THE SPATIO-TEMPORAL EVOLUTION OF IRRIGATION IN THE GEORGIA COASTAL PLAIN: EMPIRICAL AND MODELED EFFECTS ON THE HYDROCLIMATE

by

Marcus De'Andre Williams

(Under the Direction of J. Marshall Shepherd)

ABSTRACT

Agricultural landscapes comprise up to 40% of global land cover and population growth increases the need to grow current levels of agriculture. Irrigated agriculture increased globally during the last century as a result of improved technology. The impacts of this rapid expansion have been the focal point of many studies, but very few have focused on the southeastern United States. Irrigation impacts the hydrologic cycle and surface energy budget through increased evapotranspiration as a result of increased surface moisture. Georgia has experienced rapid growth in irrigated area since the early 1970s with most irrigated lands being converted from previously un-irrigated agriculture. The overarching goal of this research addresses irrigation-hydroclimate relationships in the southeastern United States, with a primary focus on southwest Georgia. While there is regional dependence on the beneficial effects of increased irrigation to improve agricultural yield, there is limited refereed literature on the influence of expansion of irrigation on Georgia's climate. The analysis conducted uses remote sensing and geographic information system (GIS) technologies to quantify past and current spatio-temporal trends in irrigated acreage in Georgia. The identification of these trends allows for the assessment of the

impacts of irrigation on local to regional hydroclimate through observation and modeling analysis.

INDEX WORDS: Irrigation, Remote Sensing, Regional Climate Change, Climate Modeling

THE SPATIO-TEMPORAL EVOLUTION OF IRRIGATION IN THE GEORGIA COASTAL PLAIN: EMPIRICAL AND MODELED EFFECTS ON THE HYDROCLIMATE

by

Marcus De'Andre Williams

B.S. Florida State University, 2006

M.S., Florida State University, 2010

A Dissertation Submitted to the Graduate Faculty of The University of Georgia in Partial Fulfillment of the Requirements for the Degree

DOCTOR OF PHILOSOPHY

ATHENS, GEORGIA

2016

THE SPATIO-TEMPORAL EVOLUTION OF IRRIGATION IN THE GEORGIA COASTAL PLAIN: EMPIRICAL AND MODELED EFFECTS ON THE HYDROCLIMATE

by

Marcus De'Andre Williams

Major Professor: J. Marshall Shepherd
Committee: Andrew J. Grundstein
Marguerite Madden
Alan P. Covich

Electronic Version Approved:

Suzanne Barbour
Dean of the Graduate School
The University of Georgia
August 2016

DEDICATION

This dissertation is dedicated to my family. They provided me with the inspiration to keep pressing forward and provided vital support to me throughout this journey. None of this would be possible without them. I would also like to thank all of the special educators who fostered my desire to learn. I also dedicate this work to my friends who have been there with me through my early childhood and who are like brothers to me. I want to especially acknowledge my wife and daughter, who are my backbone and inspiration for all my current and future achievements.

ACKNOWLEDGMENTS

I would like to thank Dr. J. Marshall Shepherd for being a mentor in my academic career and personally. I cannot think of a better mentor to learn from as an early career scientist. It is an honor to work with someone as distinguished, and famous. I would also like to thank my committee, Drs. Andrew Grundstein, Marguerite Madden, and Alan Covich for their feedback and guidance during the process. I would also like to Dr. Scott Goodrick and my colleagues at the United States Forest Service for their support and insight.

Table of Contents

1) INTRODUCTION AND LITERATURE REVIEW

1.1 Introduction and Literature Review

Agricultural production is a critical part of sustaining human life on earth. During a period known as the "Green Revolution", agricultural productivity doubled to meet rising demands of a growing population (Tilman, 1999). With an expected global population of 11.2 billion by the year 2100 (United Nations, 2015), the current levels of agricultural intensity are expected to increase to support future food demands of the population. Historically, agricultural landscapes relied on natural methods for irrigation, but more recently there has been rapid growth towards artificially irrigated landscapes. The United States Geological Survey (USGS) defines irrigation as "the controlled application of water for agricultural purposes through man-made systems to supply water requirements not satisfied by rainfall (USGS, 2016). Irrigation has rapidly expanded around the globe and can be a strain on already limited water resources. The global area equipped for irrigation was estimated to be 324 million hectares in the year 2012, with approximately 26.4 million hectares equipped for irrigation in the United States (Figure 1.1) (FAO, 2014). Growing population, decreases in the number of farms, and an overall increase in the total number of farms (Figure 1.2) (Mayo, 2016) exacerbate the need for remaining farmland to have optimal efficiency and productivity. It is postulated that the above changes increase the need for efficient irrigation as the average value of production was more than three times greater for irrigated farmland than for dryland farmland (Schaible and Aillery, 2012). From a water use standpoint, irrigation accounts for 80-90 percent of the United States' consumptive water use and much of the irrigated water is lost to atmosphere through evapotranspiration (USDA, 2012). The

bulk of this water is supplied by groundwater (38 percent global and nearly half in the United States) and is in contention with municipal water use and thermoelectric power (USDA, 2012).

Irrigation is an anthropogenic disturbance of the land surface; much like urbanization which is a widely known climate forcing that alters temperature and precipitation patterns (Mahmood et al., 2010). The literature is conclusive that irrigation significantly modifies the land surface, and it affects surface energy budgets, the water cycle, and climate (Cook et al., 2014). Figure 1.3 (Hydrologic cycle) illustrates the various aspects of the hydrologic cycle that irrigation modifies. Those branches of the hydrologic cycle affected by irrigation include precipitation, water storage in the atmosphere via increased evaporation, and ground water storage. Irrigation alters the surface energy budget (Figure 1.4) by modifying evaporation, convection, latent and sensible heat fluxes, cloud coverage, and potentially soil-heat fluxes. One common theme in irrigated areas that impacts both the local hydrologic cycle and the surface energy budget is the increase in near surface moisture. This increased moisture extending into the lower levels of the atmosphere has the ability to modify existing land-atmosphere interactions which are a critical driver of earth's climate system over continental scales (Pei et al, 2016). This modification takes place primarily through partitioning incoming solar radiation towards increased latent heating. The increase in latent heating results in decreased sensible heating that modifies temperature and evapotranspiration rates due to changes in the Bowen ratio with the Bowen ratio defined as the ratio of sensible heat flux to latent heat flux. The increased amount of near surface moisture can potentially modify existing precipitation patterns (Barnston and Schickedanz 1984, DeAnglis et al., 2010). These impacts begin at the local scale

approximately 0.5 to 5 km in size and can extend to the regional scales of 100 to 10,000 km , although the effects of irrigation on regional climate are less certain and are often region specific (Pei et al, 2016). Therefore, there is a critical need to quantify the extent of irrigated areas in order to identify what areas are impacted and to what extent. It has been postulated that increased irrigation has led to a local, and in some cases regional, cooling trend in maximum and minimum temperatures, as well as diurnal temperature range (DTR) (Greets 2002, Lobell and Bonfils 2008, Kueppers 2007, Snyder and Sloan 2007). DeAngelis et al. (2010) noted that precipitation increased by15-30% downwind of heavily irrigated areas near the Ogallala aquifer, which is part of the High Plains Aquifer System. Many of the aforementioned studies were conducted for semi-arid regions that are believed to have a heavy reliance on irrigation. However, the uncertainty of future climate change and drought frequency may lead the southeastern United States (SE US) to rely on irrigation in the same manner as the semi-arid regions. To summarize the known impacts of irrigation, literature has shown that irrigation reduces maximum temperatures, increases minimum temperatures, enhances precipitation downwind of irrigated areas, and increases low level moisture (Adegoke 2003, Barnston and Schickedanz 1984, Boucher 2004, Marshall and Pielke 2004, Sen Roy et al. 2007).

There have been efforts to map irrigated areas globally as well as in the United States and separate studies attempt to quantify the impacts of irrigation on climate. The analysis conducted here synthesizes these often separate investigations into one comprehensive study. The primary area of focus of this dissertation research is the Georgia Coastal Plain (Figure 1.1), covering an area of approximately 92, 333 km^2. The Georgia Coastal Plain landscape is characterized by

relatively gently rolling to level topography with elevations ranging from approximately 228 meters to sea level. At higher elevations, there is little level terrain except for the occasion marshy flood plain or narrow steam terrace. Soils are generally productive, well-drained, and moderately permeable. However, in areas of nearly level terrain, i.e., closer to the coast of Georgia, the soils become restrictive for agriculture and pasture (Hodler and Schretter, 1986). The 1,267 mm of annual rainfall that Georgia receives is enough to support the agriculture in the state, but the varying nature of the spatial distribution of this rainfall along with increases in drought frequency has increased the need for irrigation to support agricultural crop growth.

Agriculture is the largest industry in Georgia and contributed more than $72 billion to the state's economy in 2015 (Georgia Farm Bureau, 2016) with one out of every seven residents of the state working in agriculture or forest related fields (UGA Cooperative Extension, 2011). Southwest Georgia is responsible for a large percentage of Georgia's agricultural production (Figure. 1.5) and several of the counties in this area account for the highest agricultural water withdrawals (Figure 1.6) (Lawrence, 2016). Much of the land cover in this region was converted from un-irrigated agriculture to irrigated croplands during the early 1970s to 2008 (Martin et al., 2013).

The primary focus of this research is to investigate the hypotheses that: (1) irrigation has rapidly increased in Georgia, and (2) this rapid increase in irrigation has modified aspects of the hydroclimate such as humidity, temperature, and precipitation in the region. One interesting aspect that distinguishes this study from others is the lack of refereed literature stating the impacts of irrigation on Georgia's climate. The impact of irrigation has been investigated on

water resources, how climate change impacts irrigation demand, and impact on stream flows. Misra et al 2012 is one of the few studies that quantified the climatic impact of irrigation on Georgia's climate, but their analysis was in conjunction with other states in the southeast United States. Irrigation in Georgia has been classified as sporadic from a spatial density standpoint (Pervez and Brown, 2010) and is often not considered as having an impact in global irrigation studies. Irrigation water use is also an important issue in Georgia, as the state is in a legal dispute with Alabama and Florida over downstream usage of water. This dispute is known as the "Tri-State" water wars. The Flint river basin in Georgia has the highest amount of water use within the state and is the upstream user of water that the Florida shellfish industry is reliant upon.

A more detailed discussion of the research objectives is presented later in this chapter, but a brief summary is instructive here. This research addresses irrigation-hydroclimate relationships in the southeastern United States, with a primary focus on southwest Georgia. The first objective quantified the spatio-temporal evolution of irrigation in the Coastal Plain of Georgia. This was assessed through mapping areas equipped for irrigation in the Georgia Coastal Plain aided by Landsat satellite imagery (Figure 1.7). Building from the irrigation analysis, a simple method to estimate daily dew point temperatures using temperature and precipitation observations was developed. Chapter 2 describes the methodology and results. One of the climate system responses to irrigation is increased low level moisture and the development of a dew point estimation method allows for the capture of any long term changes in moisture content in the region using dew point temperature as a proxy. With many long-term observations of dew point

temperature existing at first order stations, which do not share common characteristics of rural and irrigated weather stations, this research objective addressed this issue.

The impact of irrigation on the hydro-climate was investigated by applying the daily dew point temperature estimation method to existing National Weather Service (NWS) Cooperative Observation Network (Coop) stations. Changes in temperature and precipitation were also evaluated. The relative response of the hydro-climate to transitioning the land surface from dry cropland, and then to an irrigated land cover was investigated using a numerical weather modeling system called the Weather Research and Forecasting (WRF) Model.

1.2 Research Objectives

Understanding the influence of past land use changes on climate is needed to improve regional projections of future climate change and inform debates about the tradeoffs associated with land use decisions (Bonfils and Lobell, 2007). The rapid expansion of irrigated area in the 20th century has remained unclear relative to other land use changes (Kueppers et al 2007). Changes in irrigation may also be expected to influence climate because soil moisture affects surface albedo and evaporation and has been shown to influence regional temperature (Dai et al, 1999). Irrigated landscapes can alter the regional surface energy balance and its associated temperature, humidity, and climate features (Sen Roy et al., 2007)

Chapter 2 identifies the spatio-temporal evolution of areas equipped for irrigation in the Georgia Coastal Plain. Prior irrigation mapping studies (Doll and Siebert 1999, Ozdogan and Gutman 2008, Siebert et al. 2005,) conducted at the global and national scale are done with very

coarse pixel size resolution (10-km to 500-m). Many of the studies produced maps that represented irrigated areas as a percentage of the pixels unit area, which does not provide information on the sub pixel location of irrigated areas. While this is sufficient for national and global applications, this level of detail is not adequate for regional analysis. Boken et al. (2004) stated that sub-county, high resolution irrigation mapping would lend better understanding to agricultural water use. This chapter answers the following research questions:

- Has irrigation increased in the Georgia Coastal Plain?
- Over what time period has irrigation increased most significantly?
- Given the spatial area of interest, where is irrigation most intense?

Chapter 3 investigates a method to estimate dew point temperatures using readily obtained daily temperature and precipitation observations. There is an absence of long term dew point temperatures outside of first order observation stations. First order stations are weather stations that are professionally maintained by the National Weather Service (NWS) or the Federal Aviation Administration (FAA) (NWS, 1999). First-order observation stations are often in areas that are not representative of agricultural areas, which created the need to develop a simple method to estimate dew point temperature and provide a metric to estimate historical dew point temperatures. Two methods of estimation were considered, a liner regression approach as well as an automated neural network approach. The neural network approach performed better, with minimum temperature, diurnal temperature range (difference between daily maximum and minimum temperature), and daily precipitation as input variables. Daily dew point temperatures

that extended back as far as observations were available can now be calculated, as they could not before this method was developed. Chapter 4 applies the daily dew point estimation method as well as analyzing temperature and precipitation methods to assess irrigation-induced changes in the region. Knowledge of the impacts of irrigation on climate is vital for understanding causes of past climate change and to anticipate the direction and magnitude of future changes in agricultural regions (Lobell and Bonfils, 2008). Chapters 3 and 4 together combine to answer the following research questions

- Has irrigation impacted hydro-climatic variables in the region?
- What type of influence, if any, has irrigation produced on hydro-climatic variables in the analysis region? Is the pre-irrigation climatology of the region different from the post-irrigation climatology?
- From the perspective of the long-term spatio-temporal characteristics of the hydro-climatic variables in the region; how are heavily irrigated surfaces different than non-irrigated surfaces?
- What hydro-climatic variable(s) is (are) most influenced by irrigation?

The aim of Chapter 5 is to investigate if there are any relative differences in the sensible and latent heat fluxes along with spatial differences in precipitation patterns between non-irrigated and irrigated land surfaces. This analysis presented a theoretical approach to quantify differences in hydro-climatic variables and their response to different land surfaces. Precipitation impacts of irrigation are often region specific (Adegoke, 2008). Pie et al. (2016) showed that

excess moisture from irrigation is transported to Georgia, but there was no mention of how the introduction of irrigation has modified the local and regional climate. The relationship is poorly understood in the analysis region (Boken et al., 2004) and has minimal observational findings to support how irrigation influences precipitation (Sen Roy et al. 2010). The proposed analysis here is focused around the following questions;

- Can irrigation theoretically impact hydro-climatic variables in humid regions?
- Has irrigation influenced moisture and precipitation transport patterns in the region?
- Are there distinct contributions to moisture and precipitation transport between two distinct representations of irrigated landscapes?

1.3 Summary

This dissertation addresses the need for a comprehensive understanding on how irrigation has influenced climate in a humid environment. Most of the studies of this nature are conducted for semiarid areas of the world because it is believed that areas with adequate rainfall do not? rely on irrigation as much. With uncertainties in drought frequency and the potential impacts of climate change, the humid Eastern United States has seen an upward trend in irrigation. This dissertation, using remote sensing methods, quantifies the high temporal and spatial resolution of the trends of irrigated areas in Georgia.

The lack of adequate long term meteorological observations in the region makes it difficult to provide a purely empirical assessment of irrigation-induced modification of the climate. To address this shortcoming, high-resolution modeling is employed to assess the relative impacts on

climate when a land surface transitions from unirrigated to irrigated agriculture. The overarching goal of the following chapters is to answer some of the uncertainties associated with irrigation and climate in the study area. This study will help to characterize the role of irrigation on hydro-climatic variables in the Georgia Coastal Plain. Although extensive literature exists for California and the Great Plains regions of the United States, a relative absence of any detailed analysis investigating the impacts of irrigation on climate in the Southeastern United States, is available. To date, this research is one of the few to create a mapped time series of irrigated area for Georgia and one of the few to provide historical analysis of long term dew point temperature trends outside of first order stations in Georgia. This research will also provide context for the impacts of irrigation in climates that are not moisture limited.

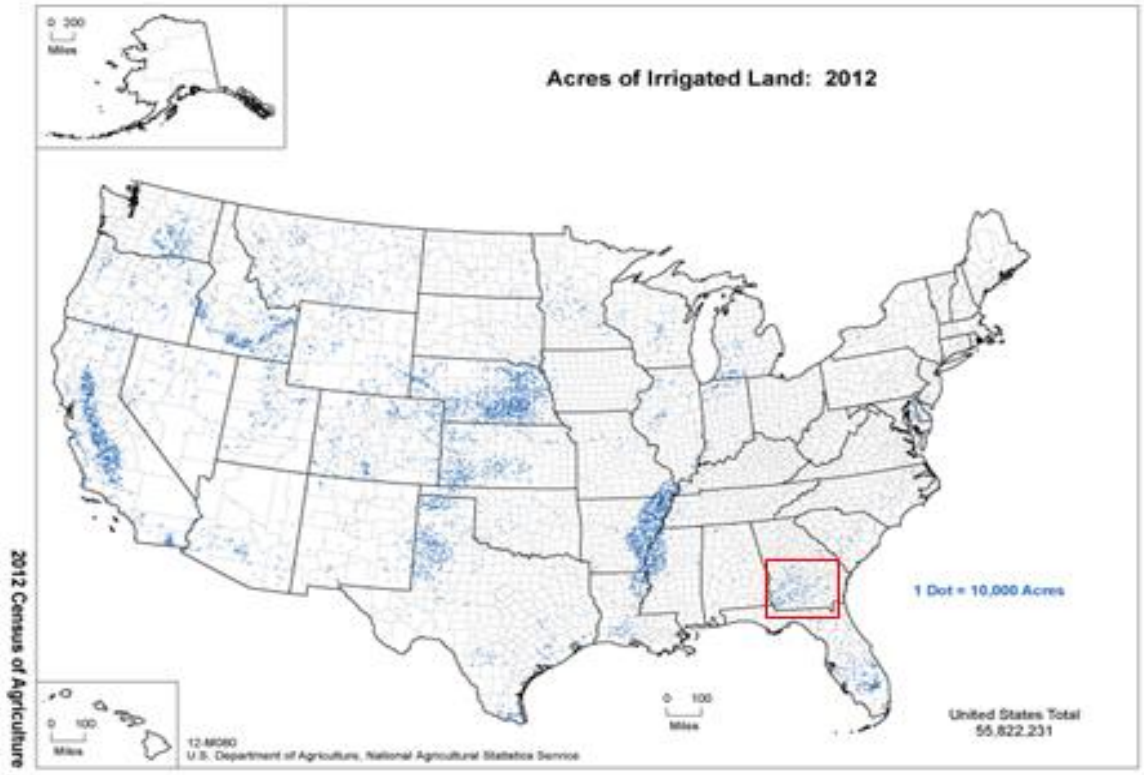

Figure 1.1: USDA map of irrigated land in 2012. Red box highlights the study area (USDA Census of Agriculture, 2012)

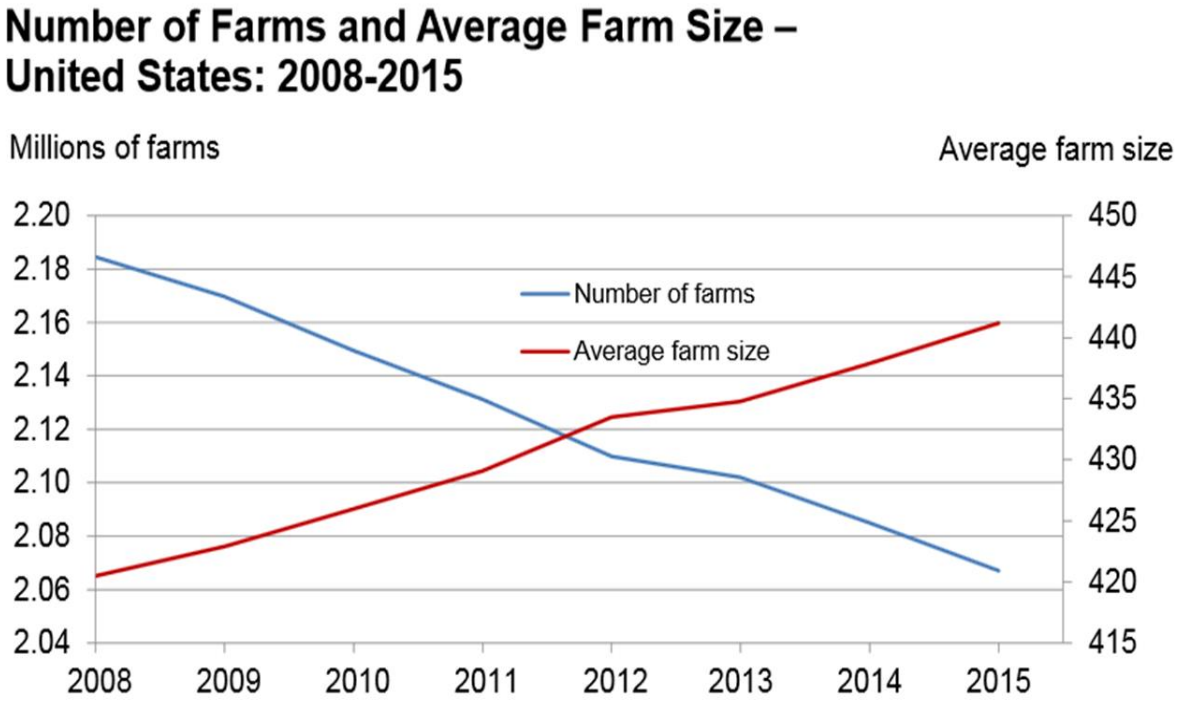

Figure 1.2: Time series of average number of farms (blue) and average farm size (red) from 2008 - 2015. Figure credit Mayo, 2016

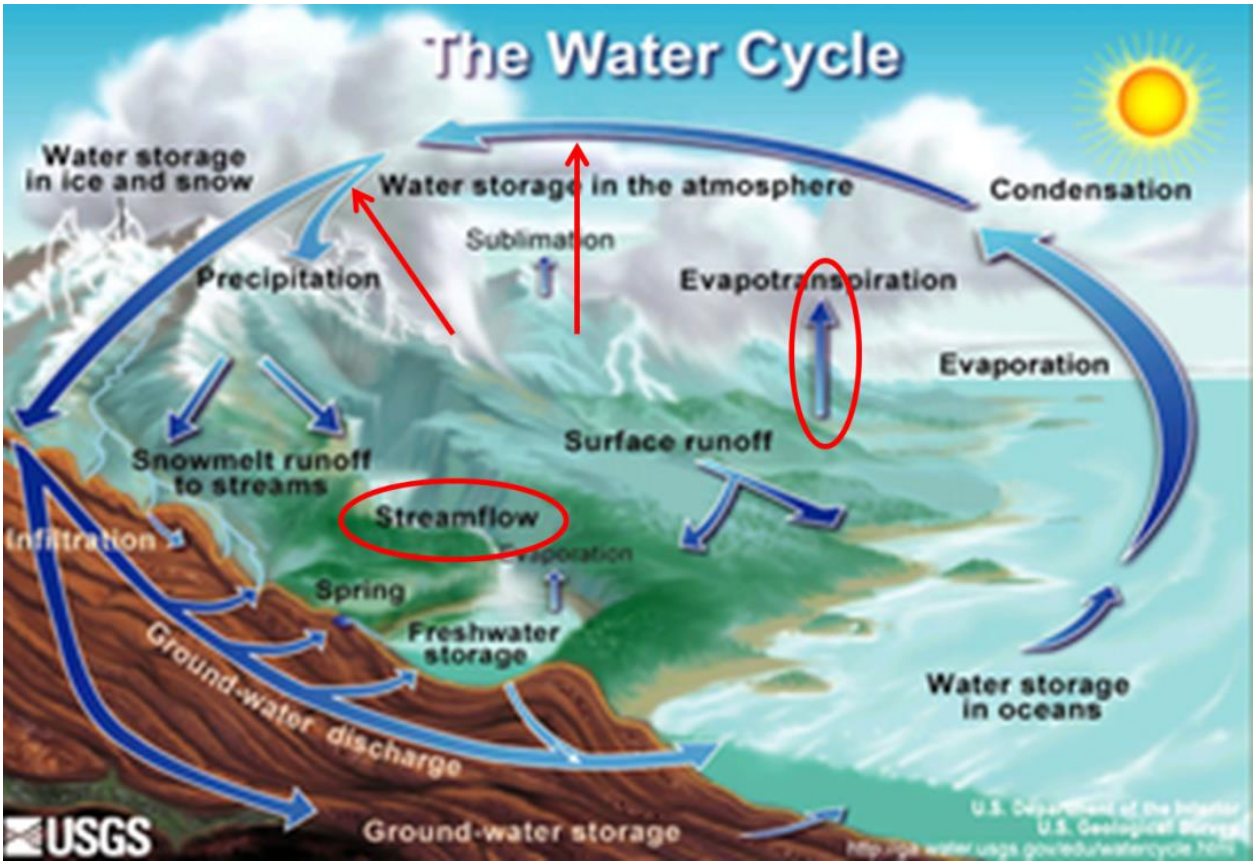

Figure 1.3: Depiction of the Hydrologic cycle. Red arrows and circles denote the impact of irrigation on the water cycle (The Water Cycle USGS, 2016).

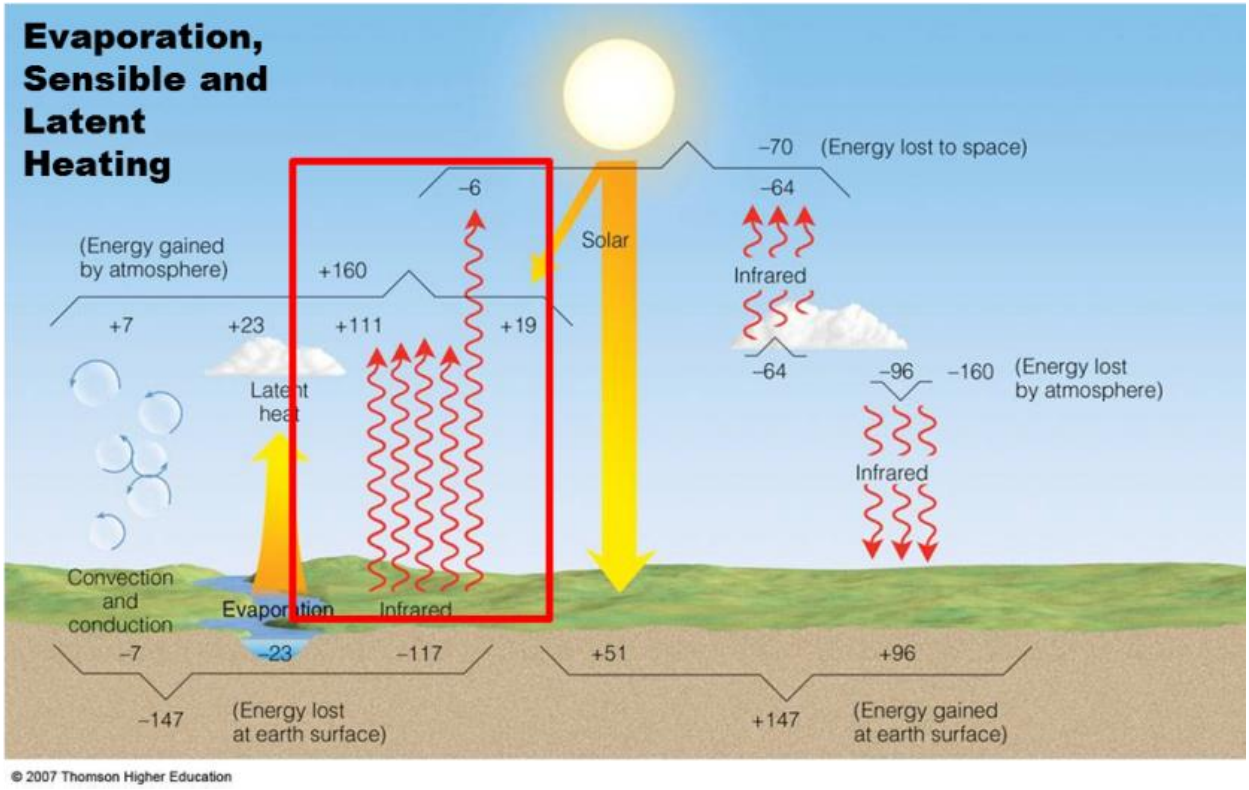

Figure 1.4: Schematic diagram of the surface energy budget. Red box represents the impacts of irrigation on the surface energy budget. Image credit Vermont State College Met 130

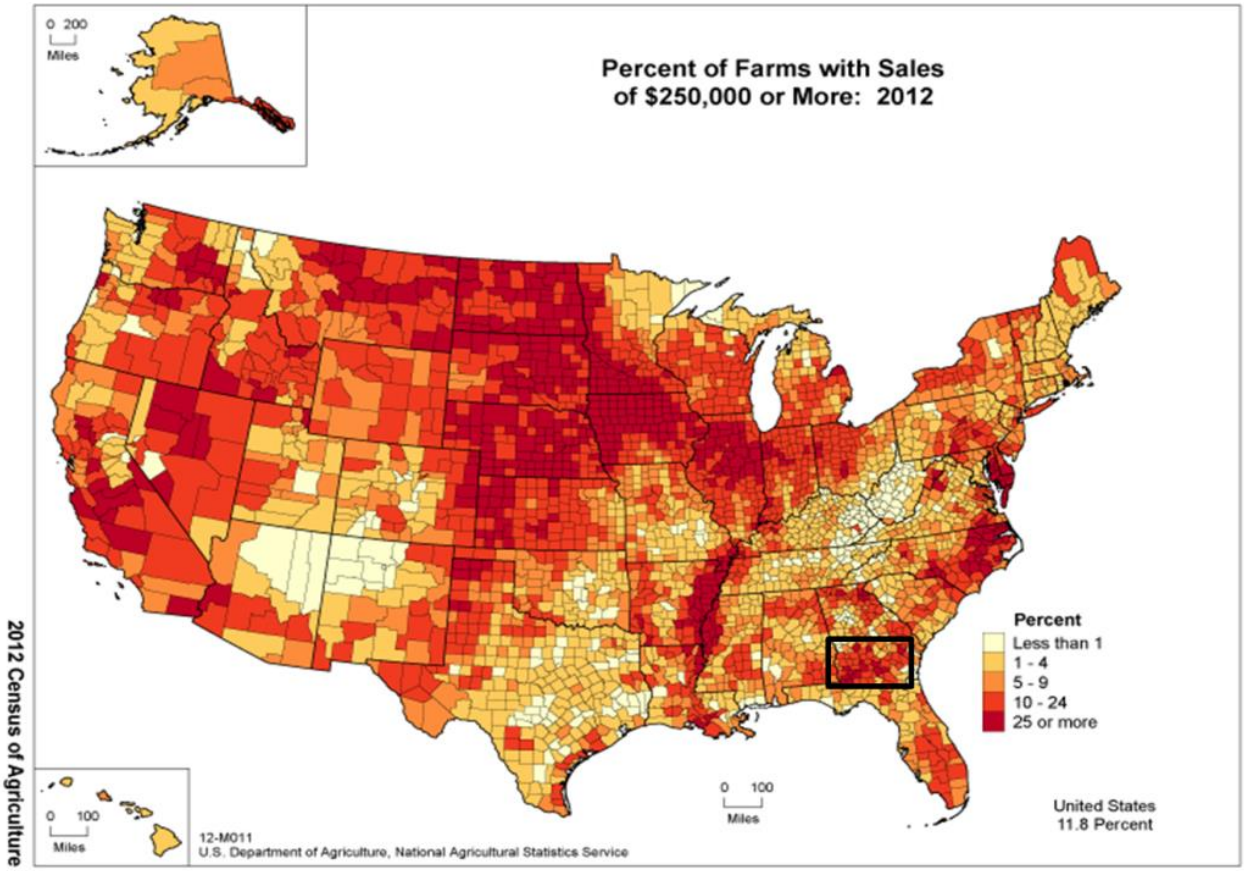

Figure 1.5: Farm sales for 2012. Shaded colors represent the percentage of farms per county with sales greater than $250, 000. Black box highlights area of interest in this study (USDA Ag Census, 2012)

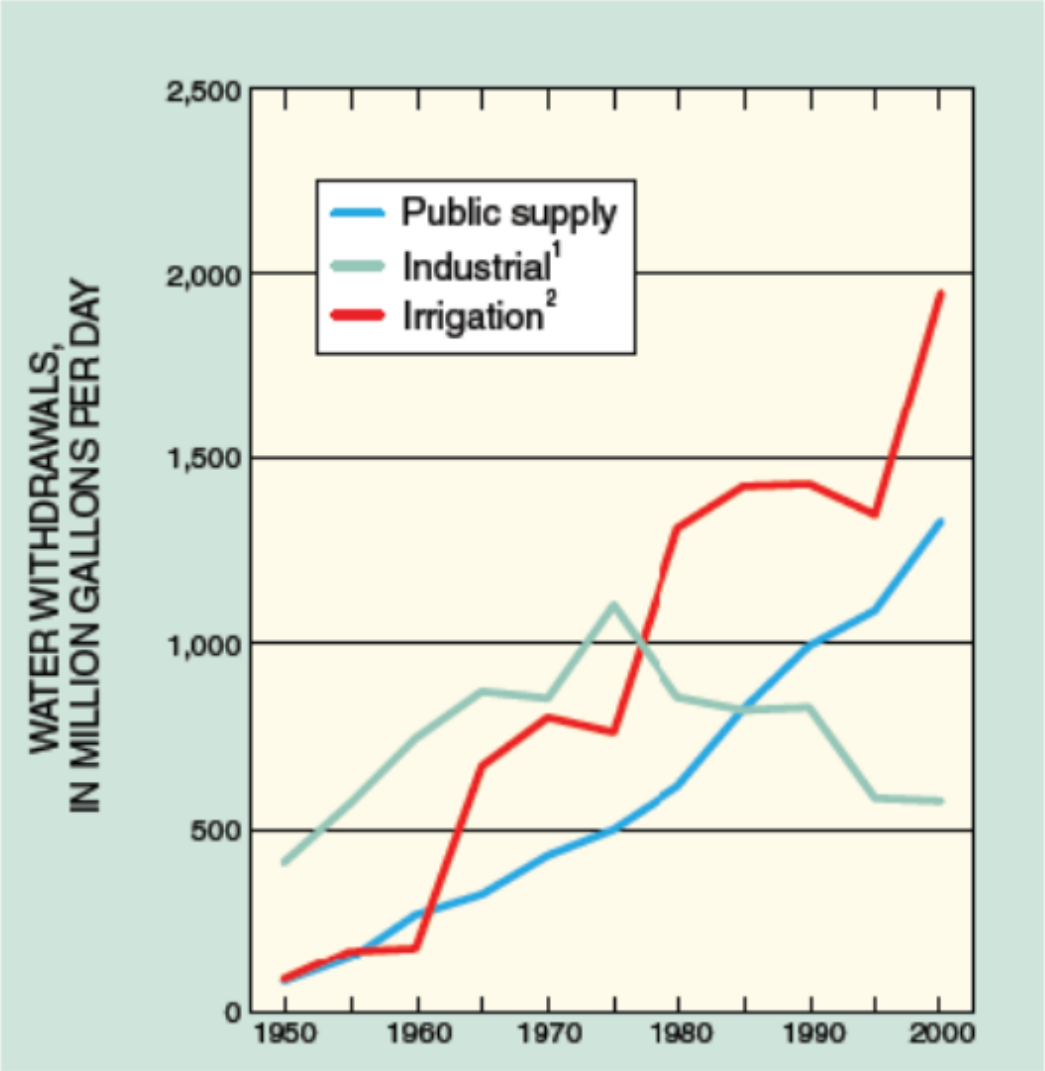

Agricultural water withdrawals for the Apalachicola-Chattahoochee-Flint (ACF) basin in Georgia have increased 1,320% from 1970-90

Figure 1.6: Diagram of water withdrawals between the public supply, industrial, and agricultural irrigation sectors in the Apalachicola-Chattahoochee-Flint Basin (Maella, 1990).

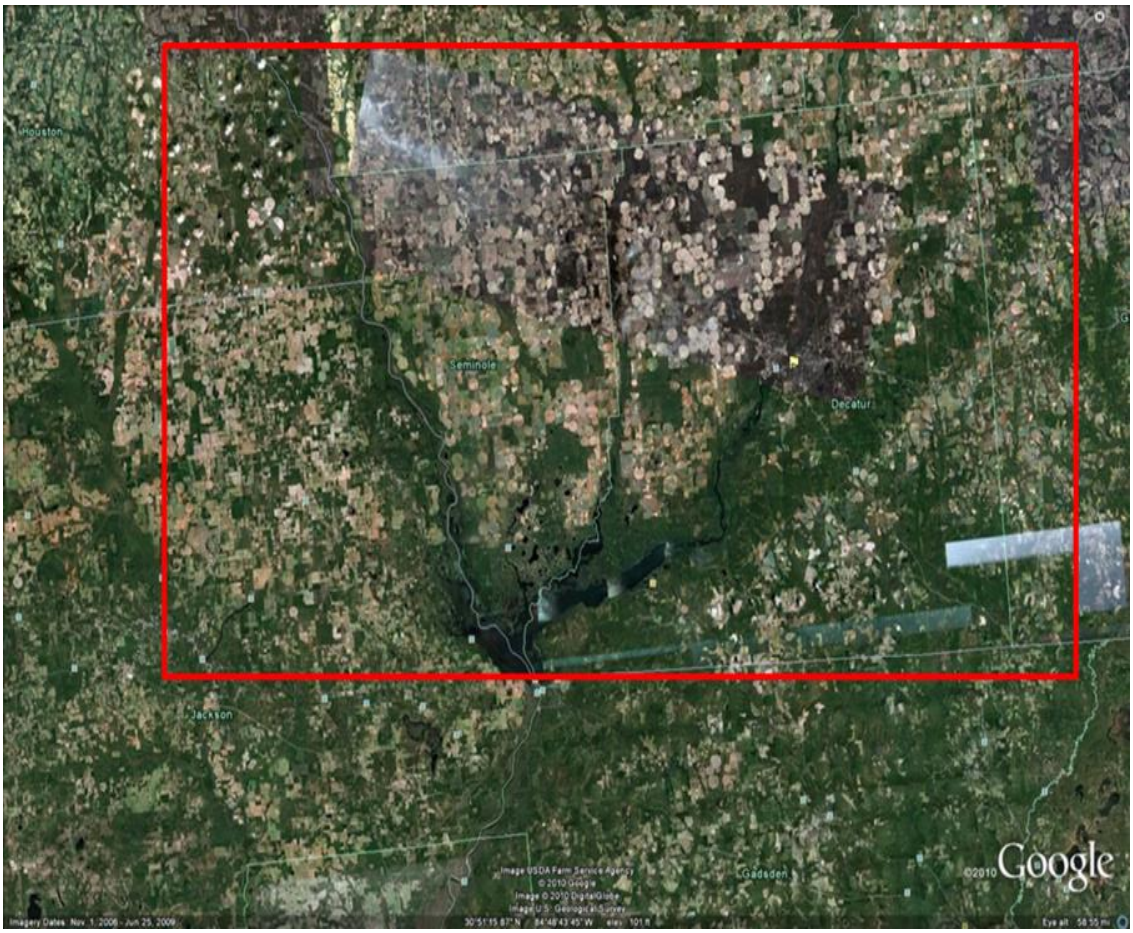

Figure 1.7: Google Earth image of southwest Georgia. Red box highlights a portion of the study area. Circular areas in image are center pivot irrigation systems. The strip of panchromatic imagery in the center a result of images from other sources being combined.

2) MAPPING THE SPATIO-TEMPORAL EVOLUTION OF IRRIGATION IN THE COASTAL PLAIN OF GEORGIA, USA

Abstract

This study maps the spatial and temporal evolution of acres irrigated in the Coastal Plain of Georgia over a 38 year period. The goal of this analysis is to create a time-series of irrigated areas in the Coastal Plain of Georgia at a sub-county level. From 1976 through 2013, Landsat images were obtained and sampled at four year intervals to manually detect Center-Pivot Irrigation (CPI) systems in the analysis region. During the 38 year analysis period there was a 4,500% increase in CPI systems detected that corresponded to an approximate 2,000% increase in total acreage. The bulk of the total acreage irrigated is contained in southwest Georgia, as seven counties in the region contained 38% of the total acreage irrigated in 2013. There was substantial growth throughout the entire Coastal Plain Region, but southwest Georgia was identified as the most heavily irrigated region of the state.

Williams M, Stegall C, Madden M, 2016: Mapping the Spatio-temporal Evolution of Irrigation in the Georgia Coastal Plain. Photogrammetric Engineering & Remote Sensing, In review

2.1 Introduction

Agriculture has always been critical for sustaining human life on earth. Improving technology and agricultural practices made it possible for world food production to double over a 31 year period between 1960 and 2000 (Tilman, 1999), which is part of a larger increased agricultural production in the 20th Century known as the Green Revolution (Evenson and Gollin, 2003). In the year 2000, approximately 15 million square kilometers of the global land cover was dominated by cropland (Ramankutty et al., 2008). With the current world population of 7.3 billion, which is expected to reach 11.2 billion by the year 2100 (UN Department of Economics and Social Affairs) and the growing demand for biofuel production (Evans 2009) the need for agricultural landscapes could potentially increase in the future. One catalyst from the rapid improvement of agricultural production was the large expansion of irrigation (Tilman et at., 2001). Irrigation can be defined as land areas that receive full or partial application of water by artificial means to offset periods of precipitation shortfalls during the growing period (Ozdogan et al. 2010). In 2000 it was estimated that 2.8 million km^2 were irrigated, with this number forecasted to increase 5.29 million km^2 ha by 2050 (Tilman 2001). Irrigation, much like urbanization, acts to alter the natural landscape properties such as partitioning latent and sensible heating at the surface of the earth which can impact surface temperature and surface moisture transport. Understanding the extent and usage of irrigation is imperative in answering questions about future water resources as it is estimated that irrigation uses over 70% of the world's consumption of freshwater (Boucher 2004, Velpuri et al. 2009). Irrigation accounts for approximately 60% of consumptive use of freshwater in the United States where estimates show that over 222,577 $km^2$of cropland are irrigated (Braneon 2014, Minchenkov 2009). For Georgia,

it is estimated that approximately 5.5 billion gallons of water per day were withdrawn from surface and ground waters in 2004 (Barnes and Keyes 2010). Agricultural water use during 2005 totaled 752 million gallons per day for irrigation, with the highest rate of irrigation occurring in the Coastal Plain region of Georgia (USGS). The primary crops irrigated in Georgia are maize, cotton and peanuts as they accounted for approximately 68% of the total irrigated acreage in 2002 (Braneon and Georgakakos, 2014).

Research has shown that irrigated croplands can impact land-atmosphere interactions and fresh water supply. Various modeling and observational studies have demonstrated that irrigation influences climate at the local, regional, and global level by enhancing evapotranspiration, altering precipitation patterns, as well as impacting minimum temperature, maximum temperature, and diurnal temperature range (Barnston and Schickedanz 1984; Greets 2002; Adegoke et al., 2003; Boucher 2004; Kueppers 2007; Lobell and Bonfils 2008; DeAngelis et al, 2010; Sen Roy et al., 2011; Cook et al., 2014 Shukla et al., 2014, Williams et al., 2015) This presents a need for accurate and detailed geospatial information on irrigated croplands (Pervez and Brown, 2010). In the United States, most mapping efforts are focused primarily on the California and the Great Plain region.

To expand and contribute to existing knowledge on the spatial and temporal changes in irrigation in Georgia, this analysis maps CPI systems through visual interpretation of Landsat satellite imagery. This shape-based method of mapping irrigation is commonly done for local scale mapping efforts. CPI systems are easy to identify in Landsat imagery because of their distinct arc-like appearance. Landsat was preferred for this analysis because of its greater spatial

coverage and the availability of imagery for more time periods. In Georgia, CPI systems are used to irrigate multiple crops and an accurate estimate of the number of CPI systems in the state could lead to better estimation of water use (Boken et al., 2004) and help identify potential climatic impacts. The analysis herein is conducted on a regional scale, with a methodology normally used for local scale studies. The goal was to produce detailed spatial extent of areas equipped for irrigation over a 38-year time frame in the Georgia Coastal Plain. The following sections include a discussion on previous mapping efforts at the global, regional, and local levels followed by information on the study area, data and methods used in our analysis. The results, conclusion and summary sections follow this.

2.2 Literature Review

Irrigation is mapped at three distinct scales; local, regional, and global. As defined by Ozdogan et al. (2010), local scales refers to one or more irrigation basins and they are typically on the order of several square kilometers in size. Regional scale studies are defined as studies that include large river basins to continental areas that extend from tens to thousands of square kilometers in area, while global scale refers to studies that attempt to map irrigation worldwide.

Most mapped irrigation studies take place at the local scale, as methods developed for one location may not be appropriate for other locations (Ozdogan et al., 2010). The methodology for local scale studies includes visual interpretation of satellite imagery or digital image classification. Manual identification of irrigated areas is often conducted for visual interpretation studies while automated classification techniques are often used for digital image classification studies. One technique to automatically detect irrigated versus non irrigated vegetation is through

digital image processing to calculate the Normalized Difference Vegetation Index (NDVI). The NDVI is a normalized ratio of the near-infrared bands and red bands (Ustin & the American Society for Photogrammetry and Remote Sensing, 2004) and the greater amount of healthy vegetation present in the sensor, the greater the NDVI value (Jensen, 2005). Pervez and Brown (2010) noted that automated techniques such as using NDVI to identify irrigated areas in humid locations can be problematic as there is little spectral difference between irrigated and non-irrigated landscape. NDVI is calculated in this study to assist in the manual detection of irrigated areas, but was not used as a stand-alone automated classification technique.

Prior irrigation mapping studies (Doll and Siebert 1999, Ozdogan and Gutman 2008, Siebert et al. 2005) conducted at the global and regional scales were performed with very coarse resolution (pixel sizes of 500-m to10-km). Many of the studies produced maps that represented irrigated areas as a percentage of the pixel unit area, which does not provide information on the sub pixel location of irrigated areas. While this is sufficient for national and global applications, this level of detail is not adequate for regional analysis. Boken et al. (2004) stated that sub county, high resolution irrigation mapping would lend better understanding to agricultural water use. Pervez and Brown (2010) attempted to make improvements on the prior irrigation maps by assimilating U.S. Department of Agriculture (USDA) National Agricultural Statistic Service (NASS) data with Moderate Resolution Imaging Spectroradiometer (MODIS) imagery. Their analysis produced maps of irrigated lands at the 250-m cell size across the conterminous U.S. for 2002. They were unable to conduct a quantitative accuracy assessment for the Eastern U.S. stating that humidity made it difficult for the NDVI to distinguish between irrigated and non-

irrigated agricultural areas. A joint effort conducted by the Georgia Environmental Protection Division EPD and the University of Georgia mapped irrigated areas in the analysis region for 2007-2008 using NAIP imagery to serve as a baseline for water resource management purposes (Braneon 2014). Our mapping analysis serves to update and provide historical context to the mapping efforts of the Georgia EPD.

The research herein has a goal to quantify the temporal and spatial evolution of areas irrigated in the Southeastern U.S Coastal Plain study region of southwestern Georgia, mainly by using satellite imagery obtained from the long-term U.S. Landsat Program. Accurate, detailed, geospatial information on irrigated croplands is essential for answering many Earth science systems, climate change, and water supply questions (Ozdogan et al., 2010). Irrigated areas are estimated through the use of time-series remote sensing data to map center pivot irrigation systems. The analysis is conducted from 10 dates of imagery acquired as early as 1976 and as current as 2013 in order to assess long-term trends in irrigation construction within the analysis region.

2.3 Study Area, Data, and Methods

Study Area

Georgia, located in the Southeastern United States, has a climate that is classified as humid subtropical climate with humid summers and mild to cool winters (Kottek et al. 2006). Georgia has a yearly average temperature of 17.4°C (63.4°F) and on average receives 1, 267 mm (49.89 in) of precipitation annually (SERCC 2015).

Georgia receives an adequate amount of rainfall to support agricultural crops such as maize, the sporadic nature of rainfall during the growing season--defined as March through October for this study--requires farmers to rely on irrigation to supplement rainfall. Using the 'Irrigated Fields with Sources in the Georgia Water Planning Region (WPR) dataset (Hook, Georgia WPR, 2015), initial analysis showed that 99% of the identified center pivot irrigation acreage occurs below the Georgia Fall Line that is approximately 60% of the total land area of Georgia. With this information, the study area was narrowed to the Georgia Coastal Plain (Figure 2.1).

Covering a total area of 92,333 km^2, the Georgia Coastal Plain landscape is characterized by relatively gently rolling to level topography with elevations ranging from approximately 228 meters to sea level. At higher elevations, there is little level terrain except for the occasion marshy flood plain or narrow steam terrace. Soils are generally productive, well-drained, and moderately permeable. However, in areas of nearly level terrain, i.e., closer to the coast of Georgia, the soils become restrictive for agriculture and pasture (Hodler and Schretter, 1986) The primary agricultural crops grown in the region are cotton, maize, and peanuts.

Data and Methods

This study used a visual interpretation-based approach to identify areas equipped for irrigation from a time-series of Landsat satellite imagery. It should be noted that areas equipped for irrigation were mapped instead of acres irrigated. This distinction is necessary as there is no firmly established way to determine if active irrigation coincided with the passing of the Landsat satellite every 16 days and recording of the images. The cloud-free images used in the analysis

were captured at various points during the growing season (March – October) over a 38-year period and a particular pivot could be in between the planting or harvest stage when the image was collected. Although band combinations and spectral enhancements can be applied to the images to highlight areas that were recently wetted, without historical ground truth data documenting actual irrigation, efforts to verify that a center pivot was operational at the time of image acquisition were not possible. Therefore, the distinction that is made in this study is areas equipped for irrigation are documented and reported as total acreage. The visual interpretation used a shape-based approach to identify center pivot irrigation (CPI) systems in the Landsat imagery. Center pivot irrigation systems are easily identified in Landsat imagery due to their arc-like appearance (Figure 2.2). This approach is easily transferable to other locations as Rundquist et al. 1989 used similar methods to create a 15-year time series of CPI systems in Nebraska from Landsat imagery.

Optical sensors of the Landsat satellite program began collecting images of the earth's surface starting in 1972 with the launch of Landsat 1. In the study area, quality images were available starting with the year 1976, Landsat scenes were selected at four-year intervals until 2008. There was a five-year interval between 2008 and the final year of 2013 due to scan line correction issues with the Landsat 7 satellite. In total, data from 10 dates covering the four Landsat satellite missions were selected. Those were Landsat 1 (1976), Landsat 2 (1980), Landsat 5 (1984-2008; sampled every four years), and Landsat 8 (2013). Table 1 provides information on the sensors and bands for all of the Landsat missions used in our analysis. The indexed path and row numbers of selected scenes were consistent for the four satellite missions.

The primary Landsat scenes analyzed were paths 17-19 and rows 37-39. The approximate size of each Landsat scene is also consistent among the four satellites with each scene size being 185 km x 185 km. Additional information about the Landsat satellite program can be found at the U.S. Geological Survey (USGS) website (USGS 2015).

The identification of the CPI systems in the Landsat images consisted of several steps:

1. Load a Landsat scene into ArcGIS;

2. Load additional shapefiles into ArcGIS that contain spatial reference data about Georgia and the Georgia Coastal Plain (including geographic coordinate system used and Universal Transverse Mercator (UTM) zones);

3. Find the best combination of bands or other spectral enhancements to highlight the CPI systems; and

4. Manually digitize the CPI systems through a process called heads-up digitizing.

Two vector shapefiles for the state of Georgia including counties, and physiographic provinces were obtained from the ESRI database of U.S. map data. ArcGIS 10.1 Desktop was used to compile all images into a single geodatabase, perform basic image processing, visual interpretation and heads-up digitizing of CPIs.

The image and vector data were georeferenced to the geographic coordinate system (GCS) (also referred to as Latitude and Longitude) tied to the North American Datum 1983 as

the spatial reference. This is done so all data layers are referenced to a common ground coordinate system.

To aid in the detection of the CPI systems, Landsat bands were selected to display additional information about the physical and biological conditions captured by the imagery. The oldest images of Landsat 1 and 2 were limited in spectral resolution as there are only four available bands from the Multispectral Sensor (MSS) sensor collecting image data at 80-m spatial resolution. For these satellites, the near-infrared, red, and green bands were composited in RGB display space to create what is known as a false color image. The NIR helped identify vegetation and soil conditions as the NIR electromagnetic (EM) energy is strongly absorbed by water and reflected by vegetation. Healthy vegetation appears red in this composite (i.e., healthy vegetation is highly reflective in the NIR portion of the EM spectrum and this band is displayed as red) and bare soil appears white (because the NIR, green, and red bands typically reflect near equal amounts of EM energy) or brown if more moisture is present and longer wavelengths are absorbed more by water. The NIR, green, and red false color composite is similar to a very near-infrared (VNIR), red, and green composite for the 7-band Thematic Mapper (TM) sensor and 8-band Operational Land Imager (OLI) sensor (both having a 30-m spatial resolution for multispectral bands). For the TM and OLI sensors, moist bare soils have a green appearance because of stronger reflectance in the relatively shorter wavelengths by moist soils.

The TM and OLI sensors also have a wider range of possible band combinations since they collect data in more bands than the MSS sensor (Table 2.1). One such combination was the blue, VNIR, and SWIR composite for the TM and OLI sensors. Moist vegetation has a bright

green appearance in this composite and moist soil appears dark purple in this composite. The purple appearance is due to the equal information (i.e., reflectance) captured by blue and SWIR bands (thereby displaying as equal levels of red and blue). There was a trial and error process to determine which combination of bands produced the best visual results for identifying CPIs and sometimes it was necessary to toggle between displaying several different band combinations in order to enhance the visual display of vegetation and levels of soil moisture. In addition, multiple bands of satellite images can be manipulated to calculate several different vegetation indices. One such index calculated in this study was the Tasseled Cap Transformation (Crist 1985, Huang et al. 2002). Calculating the tasseled cap indices gave a measure of the brightness, greenness, or wetness of a pixel in the Landsat image. This process involved a linear combination of the six bands used in the analysis with coefficients for the transformation given by Huang et al. (2002). The brightness, greenness, and wetness indices were then composited in different combinations to display spectrally enhanced images. This process produced the greatest contrast between the CPI systems and background vegetation, but was also the most labor intensive in terms of processing time. A RGB composite of the brightness, wetness, and greenness indices resulted in bare soil appearing red, wet soils appearing blue, and CPI systems with a white appearance due to about equal reflectance of bright and exposed bare ground, wet soils and healthy vegetation. Figure 2.2 provides a comparison of Landsat images of Miller County, Georgia illustrating some of the different display composites used to identify CPIs.

To capture the CPI systems in the composited Landsat scenes, circular irrigated areas were manually digitized using a procedure known as heads-up digitization. This procedure

involves visual (i.e., manual) interpretation of CPIs and using a mouse-controlled cursor to draw a vector polygon surrounding features in the raster images as displayed on a computer monitor. This method was used to create a digital boundary of CPI systems identified in the Landsat imagery. Interpretation and digitization for all images of all years was conducted by the same analyst. Although this significantly increased the length of manual labor, this was a necessary step to keep the human bias consistent through all years and allow analysis of changes over time and the calculation of ground area of the digitized CPI systems. This created a CPI shapefile for each year analyzed that can be easily disseminated to other end users, or a database of CPI systems that can be modified and updated as others see fit.

2.4 Results

This section presents data depicting the spatio-temporal evolution of areas equipped for irrigation in the Coastal Plain as well as the total increase in CPI systems during the 38-year analysis period of 1976 to 2013. The ability to detect CPI systems at the sub-county level allows for insight as to which counties have the highest total acreage irrigated and what percentage of the total land area is irrigated for each county. If a pivot spanned several counties, the digitized polygon was split and then assigned to the county that it fell in and the area was calculated for that portion.

There was considerable growth in the areas equipped for irrigation and the number of CPI systems detected. In 1976, there were 247 CPI systems detected totaling 17,162 hectares (ha) (Figure 2.3). Those numbers increased to 11,439 CPI systems (Figure 2.3) detected totaling 378,885 ha (Figure 2.3) in 2013. This accounts for an approximate 4,500% increase in CPI

systems detected and an approximate 2,000 in total acres irrigated over the 38-year analysis period. The data suggest that there were smaller pivots being added as the years progressed. The largest percent changes in CPI systems detected and total acreage were from 1980 to 1984 where there was a 151% and 145% increase, respectively (Figure 2.4). The percent changes for those particular years also coincide with a sensor change for the Landsat satellite program (i.e., the 80-m pixel Multispectral Sensor was replaced by the 30-m Thematic Mapper sensor), which could introduce increases in detection rates and acres irrigated because smaller CPIs were visible in these images. An increasing trend of acres irrigated was identified in all years analyzed, although the rate of increase was not as great as the time period between 1980 and 1984. The percent change in CPI systems and total acreage was positive for all years analyzed, with the rate of change drastically slowed after 1984. The time period between 1992 and 1996, produced the lowest percent change of any other time period. During this time there was an 11% change in CPI systems detected and an 8% change in total acreage. Initially, there was congruency between the percent change between the CPI systems and total acreage. After 1988, the difference between the two metrics increased. The largest difference occurred between 2004 and 2008, when there was a 58% increase in CPI systems compared to a 27% in total acreage. This suggests that there was a preference to install smaller CPI systems as previously mentioned.

Initially, southwest Georgia was identified as a region of dense irrigation in the images that were analyzed. There were a few other sporadic areas of irrigation throughout the analysis region, but from the onset, southwest Georgia was the core of heavy irrigation in the state. In particular, the counties of Seminole, Decatur, Miller, Baker, and Mitchell contained the most

irrigation. Even as the number of CPI systems and total acreage progressed northeastward, the southwest Georgia region remained the most densely irrigated. Maps were generated for each year analyzed, but for brevity the years 1976, 1996, and 2013 are presented (Figures 2.5-2.7). These three time periods represent the initial date in the time series (1976); a time around the midpoint of the 38 year analysis period (1996); and the last date of the time period (2013). Starting with the 1976 time period (Figure 2.5), as previously mentioned southwest Georgia contained the most CPI systems and total acreage irrigated. The total number of CPIs identified for the time period was 247, which resulted in 17,567 hectares irrigated. The counties of Seminole and Decatur were the most densely irrigated at this time. The average sizes of CPI systems are 71 hectares with the largest CPI systems covering 150 hectares. At the midpoint in 1996 (Figure 2.6), the number of CPI systems detected increased to 3,189. The largest CPI system covered 231 hectares, with a mean size of 53 hectares. During the 1996 period, densely irrigated areas expanded north and northeast of Seminole and Decatur counties. The counties of Miller, Baker, and Mitchell joined Seminole and Decatur as the counties with the highest irrigation density. The final time period, 2013 (Figure 2.7), had a total of 11,439 CPI systems that totaled 378,885 hectares. Visually, there is a substantial increase in total acreage in the eastern part of the Coastal Plain (Atlantic/Lower), but the western part of the Coastal Plain (Gulf/Upper/Lower) remains the most heavily and densely irrigated. The eastward expansion of acres irrigated was seen in each subsequent year during the analysis period. From the initial date analyzed to the last year analyzed, the geographic region that is the most densely irrigated is southwest Georgia. The region is a part of the Apalachicola Flint Chattahoochee (ACF) River Basin as irrigation represents the largest use of consumptive water in the Flint River Basin. The

largest CPI system found covered 232 hectares and the mean size also decreased to 33 hectares. The decrease in the mean size of CPI systems corroborates the initial speculation of smaller sized CPI systems in subsequent years.

To assess the counties that are the most densely irrigated, the percent of total land area and the total acreage irrigated are analyzed. It is expected that counties with a larger land area have the capacity to irrigate more. This does not necessarily mean that large counties are the most densely irrigated. Figures 2.8 and 2.9 highlight the counties with the highest totals in both areas. These figures also show that southwest Georgia is the most intensely irrigated area of the state. Southwest Georgia lies within the Flint River Basin, which along with the Central and Coastal regions of the Coastal Plain of Georgia comprise about 95% of crop production and irrigated acreage in the state (Guerra et al 2005). During the growing season, irrigation accounts for approximately 90% of water used in the Flint River Basin. Of the counties that were analyzed in the Coastal Plain, approximately seventeen had 8,000 hectares or greater irrigated (Figure 2.8) in the final year of analysis. Using 1984 as a starting point to consider data captured from Landsat satellite sensors of the same spatial resolution (30-m) between periods of analysis, many of these counties doubled the total acres irrigated during the 30-year period. Only two of those counties, Burke County and Jefferson County, are located outside of Southwest Georgia. Eleven of those seventeen counties currently have, with some counties extending back to 1984, approximately 10% of their total land area equipped for irrigation (irrigated) (Figure 2.9). Seven of those eleven counties have approximately 15% or more of their total land area equipped for irrigation. Decatur County (Lower Flint) has the highest number of total acres equipped with 30,127 ha.

Seminole County has the highest total percentage of land area irrigated with approximately 35% of the total land area. Decatur and Seminole Counties along with five other bordering counties (Baker, Calhoun, Early, Miller, and Mitchell) combined for 146,006 ha. Combined, those seven counties account for approximately 38% of the 2013 total acreage of CPI.

2.5 Discussion

All studies have some limitations due to data challenges, time constraints, or other confounding factors. This study shares some of those same challenges, with one of the greatest limitations being introduced by the data provided by the Landsat satellite program. The changes in sensors and resolution between Landsat missions could introduce spurious trends. This is not a challenge that is unique to this particular study. Also there was the nature of how the satellite images were analyzed visually to manually delineate CPIs. It would have been beneficial to create an automated detection method, but several attempts to automate the process were not successful. Manual digitization resulted in labor intensive detection of CPI systems, which was further compounded by the overall size study area. All digitization of CPI systems in the study were done by one individual in order to keep consistency from one year of analysis to another. Visual interpretation studies are often suited for local studies, but were used for regional analysis in our case. The Landsat satellite program was designed to detect changes in land cover and land use, but the sensors used and resolution available changed through time. These changes could introduce spurious increases in CPI systems detected, but this issue was not unique to our study and is common in all studies that span the same time period as our analysis. There were other

remotely sensed products available, such as aerial photography, but it was determined that Landsat was the optimal mix of temporal and spatial coverage for our analysis.

Alternative forms of aerial photographs include the National High Altitude Photography (NHAP) program, the National Aerial Photography Program (NAPP), and the National Agriculture Imagery Program (NAIP) produced by the United States Department of Agriculture.. NAIP imagery has been used for prior agricultural studies in the region. NAIP acquires areal imagery during the agricultural growing seasons in the continental USA. The first images were collected in 2003 and are available in 5-year intervals if funding is available (USDA 2015). The difference is spatial coverage between NAIP imagery and Landsat can be seen in Figure 10. Each Landsat scene is approximately 185 km x 185 km compared to the approximate 10 km by 10 km size of the NAIP imagery. NAIP imagery yields more detail, but the advantage of using Landsat images is the ability to cover a larger area for a much longer period of time. There would also be a large increase in the pre-processing necessary to create spatial references for numerous older aerial photographs. Landsat also has a higher temporal resolution compared to other forms of aerial photographs available. The ability to detect CPI systems smaller than 12 acres (5 hectares) was a limiting factor of the spatial resolution of the Landsat sensor. There were also attempts to automate the detection process through Houghton transformation and other circle detection techniques, but none produces adequate results.

Overall there was a positive trend in the number of CPI systems detected and the total acreage. Our analysis indicated that within the overall positive trend, there were year to year decreases in the rate of change. The slowdown in the rate of change could be tied to various

policies implemented in the state. One of the first policy changes was the introduction of the agricultural sector of the state was the Conservation Reserve Program (CRP) beginning in the 1980s. This program was part of the 1985 Farm Bill and was in effect from 1985 - 1992. The objective of the CRP program was to convert marginal cropland to a less intensive use, primarily trees, as 645,931 acres have been planted since 1986 (Center for Invasive Species and Ecosystem Health, the University of Georgia, 2005). This program was incentivized, paying farmers an average of $42.30 per acre (Center for Invasive Species and Ecosystem Health, the University of Georgia, 2005). Most of the land converted in the CRP program in Georgia was released in 1996, meaning that the landowner was free to use the land as they saw fit. The implementation of this policy also coincided with a drastic slowdown in the acres irrigated. As previously mentioned, from 1984 to 1996 there was a decrease in the percent change of CPI systems and total acreage. Farmers may have seen this land conversion as a more profitable long-term solution over marginal agricultural land cover.

Coinciding with the timing of the CPR program were amendments in 1988 to Georgia's Groundwater Use Act of 1972 and Water Quality Control Act that required a permit to be obtained for agricultural water users who used more than 100,000 gallons per day on a monthly basis. The permits were provided and recorded by the Georgia Environmental Protection Division (EPD). The highest irrigation rates typically occur within the Flint and Chattahoochee River Basins. This area is part of an ongoing dispute between the states of Alabama, Florida, and Georgia known as the tri-state water wars. The tri-state water wars are between based on water rights in the Alabama-Coosa-Tallapoosa (ACT) and Apalachicola-Chattahoochee-Flint (ACF)

River Basins. Although this dispute was not initially tied to agricultural water use, some of the litigation spurred policy changes that may have acted to curtail the initial rapid increase that was seen in irrigated acreage in Georgia. It is also important to note that the Flint River Basin has some of the highest agricultural water withdrawals in Georgia. Much of the water is from the Floridian aquifer (Spurgeon and Mullen, 2005).

A few changes included legislation that required CPI systems to be 80% efficient by January 1st 2020 and the Georgia EPD's intentions to produce a 20% reduction in agricultural water withdrawals in the Flint River Basin and the state's ability to restrict agricultural water withdrawals during periods of drought (Masters et al. 2009). As there are still ongoing efforts to accurately monitor the amount of water used in the agricultural sector throughout the state, this also created a desire for Georgia to quantify the amount of water used in the agricultural sector and create guidelines for farmers on how much water to withdraw to during periods of drought. To answer those questions, it is vital to know how irrigation varies spatially and how irrigation has varied over time. This work provides some critical information to answer both of those questions as our results present acres irrigated in a historical context and provides that information spatially over a 38-year time period, as opposed to a tabular format.

2.6 Conclusion

This analysis conducted a simple visual interpretation technique of Landsat satellite images to assess the spatio-temporal evolution of areas irrigated in the Georgia Coastal Plain. Acres irrigated were estimated through identifying center-pivot irrigation systems throughout the analysis region. Other research has suggested that this region has experienced upward increases

in areas irrigated, but there are few studies that display the long term spatial extent of this increase. As expected, there were significant increases in the total acres irrigated and the number of CPI systems detected in the Georgia Coastal Plain over our 38-year analysis period. There was an approximate 4,500% increase in CPI systems detected and an approximate 2,000% increase in total acres irrigated during the length of our analysis. The largest increases took place between 1980 and 1984 and there were steady year to year increases as well, although there was a dramatic slowdown in the rate of increase from 1984 to 1996. This slowdown in the rate of increase was primarily due to legislation introduced around the late 1980s such as incentive laden legislation to convert marginal agricultural land cover to a forested land cover and legislation that required permits for agricultural water withdrawals and placed restrictions on withdrawals during periods of drought. The results showed that southwest Georgia is the most densely irrigated portion of the state as there were seven counties in this area that accounted for 38% of the 2013 total acres irrigated. Ease of access to sustainable water sources, suitable soils that promote crop growth, and level topography are a few potential reasons for irrigation favoring southwest Georgia. Two counties in particular, Decatur and Seminole Counties, have the most total acres irrigated and highest percentage of total land irrigated respectively. These counties lie within the ACF River Basin, with is currently at the center of legal dispute over water rights between Alabama, Florida, and Georgia. This research will serve as a tool to aid others in the scientific community identify any ecological, climatic, or water resource impacts this increase in irrigation may have presented, as this work will serve as a baseline for spatio-temporal changes in irrigation in the Georgia Coastal Plain.

2.7 References

Adegoke, J., Pielke, R., Eastman, J., Mahmood, R., & Hubbard, K., 2003. Impact of Irrigation on Midsummer Surface Fluxes and Temperature under Dry Synoptic Conditions: A Regional Atmospheric Model Study of the U.S. High Plains. *Monthly Weather Review, 131*, 556-564.

Barnes, F., & Keyes, A., 2010. *Georgia's Water Conservation Implementation Plan*. GA: Georgia Department of Natural Resources Environmental Protection Division, pp. 1-204.

Barnston, A., & Schickedanz, P., 1984. The Effect of Irrigation on Warm Season Precipitation in the Southern Great Plains. *J. Climate Appl. Meteor. Journal of Climate and Applied Meteorology, 23,* 865-888.

Boken, V., Hoogenboom, G., Hook, J. E., Thomas, D. L., & Guerra, L. C., 2004. Agricultural water use estimation using geospatial modeling and a geographic information system. *Agricultural Water Management, 67*(3), 185-199.

Boucher, O., Myhre, G., & Myhre, A., 2004. Direct human influence of irrigation on atmospheric water vapour and climate. *Climate Dynamics, 22*, 597-604.

Braneon, C., Georgakakos, Peter, A., 2011. Climate Change Impacts on Georgia Agriculture and Irrigation. *Proceedings of the 2011 Georgia Water Resources Conference*, 11-13 April 2011, Athens, Georgia (Georgia Institute of Technology, Warnell School of Forestry and Natural Resources, The University of Georgia), pp. 1-2.

Braneon, C., 2014. *Agricultural Water Demand Assessment in the Southeast U.S. Under Climate*

Change, Ph.D. dissertation, *Georgia Institute of Technology*, 240 p.

Center for Invasive Species and Ecosystem Health, the University of Georgia., 2005. Land Use When CRP Payments End - What History Tells Us in Georgia. Retrieved November 20, 2015, from http://www.bugwood.org/crp/landuse.html

Cook, B., Shukla, S., Puma, M., & Nazarenko, L., 2014. Irrigation as an historical climate forcing. *Clim Dyn*, *44*, 1715-1730.

Deangelis, A., Dominguez, F., Fan, Y., Robock, A., Kustu, M., & Robinson, D., 2010. Evidence of enhanced precipitation due to irrigation over the Great Plains of the United States. *Journal of Geophysical Research*, *15*, D15115.

ESRI., 2007. ArcGIS Desktop Help 9.2 - welcome. URL: http://webhelp.esri.com/arcgisdesktop/9.2/index.cfm?TopicName=welcome, ESRI, Redlands, CA (last date accessed: 6 July 2015)

Evans, J., & Cohen, M., 2009. Regional water resource implications of bioethanol production in the Southeastern United States. *Global Change Biology*, *15*(9), 2261-2273.

Evenson, R., & Gollin, D., 2003. Assessing the Impact of the Green Revolution, 1960 to 2000. *Science*, *300*, 758-762.

Geerts, B., 2002. On the effects of irrigation and urbanisation on the annual range of monthly-mean temperatures. *Theoretical and Applied Climatology*, *72*(3/4), 157-163.

Guerra, L., Garcia, A., Hook, J., Harrison, K., & Boken, V., 2005. Impact of local weather variability on irrigation water use in Georgia. *Proceedings of the 2005 Georgia Water Resources Conference*, 25-27 April 2005, Athens, GA (University of Georgia,

University of Mississippi, Geoinformatics Center), pp. 1-4.

Hodler, T., & Schretter, H., 1986. *The atlas of Georgia*. Institute of Community and Area Development, University of Georgia. Athens, GA, 273 p.

Hook, J., 2010. Georgia WPR - Ag Water Demand - SW & GW Demand by WPR, URL: http://www.nespal.org/SIRP/waterinfo/State/AWD/AgWaterDemand_By_WPR.html (last date accessed: 1 November 2015)

Huang, C., Wylie, B., Yang, L., Homer, C., & Zylstra, G., 2002. Derivation of a tasseled cap transformation based on Landsat 7 at-satellite reflectance. *International Journal of Remote Sensing*, *36*(2), 1741-1748.

Jensen, J. R., 2005. *Introductory digital image processing: A remote sensing perspective* (3rd ed.). Pearson Prentice Hall, Upper Saddle River, NJ, 343 p.

Kottek, M., Grieser, J., Beck, C., Rudolf, B., & Rubel, F., 2006. World Map Of The Köppen-Geiger Climate Classification Updated. *Meteorologische Zeitschrift, 15*(3), 259-263.

Kueppers, L., Snyder, M., & Sloan, L., 2007. Irrigation cooling effect: Regional climate forcing by land-use change. *Geophysical Research Letters Geophys. Res. Lett., 34*(3), L03703.

Lobell, D., & Bonfils, C., 2008. The Effect of Irrigation on Regional Temperatures: A Spatial and Temporal Analysis of Trends in California, 1934–2002. *Journal of Climate J. Climate, 21*(10), 2063-2071.

Masters, M., Cummings, R., Daniels, B., Rowles, K., & Wilson, D., 2009. Managing Agricultural Water Use During Drought: An Analysis of Contemporary Policies Governing Georgia's Flint River Basin. *Sea Grant Law and Policy, 2*(1).

Minchenkov, A., 2009. USDA study finds 54.9 million acres of U.S. Farmland now irrigated, USDA News Release, URL: http://www.usda.gov/wps/portal/usda/usdahome?contentid=2009/12/0596.xml, United States Department of Agriculture, Washington, DC (last date accessed: 1 November 2015)

Ozdogan, M., & Gutman, G., 2008. A new methodology to map irrigated areas using multi-temporal MODIS and ancillary data: An application example in the continental US. *Remote Sensing of Environment, 112*(9), 3520-3537.

Ozdogan, M., Yang, Y., Allez, G., & Cervantes, C., 2010. Remote Sensing Of Irrigated Agriculture: Opportunities And Challenges. *Remote Sensing, 2*(9), 2274-2304.

Pervez, M., & Brown, J., 2010. Mapping Irrigated Lands at 250-m Scale by Merging MODIS Data and National Agricultural Statistics. *Remote Sensing, 2*(10), 2388-2412.

Ramankutty, N., Evan, A., Monfreda, C., & Foley, J., 2008. Farming the planet: 1. Geographic distribution of global agricultural lands in the year 2000. *Global Biogeochem. Cycles Global Biogeochemical Cycles, 22*(1), GB1003.

Roy, S., Mahmood, R., Quintanar, A., & Gonzalez, A., 2010. Impacts of irrigation on dry season precipitation in India. *Theoretical and Applied Climatology, 104*(1/2), 193-207.

Rundquist, D., Hoffman, R., Carlson, M., & Cook, A., 1989. The Nebraska center-pivot inventory - An example of operational satellite remote sensing on a long term basis. *Photogrammetric Engineering & Remote Sensing, 55*, 587-590.

Shukla, S., Puma, M., & Cook, B., 2013. The response of the South Asian Summer Monsoon

circulation to intensified irrigation in global climate model simulations. *Clim Dyn Climate Dynamics*, 21-36.

Southeastern Regional Climate Center (SERCC)., 2015. Monthly and Seasonal Climate, URL: https://www.sercc.com/climateinfo/monthly_seasonal (last date accessed: 7 July 2015)

Spurgeon, K., & Mullen, J., 2005. Estimating the Value of Irrigation Water in Georgia. *Proceedings of the 2005 Georgia Water Resources Conference*, 25-27 April 2005, Athens, GA (Georgia Institute of Technology, Institute of Ecology, The University of Georgia), pp. 1-3.

Tilman, D., 1999. Global environmental impacts of agricultural expansion: The need for sustainable and efficient practices. *Proceedings of the National Academy of Sciences, 96*(11), 5995-6000.

Tilman, D., 2001. Forecasting Agriculturally Driven Global Environmental Change. *Science, 292*(5515), 281-284.

UN Department of Economic and Social Affairs., 2015. World population projected to reach 9.7 billion by 2050, URL: https://www.un.org/development/desa/en/news/population/2015-report.html, United Nations, New York (last accessed: 11 January 2016)

USDA., 2015. National Agricultural Imagery Program (NAIP) Imagery. URL: http://www.fsa.usda.gov/programs-and-services/aerial-photography/imagery-programs/naip-imagery/, United States Department of Agriculture Farm Service Agency, Washington, DC (last date accessed 12 November 2015)

USGS. (2015). Landsat Missions: Imaging the Earth Since 1972, URL:

http://landsat.usgs.gov/about_mission_history.php, U. S. Geological Survey (last date accessed: 6 July 2015)

Ustin, S. L., & American society for Photogrammetry and remote Sensing., 2004. *Remote sensing for natural resource management and environmental monitoring* (3rd ed., Vol. 4). Lewis Publishers, Hoboken New Jersey, 736 p.

Velpuri, N., Thenkabail, P., Gumma, M., Biradar, C., Dheeravath, V., Noojipady, P., & Yuanjie, L., 2009. Influence of Resolution in Irrigated Area Mapping and Area Estimation. *Photogrammetric Engineering & Remote Sensing, 75*(12), 1383-1395.

Williams, M. D., Goodrick, S. L., Grundstein, A., & Shepherd, M., 2015. Comparison of dew point temperature estimation methods in Southwestern Georgia. *Physical Geography, 36*(4), 255-267.

	Landsat 1		Landsat 2		Landsat 5		Landsat 8	
Year(s) used	1976		1980		1984; 1988, 1992; 1996; 2000; 2004; 2008		2013	
Sensor	Multispectral Scanner (MSS)		Multispectral Scanner (MSS)		Thematic Mapper (TM)		Operational Land Imager (OLI)	
Spatial resolution	60 meters		60 meters		30 meters		30 meters	
Bands Used	Band	Wavelength (micrometers)	Band	Wavelength (micrometers)	Band	Wavelength (micrometers)	Band	Wavelength (micrometers)
	Green	0.5 – 0.6	Green	0.5 – 0.6	Blue	0.45 – 0.52	Blue	0.45 – 0.51
	Red	0.6 – 0.7	Red	0.6 – 0.7	Green	0.52 – 0.60	Green	0.53 – 0.59
	NIR	0.7 – 0.8	NIR	0.7 – 0.8	Red	0.63 – 0.69	Red	0.64 – 0.67
	NIR	0.8 – 1.1	NIR	0.8 – 1.1	VNIR	0.76 – 0.90	NIR	0.85 – 0.88
					SWIR	1.55 – 1.75	SWIR	1.57 – 1.65
					SWIR	2.08 – 2.35	SWIR	2.11 – 2.29

Table 2-1: Table providing information on the Landsat missions used in analysis

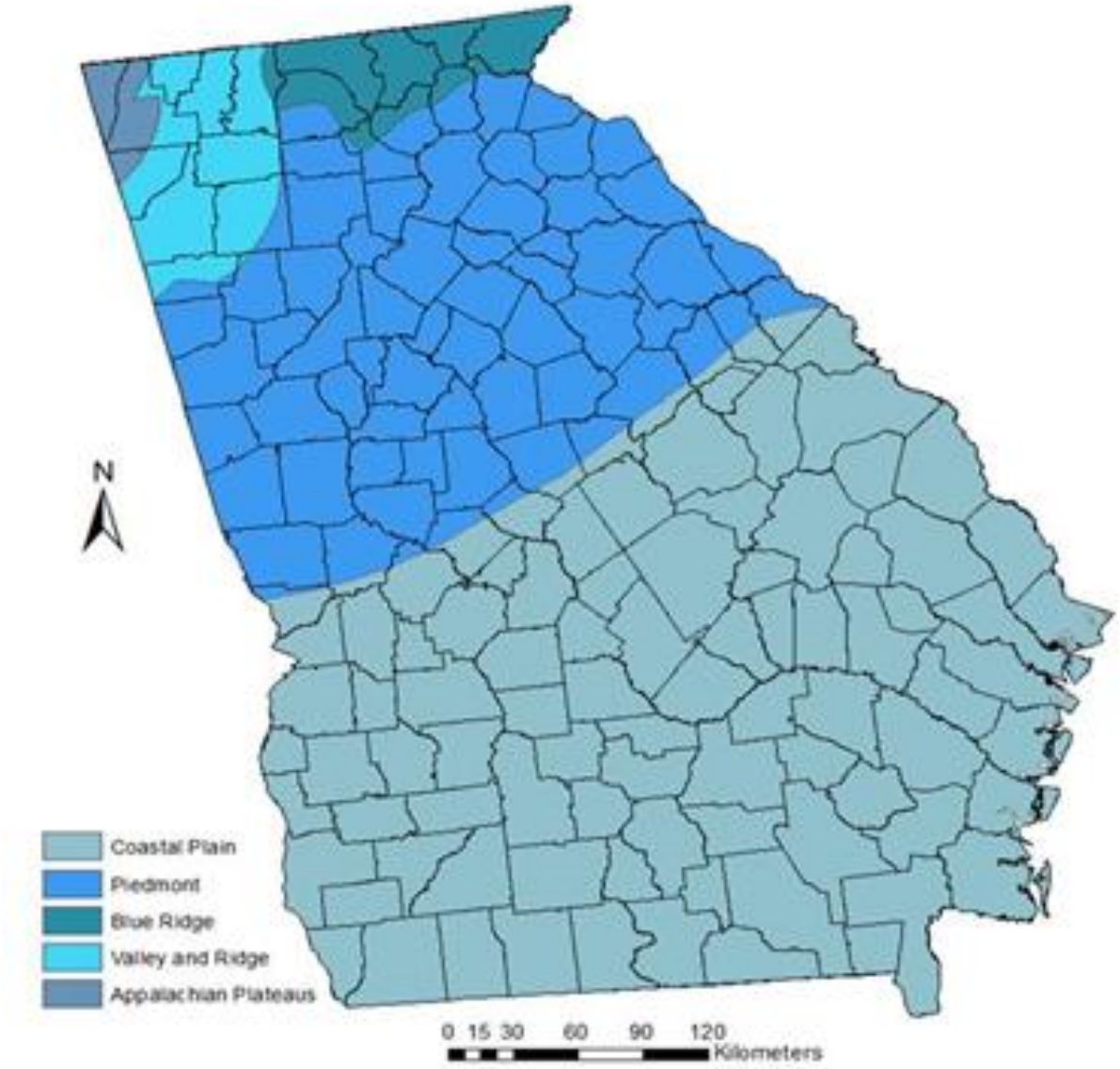

Figure 2.1: Physiographic provinces of Georgia

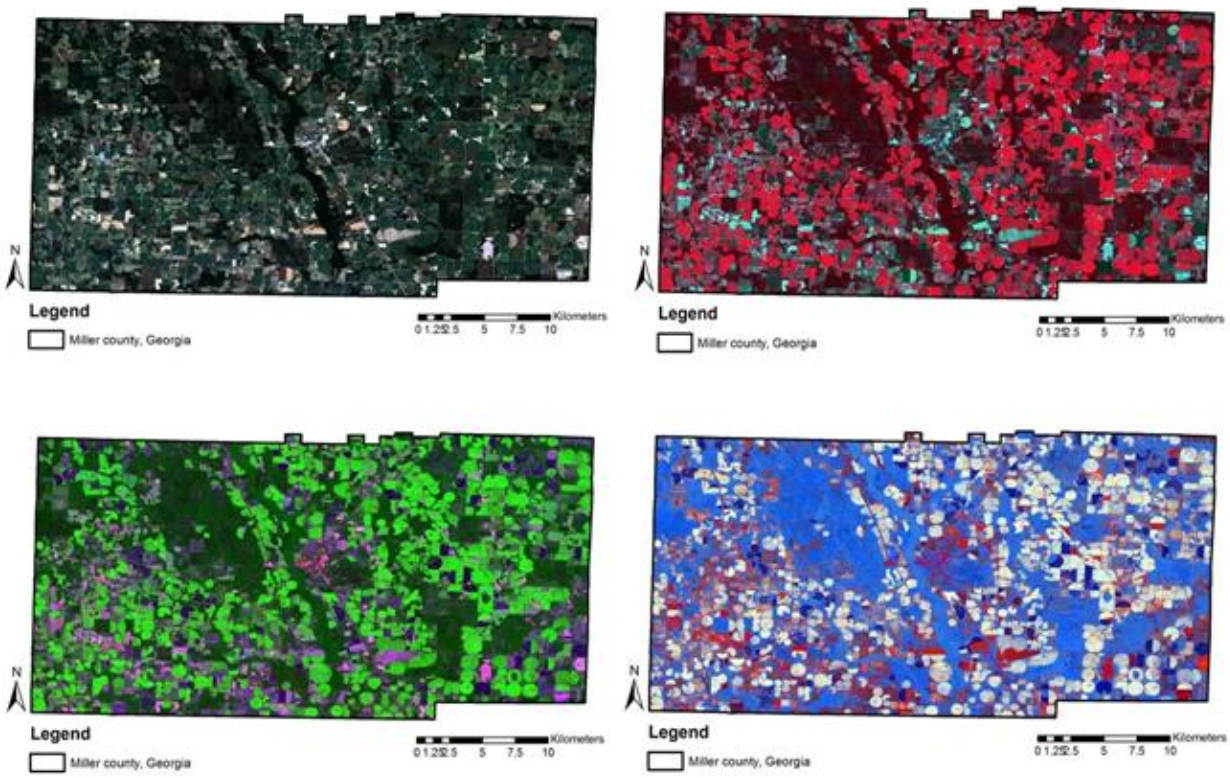

Figure 2.2: Natural, False, and Brightness, Wetness and Greenness (BWG) tasseled cap composites of Miller Country, Georgia, USA

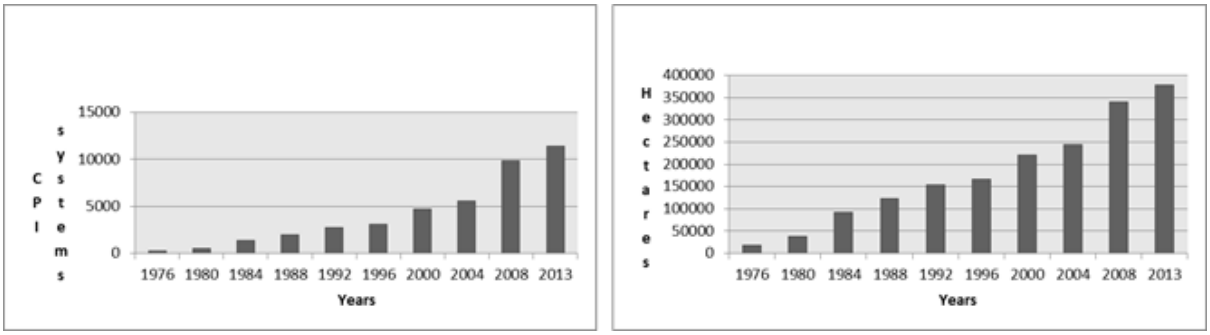

Figure 2.3: Total center pivot systems and acreage irrigated (hectares)

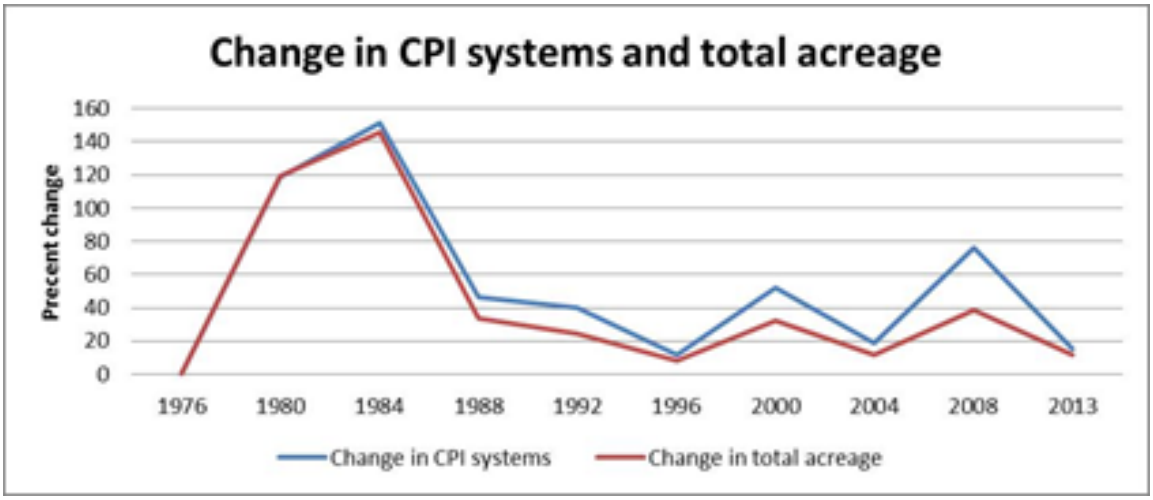

Figure 2.4: Percent change in center pivot irrigation systems (blue) and total acreage (red).

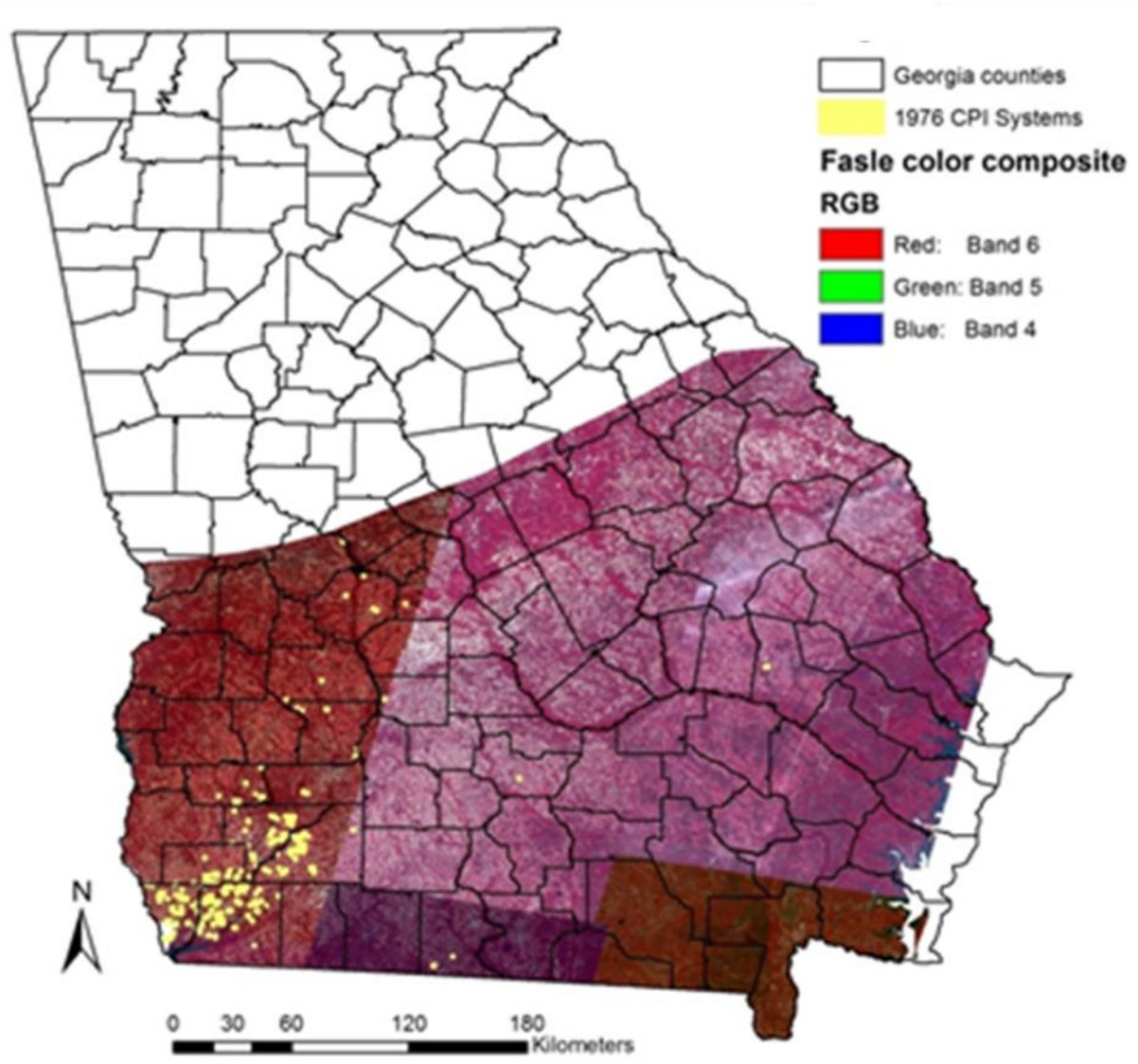

Figure 2.5: Map of 1976 CPI systems overlaid on a Landsat false color composite. The variations in the hue are due to the composite pulling from scenes from different dates.

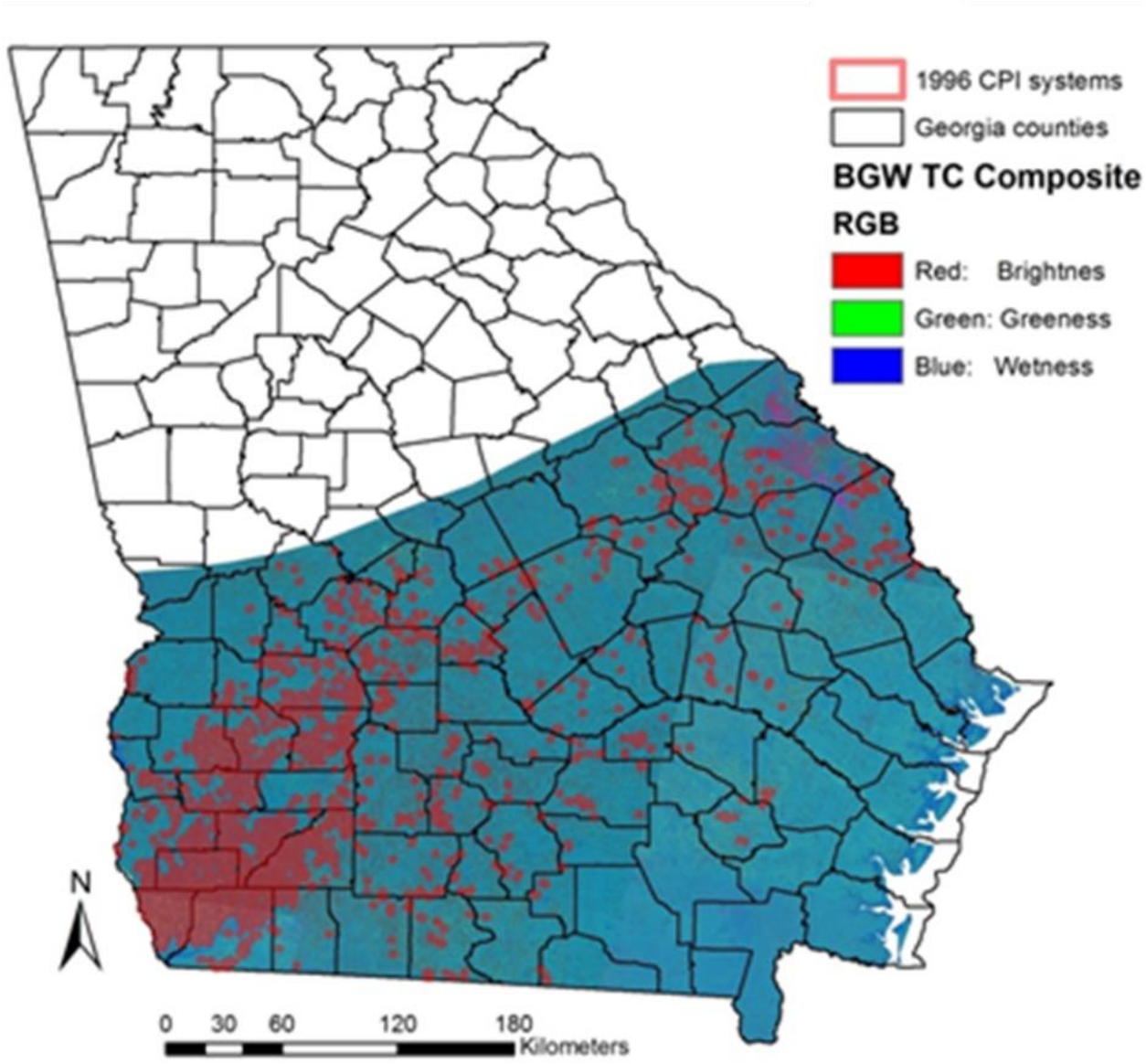

Figure 2.6: Map of 1996 CPI systems overlaid on a Landsat composite of tasseled cap indices.

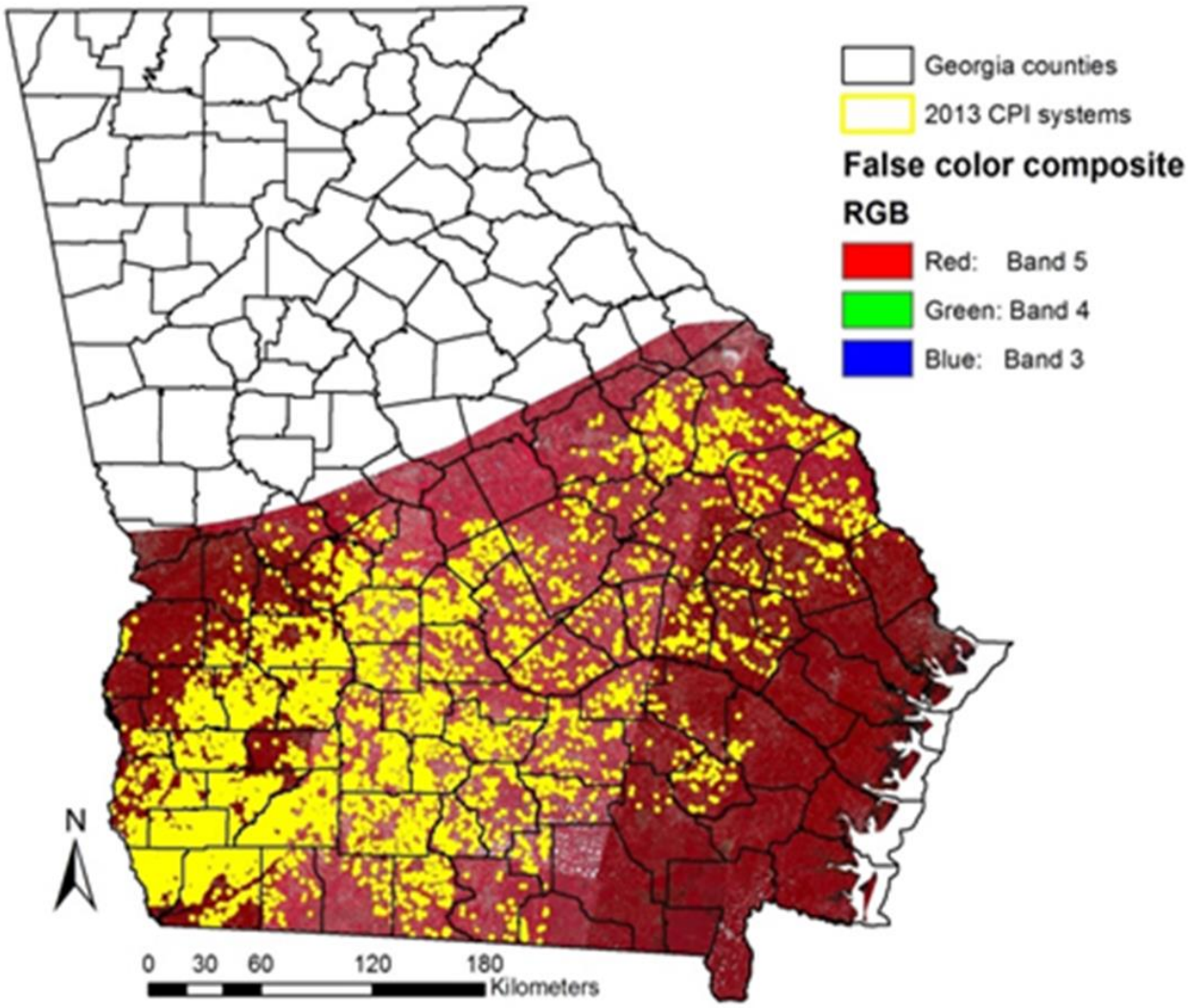

Figure 2.7: Map of 2013 CPI systems overlaid on Landsat false color composite.

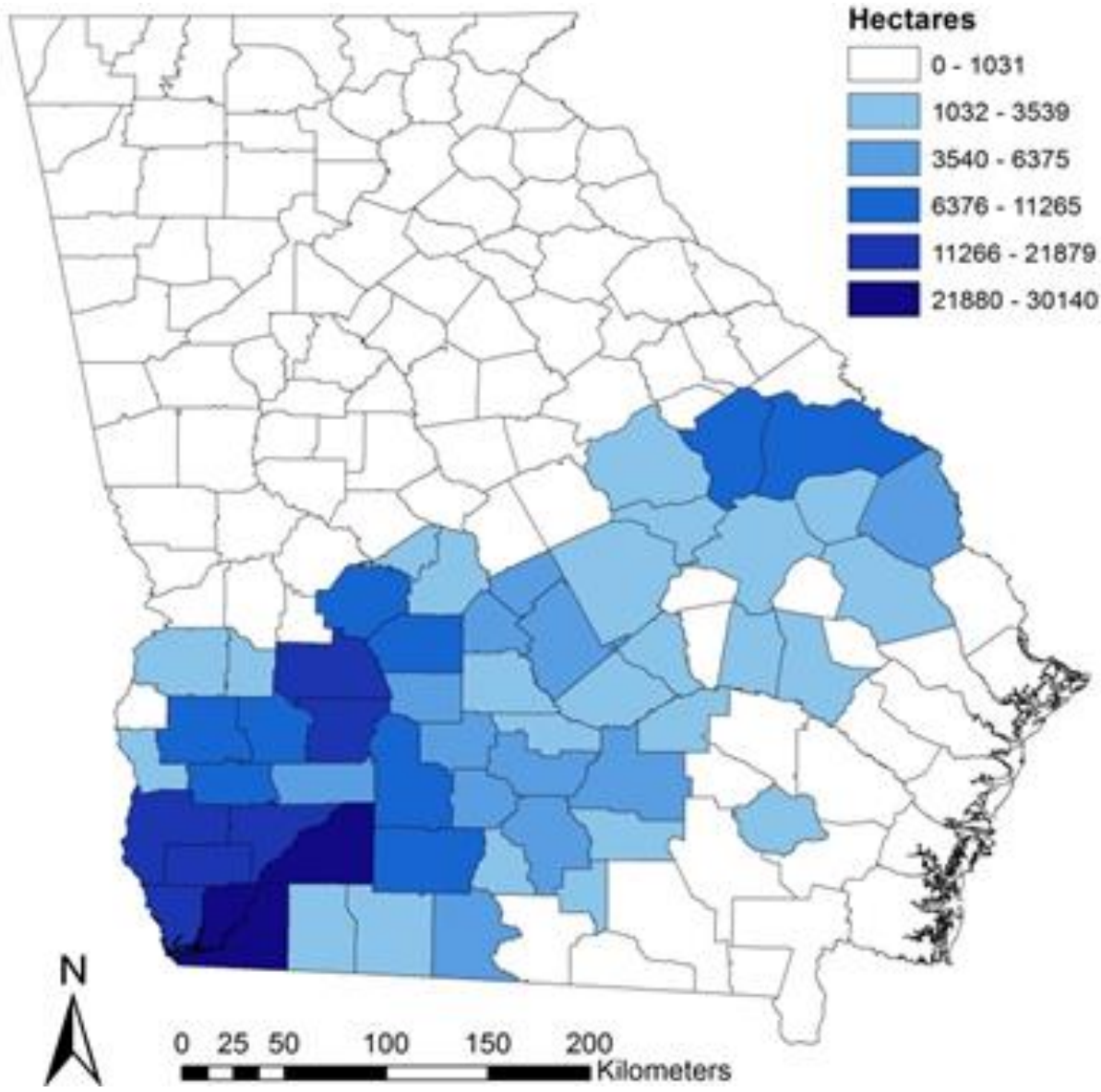

Figure 2.8 County breakdown of total hectares irrigated for 2013

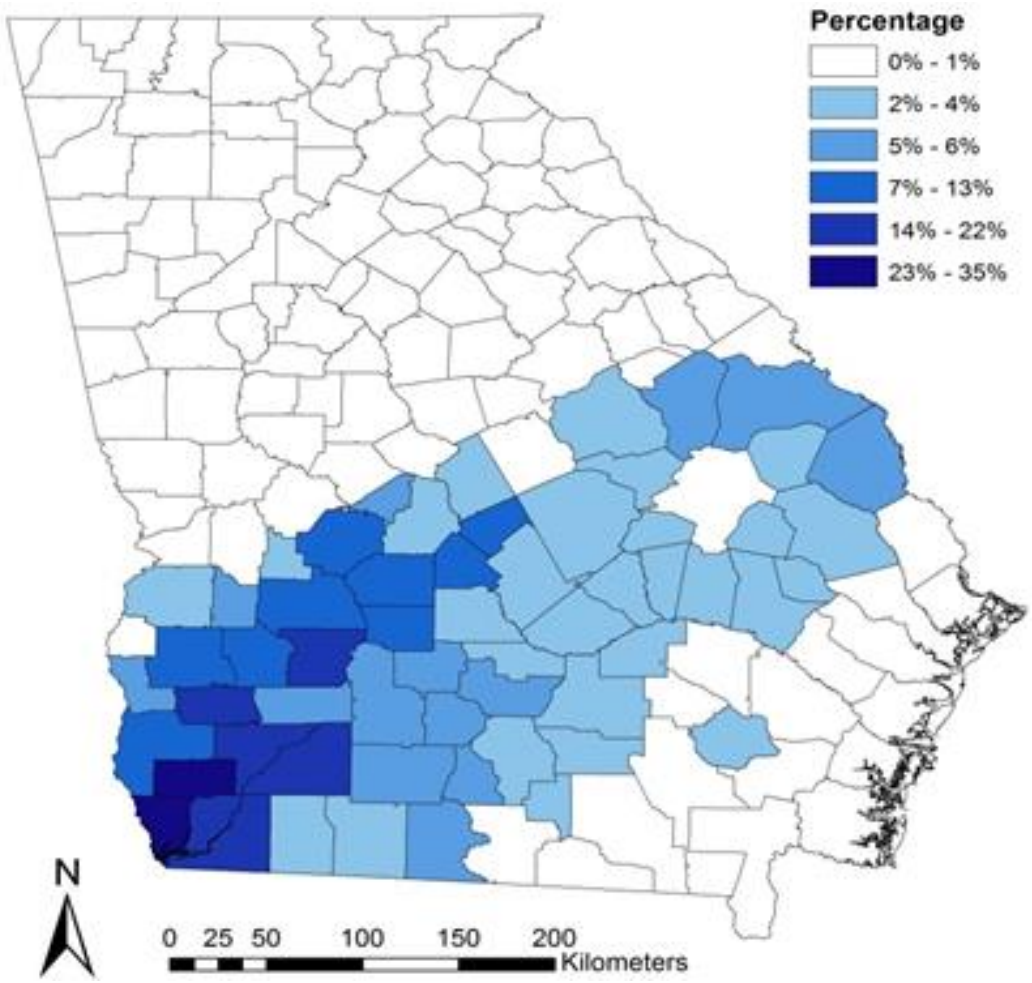

Figure 2.9 County breakdown of percent of total land area irrigated for 2013

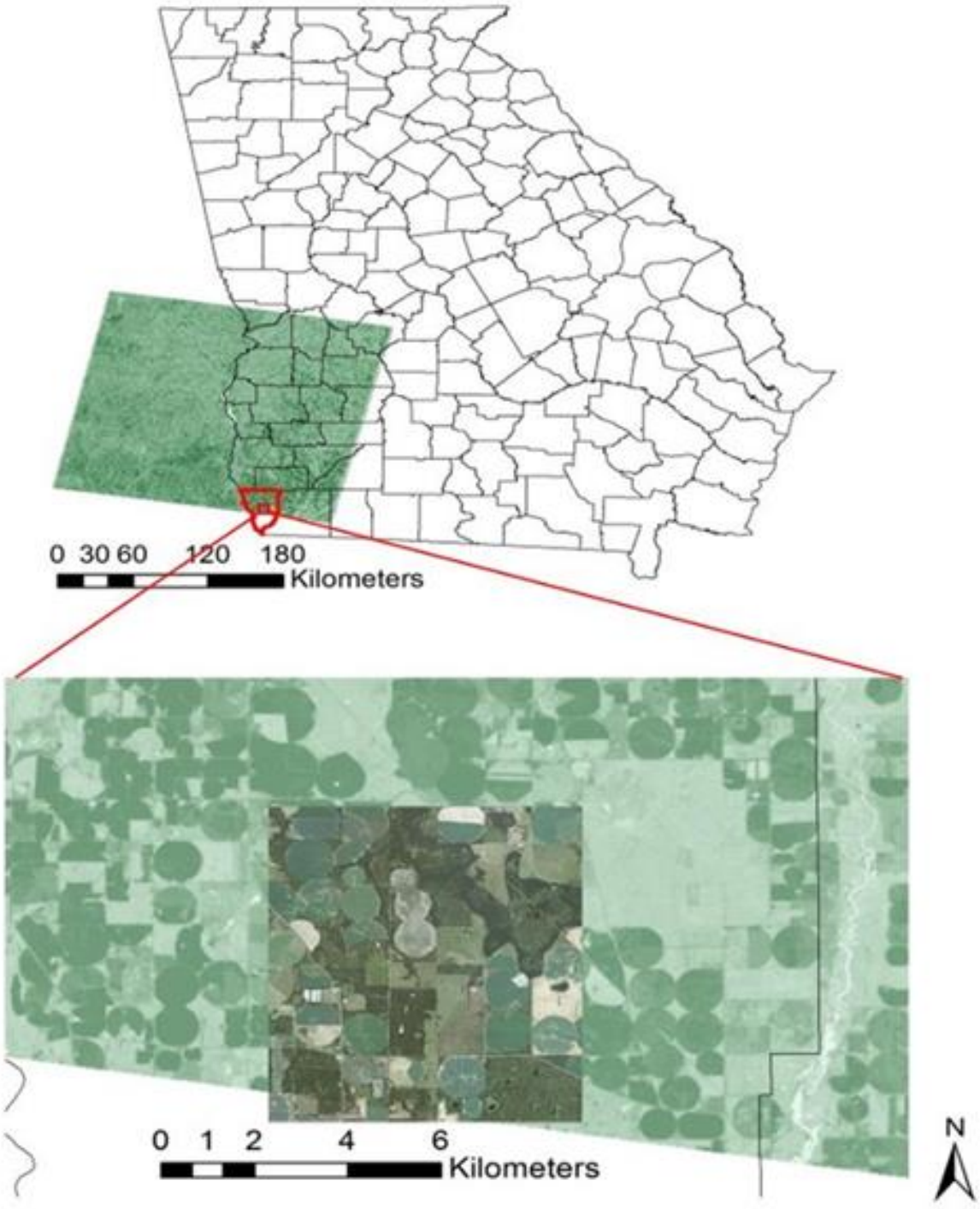

Figure 2.10 Map of NAIP imagery compared to a Landsat scene.

3) COMPARISON OF DEW POINT TEMPERATURE ESTIMATION METHODS IN SOUTHWESTERN GEORGIA

Williams et al., 2015: Comparison of Dew Point Temperature Estimation Methods in Southwestern Georgia. *Physical Geography*, in press, DOI:10.1080/02723646.2015.1011554

Abstract

Recent upward trends in acres irrigated in the United States have been linked to increasing low level surface moisture. Unfortunately, stations with dew point data for monitoring low-level moisture are sparse. Thus, models that estimate dew points from more readily observed data sources are useful. Daily average dew temperatures were estimated and evaluated at 14 stations in southwest Georgia using linear regression models and artificial neural networks. Estimation methods were drawn from simple and readily available meteorological observations, therefore only temperature and precipitation were considered as input variables. The 14 weather stations were equally partitioned into seven training stations and seven independent stations. In total three linear regression models and 27 artificial neural networks (ANN) were analyzed for the 14 sites. The two methods were evaluated using root mean square error, mean absolute error, the Pearson's correlation coefficient, the Index of Agreement, and the Coefficient of Efficiency to assess the skill of the estimation methods. Both methods produced adequate estimates of daily averaged dew point temperatures, with the artificial neural network displaying the best overall skill. Both methods displayed optimal performance for warmer dew point temperatures and showed poorer skill estimating lower dew point temperatures. The depredated skill for low dew point values is likely due to the small sample of observations around the lower dew point ranges. On average the ANN reduced root mean square error by 6.86% and mean absolute error by 8.30% when compared to the best performing linear regression model.

3.1 Introduction and Literature Review

Changing land cover can have important effects on local climate (Pielke et al. 2002, Shepherd et al. 2002, Marshall et al. 2004, Mahmood et al. 2013). The state of the land cover directly influences how incoming solar radiation is partitioned into other energy budget terms, such as sensible and latent heat. Agriculture is a predominate form of land cover, accounting for nearly 18 million km^2 (Ramankutty et al. 2006), or roughly 40% of the global land cover (Foley, 2005). Agricultural land cover is expected to increase with projected rises in population and the growing demand for biofuel production (Evans and Cohen 2009). While some agricultural landscapes rely on natural precipitation for irrigation, there has been rapid growth towards artificially irrigated landscapes (Harrison 2001, Tillman 2001). This introduction of water at the surface has the ability to change the low level near surface moisture content (Ferguson and Maxwell 2011). Increased low level moisture has been linked to the 1995 and 1999 Midwestern heat waves (Changnon et al 2003). Hot humid weather can cause heat stress in humans (Gaffen and Ross 1998), increasing their chances of experiencing heat related morbidity or mortality (Bently and Stallins 2003, Lipmann et al., 2013). It is difficult to assess these postulated changes in moisture content because of the lack of sufficient data outside of first order observation stations. Thus, there is a need to model and estimate low level moisture from readily available meteorological data.

Early methods for estimating low level moisture involved using daily minimum temperature as a proxy for dew point temperature. This assumption is not always valid if there are large diurnal variations in dew point temperature and if minimum temperature stays well

above dew point temperature (Kimball et al. 1997). Kimball et al. (1997) used annual precipitation, potential evapotranspiration, mean daily net solar radiation, as well as temperature (maximum, minimum, and mean) to produce a more accurate assessment of daily dew point temperature across the United States and Alaska, primarily at first order observation stations. Hubbard et al. (2003) expanded on the efforts of Kimball and evaluated an additional four regression equations for the Northern Great Plains in the United States. The goal of their study was to produce a dew point temperature estimation method that required less complex input data than Kimball et al. (1997). They wanted to take advantage of meteorological data provided by the National Weather Service Cooperative (NWS Coop) weather stations. Their analysis found that a combination of maximum (Tx), minimum (Tn), and mean (Tm) temperature are the best estimators for daily dew point temperature. An alternative method for estimating low level moisture is through artificial neural networks (ANN). Jain et al. (2008) estimated evapotranspiration (ET) using an ANN from limited input variables. Their estimation model included hourly temperature, dew point, sunshine radiation, wind speed, and humidity in Reynolds Creek Experimental Watershed. Shank et al. (2008) developed ANN models to predict dew point temperature at two hour intervals, up to 12 hours in advance. Their methods incorporated dew point temperature, relative humidity, vapor pressure, wind speed, and solar radiation from the Georgia Environmental Automated Monitoring Network (GEAMN) to develop and train the ANN.

The purpose of this study is to estimate daily dew point temperature using linear regression models and an ANN for portions of Southwest Georgia using daily meteorological data, an

understudied area that has undergone rapid agricultural expansion since the 1970s (Harrison 2001). This study aims to give insight into which meteorological variables sufficiently estimate dew point temperature in the analysis region. A secondary objective is to evaluate the performance of the linear regression models in an area outside of the Great Plains to determine if there are any differences in the variables needed to successfully estimate dew point temperature. Southwest Georgia experiences a higher amount of annual precipitation than the Great Plains and also suffers from less continentality (Rohli and Vega 2008). Precipitation could be an important factor in estimating daily dew point, as the highest dew point ever recorded in the United States was partly caused by heavy rains the morning of the event (NWS WFO Grand Forks, ND). Shank et al (year?) gave insight as to how an ANN performed in the region from an error standpoint, but their analysis included observed dew point temperatures as an input variable. This study analyzes a different geographic location from Hubbard et al. (2003) and focuses on a smaller spatial extent than Kimball et al. (1997). The ANN analysis is not aided by the inclusion of dew point temperature or any moisture parameter because the focus is on producing a daily estimate versus a prediction. Qualitative comparisons of the performance of the two estimation techniques are assessed from an error standpoint. The development of a valid estimation technique is a vital step in the goal of characterizing the influence of irrigation on climate in the study region. This region has experienced rapid growth in acres irrigated (Harrison 2001), but little is known about the influence of irrigation on the climate. This research will provide a tool to answer the question about the impact of irrigation in the region. Section 3.2 will provide a description of the data and methodology applied which entails a breakdown of the linear

regression and ANN models. This is followed by the results and discussion section, where the performance of each method is evaluated, and then the conclusion.

3.2 Data and Methodology

Data

The dataset used in this study is the Georgia Automated Environmental Monitoring Network (GEAMN, Hoogenboom 2000). The GAEMN, established in 1991, is maintained by the University of Georgia and has a 1s temporal resolution that is aggregated into 15 minute averages or totals. There are over 75 stations in the network throughout Georgia that record weather variables including air temperature, relative humidity, vapor pressure, wind speed and direction, and solar radiation. Dew point temperature is calculated from the collected variables. This study uses daily aggregates of maximum and minimum temperature, precipitation, and dew point.

Linear Regression

The regression equations are adapted from Hubbard et al. 2003, hereafter referred to as H03. H03 was developed using station data in the Great Plains region. The analysis herein employed three out of the five total regression equations developed by H03. The equations used are as follows:

H03 Method 1: $T_d = \propto(T_n) + \beta(T_x - T_n) + \gamma$ (1)

H03 Method 3: $T_d = \propto(T_m) + \beta(T_n) + \gamma(T_x - T_n) + \lambda$ (2)

H03 Method 4: $〚 T〛_d = \propto(T_n) + \beta(T_x - T_n) + \gamma(P_{daily}) + \lambda$ (3)

Where Dew point temperature, Tx, Tn, Tm, and Pdaily are the daily dew point temperature; maximum, minimum, and mean daily temperature; and daily precipitation, respectively. The coefficients of the regression equations are represented by ∝,β,and, β, and λ. Figure 3.1 shows the GEAMN stations used in this study. The stations labeled in blue represent the stations used in the development of the regression models and the stations labeled in red represent the independent stations. Method 1 (eqn. 1) uses minimum temperature and the diurnal temperature range (DTR) to estimate dew point. Method 3 (eqn. 2) includes the mean temperature in addition to the minimum temperature and the DTR. Method 4 (eqn. 3) uses minimum temperature, DTR, and daily precipitation to estimate daily dew point temperature.

Different configurations of precipitation were also included in equation 3, in place of the P_daily variable, to determine if there was any improvement in model skill. The different configurations include three, five, and seven day totals and averages. The different configurations of precipitation showed no improved model skill, so P_daily is the primary configuration of precipitation used in the analysis.

To determine the coefficients for the regression models and to evaluate the initial performance of the regression models, a subset of seven stations with the longest continuous period of record within the region (Figure 2.1, blue) is selected. The data from the seven stations are aggregated to determine the coefficients only, and then each station is analyzed on an individual basis. The performances of the three models are evaluated for each station before

choosing the best model to perform test on independent data not used in model training. The independent stations in the analysis (figure 2.1, red) are not used in the development of the model coefficients or in the initial estimates of the model performance. The model evaluation parameters presented in this analysis are selected to ensure a robust viewpoint of possible error and biases, and to avoid solely relying on correlation parameters as high correlations can be achieved by poor models (Legates and McCabe, 1999). The three models are evaluated using the root mean square error (RMSE), the mean absolute error (MAE), the Pearson's correlation coefficient (R), the Index of Agreement (d), and the Coefficient of Efficiency (E). Readers are encouraged to review Legates and McCabe (1999) for a detailed overview of the d and E model validation statistics. As previously stated, a single set of coefficients is developed from a combination of the seven developmental stations. The decision to merge the data sets is made to ensure the models can adequately estimate dew point temperatures for varying climatic regimes within the region.

Artificial Neural Network

The ANN used in this study is a feed-forward multilayer perceptron (algorithm) with one hidden layer using sigmoid activation functions and trained using back-propagation as implemented in pyBrain version 0.3.1 (Schaul et al. 2010) with python programming language version 2.7.3. The basic network design is shown in Figure 2. A number of potential networks were evaluated. These networks differ in the number of input variables and the number of processing nodes in the hidden layer. Inputs to the network include minimum temperature, temperature range, and 0 to 5 days of antecedent precipitation. A constant bias input node with a

value of unity is also included. The number of nodes in the hidden layer varies from a minimum of two to a maximum equal to the number of inputs for the network (up to eight). In total, 27 ANNs are evaluated. Data for ANN training and testing are partitioned in an identical manner to the regression models.

3.3 Results and Discussion

Linear Regression

The three methods performed comparably from an error and model evaluation standpoint. The RMSE, MAE, R, d, and E values were only separated by hundredths for all three models for all stations within the training data set. The Pearson's correlation coefficient (R), d, and E all indicate improved performance when they are closer to unity. Overall, Method 4 had the lowest errors and the highest model evaluation statistics. This was a different result from H03, as Equation 2 in our analysis was their best performing method. As expected, their analysis region has a different climatic regime from our analysis region. This result shows that daily precipitation is an important factor in estimating daily dew point values. As a refresher Equation 3 incorporated minimum temperature, the difference between maximum and minimum temperature and the addition of daily precipitation. The equation with included coefficients is as follows:

$$T_d = 1.00681512(T_n) + 0.17912155(T_x - T_n) + 0.05591049(P_{daily}) - 1.789463 \quad (4)$$

The results of the model evaluation and error statistics are displayed in tables one through three. For most of the stations in the developmental dataset, the R, and d statistics were nearly identical

amongst the three methods. For most stations R ranged from 0.94 to 0.96. The only noticeable variation was in the RMSE, MAE, and the E statistic. This speaks to the robustness of the equations developed by H03. From a physical standpoint, Method 4 accounts for the relationship between dew point and minimum temperature (Hubbard et al., 2003), the diurnal temperature range is indicative of the moisture content of an air mass (H03). The inclusion of precipitation captures the partitioning of energy to latent heating, especially in the summer months when the atmospheric demand for water is highest.

We observed some biases in the models at high and low dew points. This result was present in all three methods, although only Equation 3 is shown here. This is captured in the scatter plot of estimated and observed dew point values from the Arlington automated weather station (Figure 2.3). Figure 2.3 shows a greater tendency for the model to underestimate values on the low end of dew point spectrum. Arlington is used as a representative station because it has the lowest RMSE and MAE for the selected method. Other stations are expected to perform comparably to the Arlington station. There is also a tendency for the overestimation of dew point at the high end. Even with the discrepancies mentioned above, Equation 3 does an adequate job of capturing the observed variability. The overall performance of the model is adequate as well, as approximately 85% of the estimated values are within 3°C of the observed values (fig. 2.4).

Since the method that included precipitation performed the best, it was a natural inquiry to see if different variations of precipitation improved the skill of the model. The underlying premise of this hypothesis is to analyze whether there is a “soil moisture memory” component to the estimation of dew point, as modeling studies suggest that wet soils are thought to influence

ET rates, thus influencing the dew point temperature (Dirmeyer et al. 2009, Dirmeyer et al., 2012, Koster and Suarez, 2000). To test this theory, three, five, and seven day totals and averages were added in place of the daily precipitation. It was also required to develop a new set of coefficients for each variation of precipitation tested. It is possible that the additional days of precipitation were a poor fit for the regression equations as additional precipitation information slightly degraded the model performance when compared to the regression model with daily precipitation (table 2.5).

The model performance was evaluated on an annual basis. This measure was taken to ensure a robust model performance, capable of handling a wide array of climatic conditions. Essentially, the model will be applied when irrigation rates are at their highest, the growing season (April – September). During the growing season, the model displays an improved skill and has an optimal performance during this period. This was tested by developing a set of coefficients for October to November for all years. The coefficients of the growing season data set are then applied to the Arlington training station. The growing season regression model reduced the RMSE and the MAE by 17% (table 2.5).

Artificial Neural Network

The first step in applying an ANN to the problem of estimating dew point temperature is to determine the combination of inputs and hidden nodes that provide the best performance. The number of inputs is dependent upon the number of day's worth of precipitation data we wish to include in the analysis and ranges from zero to five. Other inputs included in all networks are

minimum temperature, temperature range and a constant bias neuron whose value is always equal to unity. There is no formula for determining the optimal number of nodes in the hidden layer of a network. It is generally suggested that the number of hidden nodes should be between the number of inputs and the number of outputs (Heaton 2013). For this study we will test networks with number of hidden nodes ranging from 2 to the number of inputs.

Figure 2.5 shows how number of inputs and hidden nodes affected network performance as expressed by mean absolute and root mean square errors for 27 different networks. Examining the figure from left to right, the first network (3_2) relies on only minimum temperature and temperature range to determine dew point. Addition of an additional hidden node (3_3) allows the network to better fit the data. Addition of the current days precipitation (4_2) allows for further improvement in the network performance. Expanding the network beyond 4 inputs and 2 hidden nodes did not lead to an appreciable improvement in network performance. For the remainder of the study the ANN architecture used is that of four inputs (minimum temperature, temperature range, daily precipitation and a constant) with two hidden nodes.

Overall the ANN outperformed the regression methods of H03 as shown in table 2.6 for the training data and table 2.7 for the validation data. For all stations the ANN displayed lower error values and was equal to or better on the other performance metrics as well. Direct comparison between the ANN and H03 equation 3 shows that on average the ANN reduced RMSE by 6.86% and MAE by 8.30% (table 2.8). One area where the ANN offered little improvement is for low dew point temperatures (Figure 6). For dew points in the 20°- 30° C range, the ANN has an absolute error within 2° C of the observed for 90% of the cases and 60% of the time the error is

1° C. However, performance for the lower end of the dew point spectrum drops off quickly. When the dew points are between 0°-10° C, only 50% of cases are within 2° of the observed dew point and only 24% within 1° C. Fortunately, the growing season of southwest Georgia is characterized by dew point values in the range where the ANN estimates are most accurate. Note that the ANN was not retrained using only growing season data as was done for the regression model

3.4 Conclusion

The overarching goal of this study was to develop a daily dew point estimation method adapted for southwest Georgia. An estimation method is needed because of the poor availability of long term dew point observations in the region. It was also desired to make the estimation draw from readily available temperature and precipitation observation from NWS COOP stations in the region. The linear regression equations developed by H03 were adapted and applied to our region of interest. Three of the five methods used in H03 were used here, with H03 Equation 3 performing the best from an error standpoint. It is reasonable to believe that Equation 3 can be generalized across the southeast. On average, H03 Equation 3 performed equal to, or better in all five measures of performance for the training stations (tables 2.1-2.3). It was shown that the model performs best during the growing season, when irrigation rates are at their highest, and that additional precipitation information actually degrades model performance. An artificial neural network (ANN) is also employed to estimate dew point.

Seven automated weather stations from the GEAMN were selected to train and validate each the estimation model for each technique. On an annual basis the ANN performed best, only

bettered by the growing season version of the regression model. A growing season only version of the ANN was not tested, and is something that can be explored in the future to see if there is any improvement in the skill of its estimation. Each technique tested performed adequately for the region and should be able to assist in a retroactive analysis in dew point estimation in the study region. Estimating dew point from limited meteorological variables has been successfully demonstrated in the Great Plains region, and now in southwest Georgia. This gives confidence into the validity of dew point estimates derived from other variables, which can be applied to construct dew point climatology for data poor regions. The next chapter of this dissertation applies the estimation method developed here to study the influence of agricultural irrigation in the region by evaluating changes in dew point. This analysis also presents the ability to investigate and assess historical trends in dew point temperatures outside of first order station, which would be the first analyses to date.

3.5 References

Adegoke, J. O., Pielke, R. A., Eastman, J., Mahmood, R., & Hubbard, K. G. (2003). Impact of Irrigation on Midsummer Surface Fluxes and Temperature under Dry Synoptic Conditions: A Regional Atmospheric Model Study of the U.S. High Plains. *Monthly Weather Review*, *131*(3), 556-564.

Harrison, K. A. (Director) (2001, March 26). Agricultural Trends in Irrigation. *Proceedings of the 2001 Georgia Water Resources Conference*. Lecture conducted from Institute of Ecology, Athens.

Bentley, M. L., & Stallins, J. A. (2008). Synoptic evolution of Midwestern US extreme dew

point events. *International Journal of Climatology*, *28*(9), 1213-1225.

Changnon, D., Sandstrom, M., & Schaffer, C. (2003). Relating changes in agricultural practices to increasing dew points in extreme Chicago heat waves. *Climate Research*, *24*, 243-254.

Deangelis, A., Dominguez, F., Fan, Y., Robock, A., Kustu, M. D., & Robinson, D. (2010). Evidence of enhanced precipitation due to irrigation over the Great Plains of the United States. *Journal of Geophysical Research*, *115*(D15), 1-14.

Dirmeyer, P. A., Schlosser, C. A., & Brubaker, K. L. (2009). Precipitation, Recycling, and Land Memory: An Integrated Analysis. *Journal of Hydrometeorology*, *10*(1), 278-288.

Dirmeyer, P. A., Jin, E. K., Kinter, J. L., Cash, B. A., Manganello, J., Huang, B., et al. (2012). Evidence for Enhanced Landâ€“Atmosphere Feedback in a Warming Climate. *Journal of Hydrometeorology*, *13*(3), 981-995.

Evans, J. M., & Cohen, M. J. (2009). Regional water resource implications of bioethanol production in the Southeastern United States. *Global Change Biology*, *15*(9), 2261-2273.

Foley, J. A. (2005). Global Consequences Of Land Use. *Science*, *309*(5734), 570-574.

Gaffen, D. J., & Ross, R. J. (1998). Increased summertime heat stress in the US. *Nature*, *396*, 529-530.

Heaton, J. (2013). *Introduction to Neural Networks for Java* (2 ed.). Chesterfield, MO: Heaton Research Inc.

Hoogenboom, G. (2000). The Georgia automated environmental monitoring network. *Preprints of The 24th Conference on Agricultural and Forest Meteorology*, *24*, 24-25.

Hubbard, K., Mahmood, R., & Carlson, C. (2003). Estimating daily dew point temperature for the northern great plains using maximum and minimum temperature. *Agronomy Journal*, *95*, 323-328.

Jain, S. K., Nayak, P. C., & Sudheer, K. P. (2008). Models For Estimating Evapotranspiration Using Artificial Neural Networks, And Their Physical Interpretation. *Hydrological Processes*, *22*(13), 2225-2234.

Kimball, J., Running, S., & Nemani, R. (1997). An Improved Method For Estimating Surface Humidity From Daily Minimum Temperature. *Agricultural and Forest Meteorology*, *85*(1-2), 87-98.

Koster, R. D., & Suarez, M. J. (2001). Soil Moisture Memory in Climate Models. *Journal of Hydrometeorology*, *2*(6), 558-570.

Legates, D., & Jr., G. M. (1999). Evaluationg the use of "goodness-of-fit" measures in hydrologic and hydroclimatic model validation. *American Geophysical Union*, *35*(1), 233-241.

Li, B., McClendon, R., & Hoogenboom, G. (2004). Spatial Interpolation of weather variables for single locations using artificial neural networks. *Transactions of the ASAE*, *47*(2), 629-637.

Lippmann, S. J., Fuhrmann, C. M., Waller, A. E., & Richardson, D. B. (2013). Ambient temperature and emergency department visits for heat-related illness in North Carolina, 2007â€“2008. *Environmental Research*, *124*, 35-42.

Lippmann, S. J., Fuhrmann, C. M., Waller, A. E., & Richardson, D. B. (2013). Ambient

temperature and emergency department visits for heat-related illness in North Carolina, 2007â€“2008. *Environmental Research*, *124*, 35-42.

Mahmood, R., Nair, U., Gameda, S., Hale, R., Carleton, A. M., Mcalpine, C., et al. (2013). Land cover changes and their biogeophysical effects on climate. *International Journal of Climatology*, *1*, 1-25.

Marshall, C. H., Pielke, R. A., Steyaert, L. T., & Willard, D. A. (2004). The Impact of Anthropogenic Land-Cover Change on the Florida Peninsula Sea Breezes and Warm Season Sensible Weather. *Monthly Weather Review*, *132*(1), 28-52.

Pielke, R. A., Marland, G., Betts, R. A., Chase, T. N., Eastman, J. L., Niles, J. O., et al. (2002). The influence of land-use change and landscape dynamics on the climate system: relevance to climate-change policy beyond the radiative effect of greenhouse gases. *Philosophical Transactions of the Royal Society A: Mathematical, Physical and Engineering Sciences*, *360*(1797), 1705-1719.

Rohli, R. V., & Vega, A. J. (2008). *Climatology*. Sudbury, Mass.: Jones and Bartlett Publishers.

Sandstrom, M., Lauritsen, R., & Changnon, D. (2004). A Central-U.S. Summer Extreme Dew-Point Climatology (1949-2000). *Physical Geography*, *25*(3), 191-207.

Schaul, T., Bayer, J., Wierstra, D., Sun, Y., Felder, M., Sehnke, F., et al. (2010). PyBrain. *The Journal of Machine Learning Research*, *11*, 743-746.

Shank, D., McClendon, R., Paz, J., & Hoogenboom, G. (2008). Ensemble Artificial Neural Networks for prediction of dew point temperature. *Applied Artificial Intelligence*, *22*, 523-542.

Shepherd, J. M., Pierce, H., & Negri, A. J. (2002). Rainfall Modification by Major Urban Areas: Observations from Spaceborne Rain Radar on the TRMM Satellite. *Journal of Applied Meteorology*, *41*(7), 689-701.

Tilman, D. (2001). Forecasting Agriculturally Driven Global Environmental Change. *Science*, *292*(5515), 281-284.

Webmaster, F. (2008, June 10). Hottest Place On Earth?. *NWSFO Grand Forks, ND*. Retrieved June 21, 2014, from http://www.crh.noaa.gov/news/display_cmsstory.php?wfo=fgf&storyid=71074&source=2

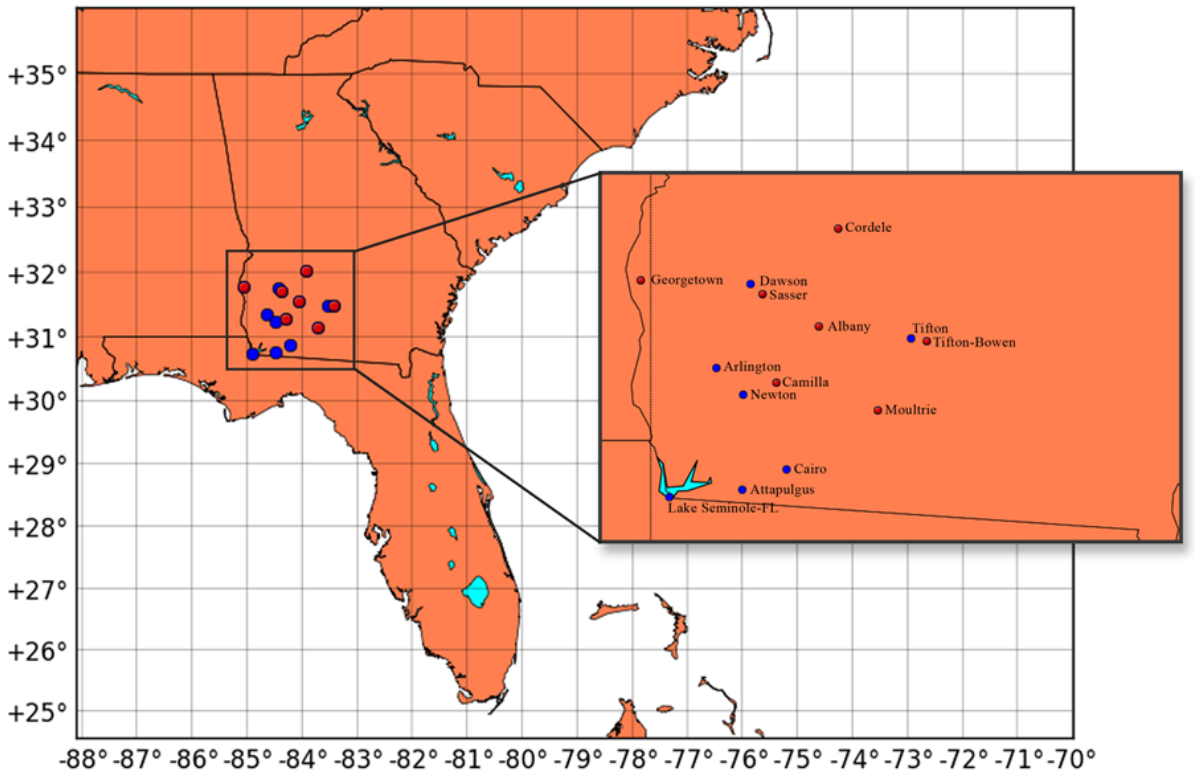

Figure 3.1 Map of stations used in development of the regression models (blue) and testing of the regression models (red)

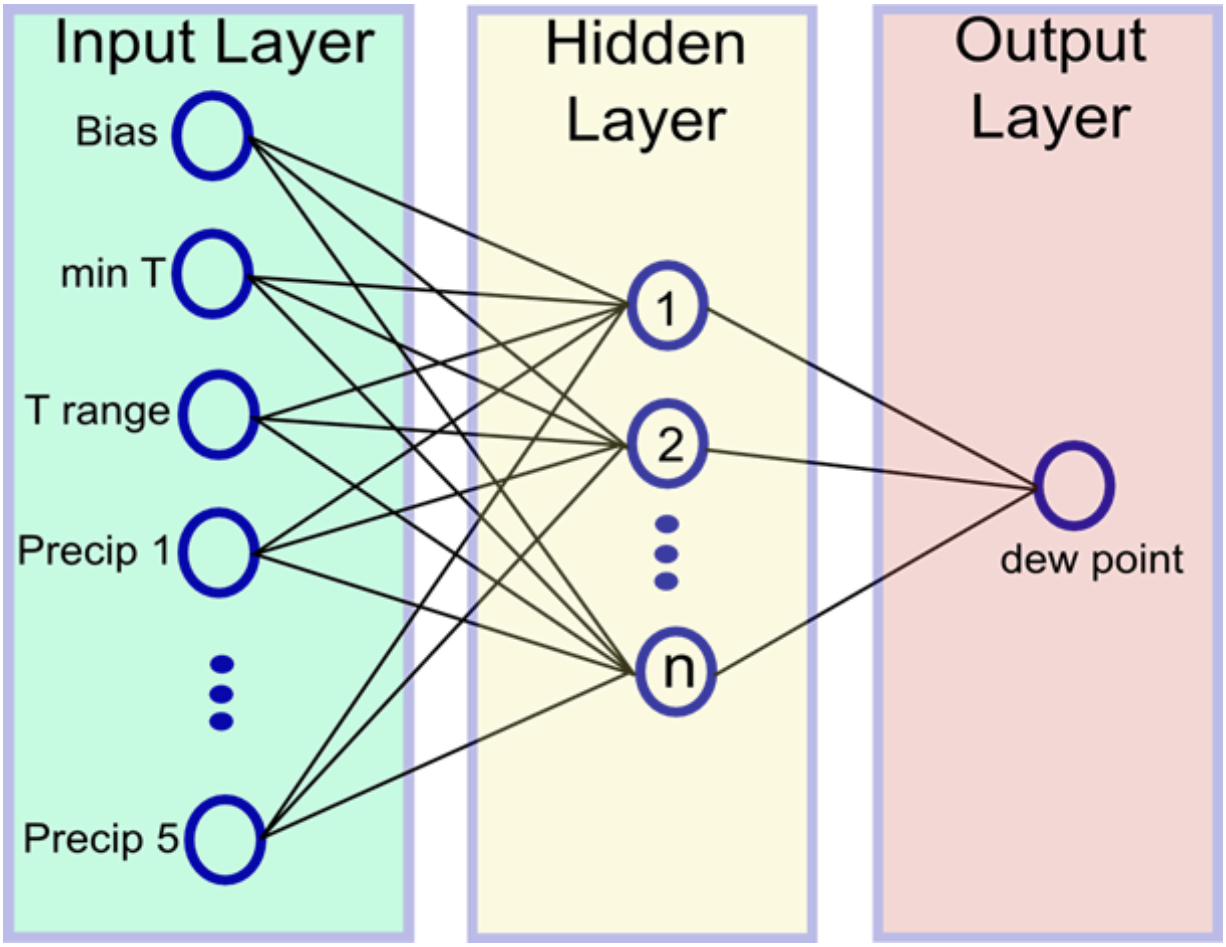

Figure 3.2 Basic network design of the ANN. This ANN is a feed-forward multilayer perceptron with one hidden layer using sigmoid activation functions and trained using back-propagation. The ANN consists of an input layer, a hidden layer, and an output layer.

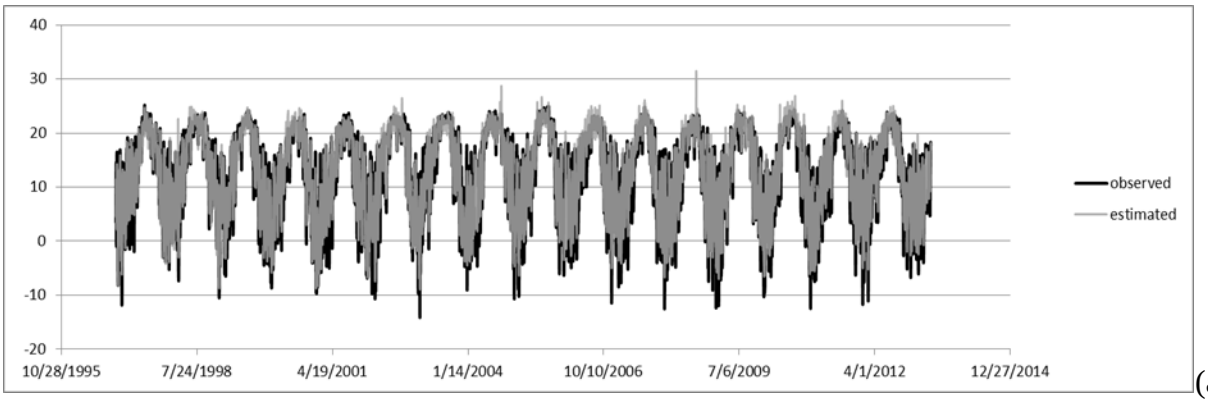

(a)

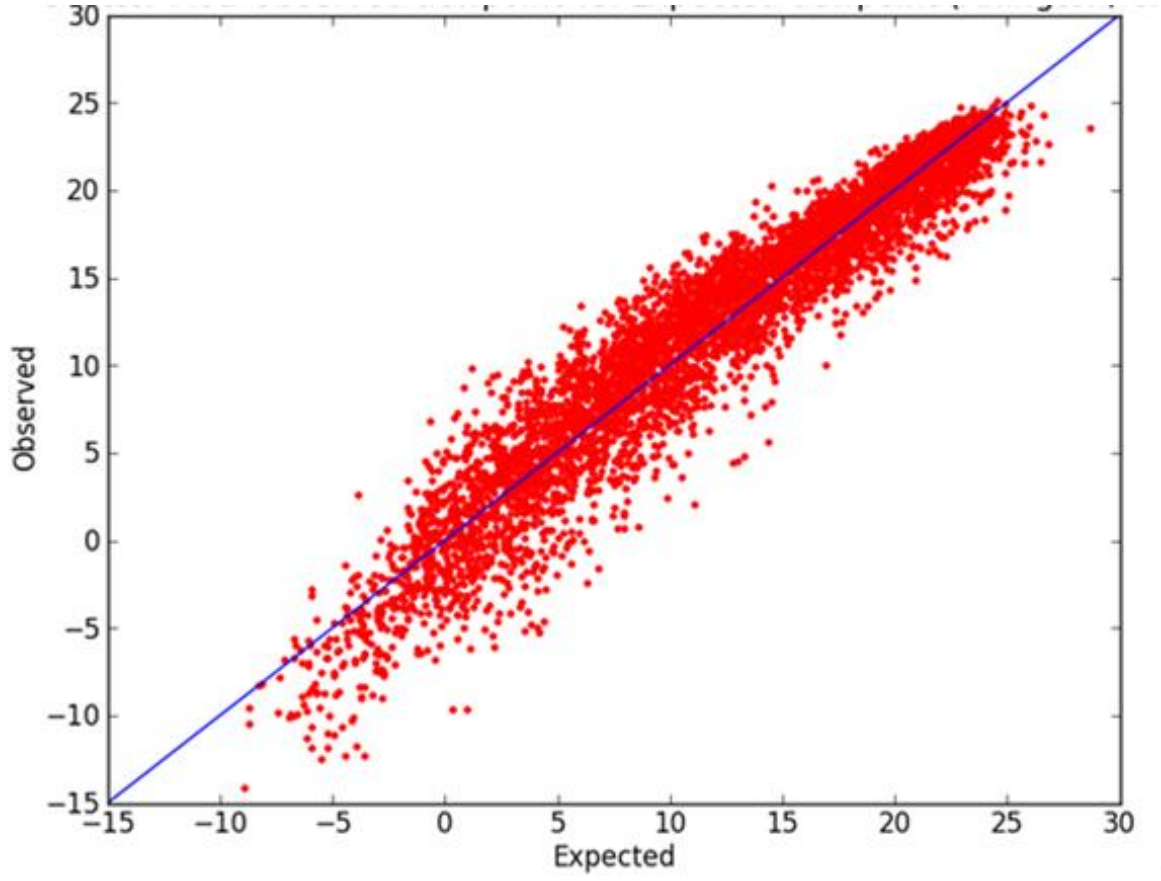

(b)

Figure 3.3(a) Time series of observed and estimated dew point temperatures of H03 Equation 3 for Arlington automated weather station. The black line represents observed values and the grey line represents the estimated values. The x-axis represents the date and the y-axis represents temperature in degrees Celsius. (b) Observed versus Estimated scatter plot for Arlington GEAMN station. The x-axis and y-axis are shown in degrees Celsius.

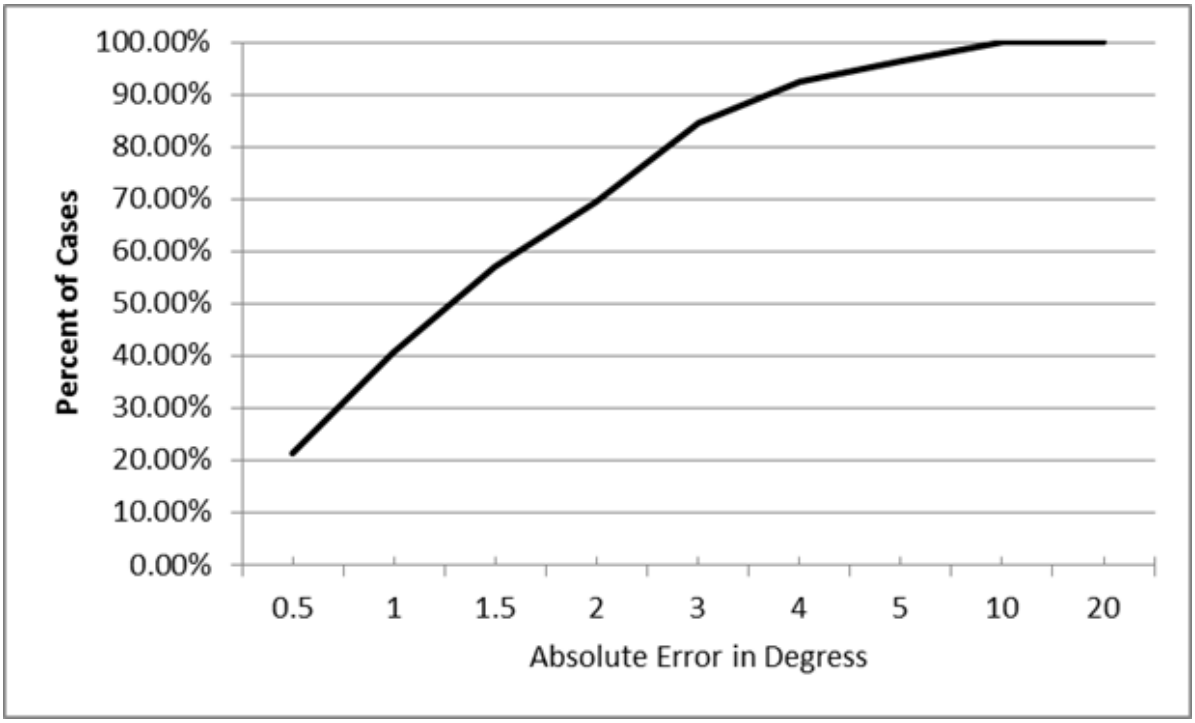

Figure 3.4 Performance of Equation 3 for the Arlington automated weather station. The x-axis represents the absolute error in degrees and the y-axis represents the percent of cases associated with the corresponding error.

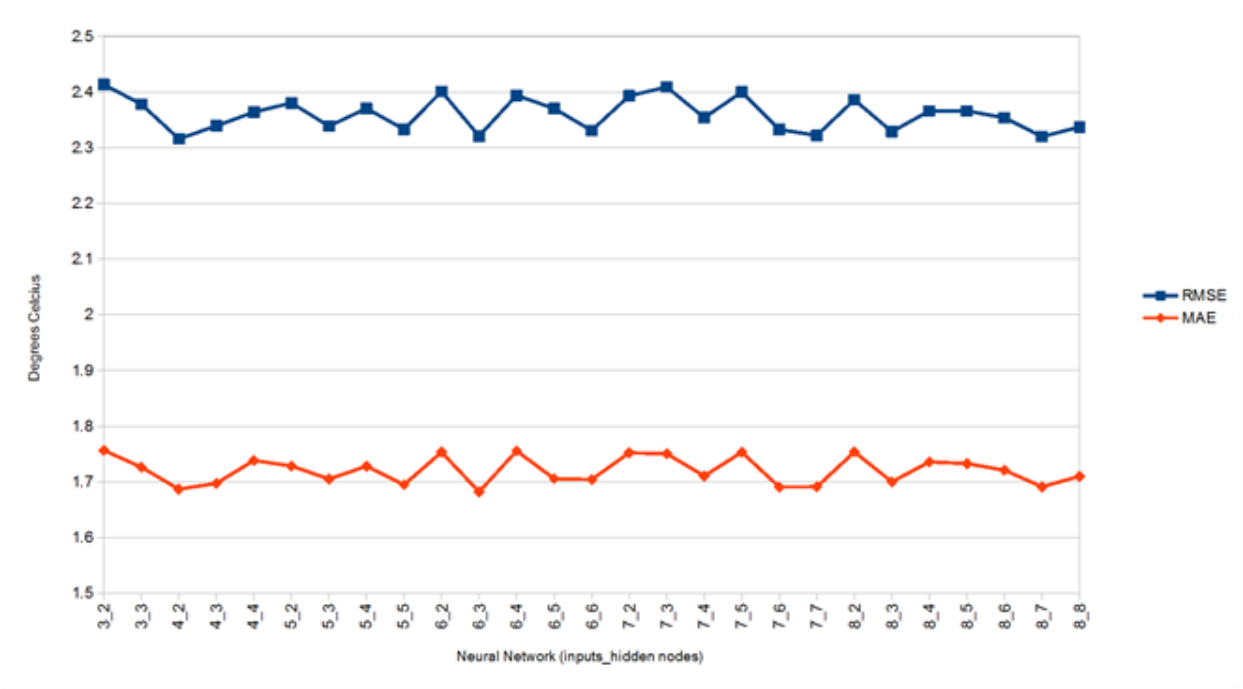

Figure 3.5 Performance comparison of various neural network architectures for dew point estimation. Network architectures are given on x axis and are defined by the number of input and hidden nodes: 3_2 represents a network with 3 inputs and 2 hidden nodes.

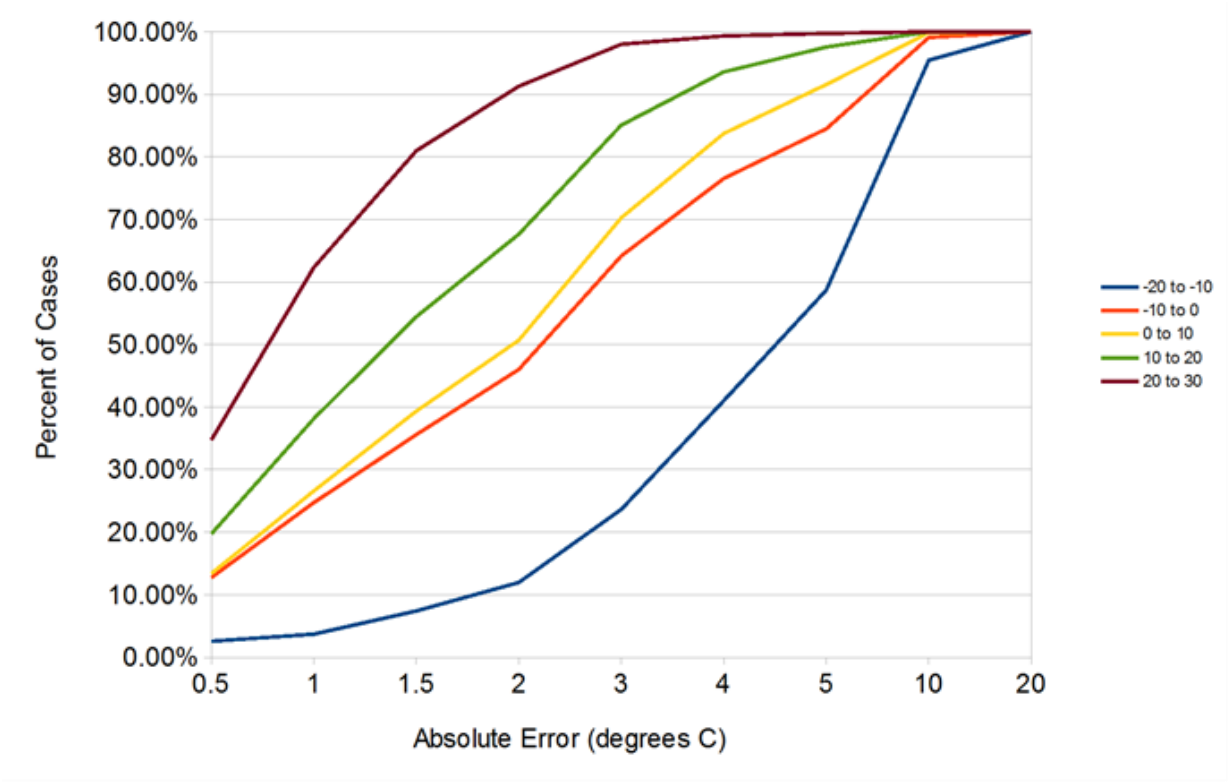

Figure 3.6 Performance of the ANN represented as a percentage for varying dew point temperature ranges. The x-axis represents the absolute error in degrees and the y-axis represents the percent of cases for the given absolute error.

	RMSE	MAE	R	D	E
Arlington	2.25	1.69	0.96	0.98	0.92
Attapulgus	2.68	1.99	0.95	0.97	0.89
Cairo	2.4	1.77	0.95	0.98	0.91
Dawson	2.8	1.91	0.94	0.97	0.89
Newton	2.31	1.7	0.96	0.98	0.92
Sneads	2.57	1.82	0.94	0.97	0.88
Tifton	2.58	1.94	0.95	0.97	0.91
Average	**2.51**	**1.83**	**0.95**	**0.97**	**0.9**

Table 3-1 Error and model evaluation statistics of Equation 1 for the individual stations. The coefficients for the regression equation are derived from a merged data set containing data from all seven stations listed below. The model

evaluation parameters are root mean square error (RSME), mean absolute error (MAE), Pearson's correlation coefficient (R), index of agreement (D) and the coefficient of efficiency (E).

	RMSE	MAE	R	D	E
Arlington	2.24	1.73	0.96	0.98	0.92
Attapulgus	2.65	1.99	0.95	0.97	0.9
Cairo	2.38	1.78	0.96	0.98	0.91
Dawson	2.69	1.93	0.95	0.97	0.9
Newton	2.31	1.74	0.96	0.98	0.92
Sneads	2.54	1.81	0.94	0.97	0.89
Tifton	2.59	1.98	0.95	0.97	0.91
Average	**2.48**	**1.85**	**0.95**	**0.97**	**0.9**

Table 3-2 Same as Table 1, except for Equation 2.

	RMSE	MAE	R	D	E
Arlington	2.2	1.65	0.96	0.98	0.93
Attapulgus	2.62	1.95	0.95	0.97	0.9
Cairo	2.33	1.72	0.96	0.98	0.92
Dawson	2.72	1.87	0.95	0.97	0.9
Newton	2.26	1.67	0.96	0.98	0.93
Sneads	2.52	1.79	0.94	0.97	0.89
Tifton	2.52	1.91	0.96	0.97	0.91
Average	**2.45**	**1.79**	**0.95**	**0.97**	**0.91**

Table 3-3 Same as Table 1, except for Equation 3.

	RSME	MAE	R	D	E
Albany	2.9	2.21	0.95	0.97	0.88
Cordele	2.46	1.87	0.96	0.98	0.91
Georgetowr	2.43	1.83	0.96	0.98	0.91
Moultrie	2.35	1.72	0.96	0.97	0.9
Sasser	2.5	1.86	0.96	0.97	0.9
Tifton-Bowe	2.44	1.83	0.96	0.97	0.9
Average	**2.51**	**1.88**	**0.95**	**0.97**	**0.9**

Table 3-4 Error and model evaluation statistics for the independent stations using Equation 3.

	RMSE	MAE	R	D	E
Growing	1.82	1.37	0.96	0.98	0.91
Daily Precip	2.2	1.65	0.96	0.98	0.93
3 day precip	2.29	1.74	0.96	0.98	0.92
Average	**2.1**	**1.58**	**0.96**	**0.98**	**0.92**

Table 3-5 Error and model evaluation for Arlington during the growing season, daily precipitation, and three day precipitation using H03 Method 4.

	RMSE	MAE	R	D	E
Arlington	2.08	1.57	0.97	0.98	0.93
Attapulgus	2.55	1.88	0.95	0.97	0.9
Cairo	2.22	1.59	0.96	0.98	0.92
Dawson	2.36	1.72	0.96	0.98	0.92
Newton	2.13	1.58	0.97	0.98	0.93
Sneads	2.46	1.71	0.95	0.97	0.9
Tifton	2.35	1.77	0.96	0.98	0.92
Average	2.31	1.69	0.96	0.98	0.92

Table 3-6 Error and model evaluation statistics of the ANN for the individual stations.

	RMSE	MAE	R	D	E
Albany	2.7	2.01	0.96	0.97	0.9
Cordele	2.26	1.68	0.96	0.98	0.92
Georgetowr	2.24	1.67	0.96	0.98	0.93
Moultrie	2.25	1.67	0.96	0.98	0.92
Sasser	2.27	1.66	0.97	0.98	0.93
Tifton-Bowe	2.32	1.68	0.96	0.98	0.92
Average	**2.34**	**1.73**	**0.96**	**0.98**	**0.92**

Table 3-7 Same as table 6, except for independent stations.

	Neural Network		Regression		Precent Improvement	
	RMSE	MAE	RMSE	MAE	RMSE	MAE
Albany	2.7	2.01	2.9	2.21	6.85%	8.92%
Cordele	2.26	1.68	2.46	1.87	8.04%	10.11%
Georgetowr	2.24	1.67	2.43	1.83	7.74%	8.61%
Moultrie	2.25	1.67	2.35	1.72	4.24%	2.93%
Sasser	2.27	1.66	2.5	1.86	9.33%	10.79%
Tifton-Bowe	2.32	1.68	2.44	1.83	4.99%	8.44%
Average	**2.34**	**1.73**	**2.51**	**1.89**	**6.86%**	**8.30%**

Table 3-8 Comparison of RMSE and MAE for Equation 3 and the ANN for the independent stations.

4) INTEREPOCHAL CHANGES IN TEMPERATURE, HUMIDITY, AND PRECIPITATION ASSOCIATED WITH INCREASING IRRIGATION IN THE GEORGIA COASTAL PLAIN

Abstract

Through the introduction of increased near surface moisture, artificial irrigation has the potential to have a significant impact on temperatures and precipitation locally. Using National Weather Service Cooperative Network Observation station daily temperature and precipitation data at 19 stations in the Georgia Coastal Plain from 1938 to 2013, this study explores the possibility that irrigation has modified the hydroclimate through changes in temperature, humidity and precipitation. Dew point temperatures are calculated by a dew point estimation method developed by Williams et al., (2015). Dew point temperatures are used as a measure of humidity in this analysis. The data are divided into consecutive epochs (1938-1975 and 1976-2013) that represent pre- and post-irrigated land cover in the Georgia Coastal Plain. Interepochal differences in monthly average minimum and maximum temperature, dew point temperatures, and average total precipitation are explored. Some stations displayed a significant increase in temperatures during the post irrigation period, and there was a region wide decrease in April precipitation during the post irrigation epoch.

4.1 Introduction and Literature Review

In 2013, there were approximately 324 million ha equipped for irrigation worldwide, with the United States accounting for 26.4 million ha (Food and Agriculture Organization, 2014). In the United States, nearly half of water used for irrigation is drawn from groundwater resources (FAO, 2014). This removal of water from groundwater storage onto the surface creates a disruption in the hydrologic cycle. Artificial irrigation is an anthropogenic disturbance to the land surface. Much like urbanization, irrigation has the ability to modify the surface energy budget, cloud cover, local circulation patterns and consequently, the hydrologic cycle. There is a critical need to quantify the impacts of irrigation on the land surface and the resultant impact on the coupled climate system.

Observation and modeling evidence has found that irrigation reduces air temperature and increases humidity via the repartitioning of latent heat flux and sensible heat flux (Moore and Rojstaczer 2002; Adegoke et al. 2003, 2007; Douglas et al. 2006; Bonfils and Lobell 2007; DeAngelis et al. 2010; Kueppers and Snyder 2012; Sridhar 2013). If an irrigated area is large enough, secondary circulations can develop within adjacent unirrigated areas (Segal et al. 1998, Douglas et al. 2009, Shukla et al., 2013). The primary modifications to the hydrologic cycle and surface energy budget caused by irrigation include altering the Bowen ratio (ratio between sensible and latent heating) and enhancing precipitation down wind of irrigated areas often in lieu of decreasing precipitation over irrigated regions/areas (Pei et al. 2016). Agricultural expansion and increased irrigation has been attributed to second-order health hazards. For example, Chagnon et al. (2003) attributed increased agricultural irrigation, which produced

anomalously high dew point values, to extreme heat waves in the Chicago area. Fatalities associated with heat waves often occur at night, due to higher than normal daily minimum temperatures that prevent the body from cooling. Higher dew point temperatures impact the amount minimum temperatures cool.

Georgia, particularly the Coastal Plain region, has experienced rapid growth in irrigated area. Although Georgia receives an adequate amount of annual precipitation, the uncertainty in the spatial distribution of rainfall results in irrigation being favored to sustain profitable crop production (Salazar et al. 2012). Geographic analysis of the irrigated acreage in the Coastal Plain region found the area equipped for irrigation increased 2000% from 1976 until 2013 (Williams et al., 2016, in review). The impacts of irrigation on the climate of Georgia are underrepresented in peer reviewed literature. Misra et al. (2012) was one of the first studies to address the impact of irrigation on climate in the region, and their analysis found that irrigation had a meaningful impact on summer minimum temperature trends in Georgia. Using model simulations to evaluate the impact of irrigation on climate in the United States, Pei et al. (2016) found that evaporated irrigation water from the High Plains region is transported to the lower Midwest and parts of the Southeast. Their analysis did not mention the Southeast as a source of irrigation-induced climate change. Georgia has been classified as an area of sporadic irrigation compared to more densely irrigated regions of the United States (Pervez and Brown, 2010) and that could explain the lack of peer-reviewed literature. Georgia is outside of the top ten states in total acres irrigated, and those states combined accounted for 71 percent of the total acres irrigated (Fig. 4.1; USDA, 2012). It is postulated that the impacts of irrigation are localized, and these local changes are not

of interest to many of the large scale studies on irrigation and climate. These local changes in land cover, however, are important and need quantification in the context of other climate forcings such as urbanization, aerosols and greenhouse gasses.

The research conducted in this chapter is concerned with the following questions: (1) has change in irrigation intensity in the region effected the hydroclimate, (2) if so, what variable is impacted most, and (3) what time of year are changes most pronounced?. It is hypothesized that changes in intensity have altered the hydroclimate in the region and it is expected that minimum temperatures or dew point temperatures are impacted most. Since summer (June, July, August) is when irrigation application rates are the highest, it is expected that the greatest change is seen during the summer months. This analysis is done by comparing epochal differences in average maximum, minimum, and dew point temperatures as well as average total precipitation at select stations in the region. The spatial extent of irrigated acreage of Georgia is not as large as some regions in the United States, so our analysis determines if the impacts to the hydroclimate are localized or if there is a region wide response. The following section briefly describes the data and methods used for this analysis. An analysis of the results is then presented, followed by concluding remarks.

4.2 Data and Methods

Data from a total of 19 National Weather Service Cooperative (NWS Coop) observation stations were analyzed to identify and detect changes in hydro-climatic variables in the Georgia Coastal Plain (Figure 4.2). The NWS Coop data set provides daily maximum and minimum temperature, 24 hour precipitation totals, and snowfall observations. For the study of interest,

only temperature and precipitation observations were analyzed from the NWS Coop stations. Specially, average minimum, maximum, dew point temperatures and average total precipitation were analyzed. The study employed data from unadjusted NWS Coop stations in lieu of the often used biased corrected United States Historical Climatology Network (USHCN) data set. This choice was made for two primary reasons: 1) the desire to preform analysis on raw, daily data that did not undergo any bias correction; and 2) it was critical to include the maximum amount of stations in our analysis and it is known that there are a limited amount of stations that qualify for the criteria set forth by the USHCN data set. Detailed information on the method for calculating dew point temperatures can be found in Williams et al. (2015).

The daily observations for maximum and minimum temperature, dew point temperatures, and 24 hour total precipitation were aggregated to monthly values. Once the monthly values are calculated, they are then broken into two equal 38-year epochs. Epochal analysis has been established as an accepted method to investigate climatological changes (Diem and Mote, 2005; Zhao and Shepherd, 2012). The two epochs are defined as a pre-irrigation epoch (1938 – 1975) and a post-irrigation epoch (1976-2013). All stations analyzed did not contain data for the entire 76-year period, so some epochs are truncated or adjusted depending on the availability of data. Differences between the two epochs are calculated for each month, as well as differences for boreal summer, the growing season (April – September) and boreal winter. An independent t-test with equal variances was employed to determine if there was a significant difference between the two epochs. The epochs in this analysis correspond to a mapped time series of irrigation in the Georgia Coastal Plain (Williams et al. 2016). In this study, 1976 is considered the genesis of

irrigation and 2013 serves as the final date of mapped irrigated acres based on prior analyses of areas equipped for irrigation in the Georgia Coastal Plain.

4.3 Results

Herein, differences in temperature and precipitation between the pre- and post-irrigation epochs are discussed. For clarity, decreases or increases in a variable refer to changes in the post irrigation epoch. When comparing the pre-irrigation epoch to the post-irrigation epoch, it was expected that summer and growing season would display the greatest differences. Physically, irrigation increases moisture in the lower levels of the atmosphere resulting in increased latent heating and decreased sensible heating. Evapotranspiration increases locally and often this evaporated water from irrigation falls as precipitation down wind of irrigated regions. Irrigation starts during the growing season and reaches its peak intensity during boreal summer (June, July, and August). During these seasons it is hypothesized that minimum and dew point temperatures would increase, maximum temperatures would decrease, and there would be an increase or reduction in summer precipitation during the post irrigation epoch due to the physical reasons mentioned above. To test the significance in the differences in temperature in precipitation between the two regimes, the student t-test was employed.

Temperature

Pre-irrigation minimum temperatures were generally warmer in the region, outside of June, July, August, and November (Fig. 4.3). The increase in June, July and August lead to a cumulative summer increase in minimum temperatures as the mean summer minimum temperature increased from 20.1°C during the pre-irrigation epoch to 20.3°C during the post

irrigation epoch. A subset of eight stations had statistically significant ($\alpha = .05$) increases in minimum temperatures during the post irrigation epoch. Those stations were Alma, Colquitt, Cordele, Glennville, Fitzgerald, Moultrie, Thomasville, and Tifton. The increase in post irrigation generally occurred in July and August, with two stations also showing an increase in June minimum temperatures. Those stations were Alma and Colquitt. Averaging the pre and post irrigation minimum temperatures for these eight stations; increases of 0.46°C, 0.72°C, 0.55°C, and 0.92°C were found in June, July, August, and November respectively. It is possible that the average of the subset of stations strongly influences the trend summer temperatures when all stations are averaged. There were four additional stations were summer minimum temperatures increased, but the decrease was not statistically significant. Figure 4.4 shows the monthly and seasonal differences between the two subsets of stations. Noted is an increase in November post irrigation minimum temperatures, but this increase was statistically significant at only the Alma and Thomasville locations

Pre-irrigation dew point temperatures were also generally higher in the region. Several stations showed a statistically significant decrease in dew point temperatures. Many of the decreases were found in times that were likely outside of the influence of irrigation. Figure 4.5 shows that pre-irrigation dew point temperatures were higher in all months except for June, July, August, and November. A similar pattern was found in minimum temperatures. There was a subset of six stations where dew point temperatures increased during the post irrigation epoch. Those stations were Alma, Colquitt, Cordele, Moultrie, Thomasville, and Tifton. All six stations displayed an increase in July, August and cumulative summer post irrigation dew point

temperatures. Additional increases were found in March (Alma), June (Alma and Colquitt), November (Alma and Thomasville), and growing season (Alma).

Maximum temperatures were higher during the pre-irrigation epoch for all months except March and November (Fig. 4.6). Decreased maximum temperatures were expected at the six stations that saw increases in minimum and dew point temperatures, but decreases in maximum temperatures were not confined to those six stations in particular. The largest interepochal differences were found in January and August. Maximum temperatures decreased by 1.39°C during the post irrigation epoch, with 10 of the 19 stations showing a statistically significant decrease in maximum temperatures. The average decrease in August maximum temperatures were 1.6°C with only three stations displaying a statistically significant difference. Average July maximum temperatures decreased by 0.96°C, but surprisingly there was not a single station where a significant change in July maximum temperatures was found. There were more stations, five total, that showed increased July maximum temperatures during the post irrigation epoch. Speculatively, there appears to be confounding factors outside of irrigation influencing maximum temperatures in the stations analyzed. One such factor may be the amount of urban area around a particular station. The results here are comparable to other areas where irrigation has increased, and agree with trends found in Misra et al. (2012), although included here are stations that were not in their analysis.

Precipitation

There was a region wide response in decreased precipitation in April during the post irrigation epoch (Fig. 4.8). Stations in closer proximity to irrigation displayed a decrease in July precipitation although the decrease was not always significant ($p = .05$). The decreases were usually contained within the months of April and July although a few stations saw decreases in May. A secondary and less robust response was an increase in January and November precipitation. Blakely, Georgia had a decrease in July average total precipitation of 40.7 millimeters (mm), which was the largest July decrease of any of the stations found. On average, the decrease in July average total precipitation was 17.54 mm. The station in Blakely had an 8-year period of missing values which could lead to a spurious decrease in precipitation in the post-irrigation epoch. There was not a single station that showed an increase in post-irrigation precipitation during the summer months. This could potentially imply that there is a net loss of water in the region when considering the decrease in precipitation and the loss of water through increased evapotranspiration. There was a widespread decrease in April average total precipitation. This response occurred in several stations and was not confined to the subset of six stations that showed increased minimum and dew point temperatures. The largest decrease in April precipitation during the post irrigation epoch, which was 50 mm, occurred in Thomasville, Georgia. The average decrease in post-irrigation April precipitation was 26.43 mm. The change in April precipitation is not likely due to increased irrigation as April is the onset of the growing season and likely the initial start of irrigation in the region. This result is important because it has implications on the irrigation trends in the future. During their analysis in estimating the water use trends for growing maize in Georgia, Salazar et al. (2012) found the seasonal irrigation

demand showed that there was an increasing trend in the amount of irrigation required from the beginning of the season in March (10.3 mm) to the mid-season in May with an average of 79.2 mm. The increase of irrigation required for the early spring period corresponds with the significant decrease in average total precipitation in April.

4.4 Discussion

Availability of quality long-term stations in the densely irrigated areas was an issue. Of the 19 stations that were analyzed, only three stations were in the most densely irrigated portion of the state. One of those stations, the Blakely, Georgia location, had an 8-9 year period in the 1990s when observations were not available. These missing data could potentially skew the differences found between the two regions. The counties with the highest total land area used for irrigation, Seminole County and Decatur County, did not have any stations with reliable long-term observations. There were only a total of five stations where minimum and dew point temperatures showed the expected response to increasing irrigation. Those stations were Alma, Colquitt, Cordele, Moultrie, and Tifton. These stations all had a statistically significant increase in June, July, and August average minimum and dew point temperatures.

Two locations of interest are Albany and Camilla. They share close proximity to the subset of six stations identified in the previous section, but their response to increased irrigation differed. Figure 4.9 shows the location of the station in Albany and its proximity to center pivot irrigation (CPI systems). Locally, there are few CPI systems around the station and irrigation density as a whole is sporadic. Minimum, dew point, and maximum average temperatures (Figure 4.10) decreased during the post-irrigation epoch outside of the summer months. During

the summer months, the magnitude of the difference between the two epochs decreased and there were no significant differences ($p = .05$). The Camilla, GA (Fig 4.11) location saw a decrease in average minimum and dew point temperatures in the summer months (Fig 4.12) during the post-irrigation epoch but the differences were not significant. Camilla was one of the few stations with significant decreases in post irrigation June and August maximum temperature. It is possible that the response to increased irrigation impacts maximum temperatures more than any other variable. It appears that the climatic response to increased irrigation is damped at this location by other climate forcings such as urbanization.

The Alma, GA location is included in the subset of six stations that saw increased minimum and dew point temperatures during the post irrigation epoch. This result was unexpected as it was not in an area intensely irrigated as the other five. Statistically significant increases during the post irrigation epoch in minimum and dew point temperatures were found in March, June, July, August, and November. There were no significant changes in average maximum temperature. These changes could be due to factors not related to irrigation, as the Alma, GA NWS Coop station is located at an airport. The fact that the significant differences were only found in minimum and dew point temperatures leads to hypothesis that the increases are possibly due to advection of moisture as humidity should decrease as the amount of impervious surfaces around a station increases. Backward trajectories were calculated using the HYSPLIT model for July 1-2, 2008 for the location of the Alma station. The trajectories show that on these two particular days, the air mass ending in Alma traveled through densely irrigated areas of southwest Georgia (Fig 4.13). Looking at the wind rose diagram for Alma, GA (Fig.

4.14), there are a large percentage of westerlies and the average wind direction for the months of June, July, and August is 201.83 degrees. This south-southwest average direction would bring an air mass to the region that spent time traveling over densely irrigated areas. This issue needs to be further investigated as there could be other confounding factors that contribute to the increased minimum and dew point temperatures. Urbanized areas and impervious surfaces increase minimum temperatures, but increases in dew point temperatures are not characteristic of that type of land cover change.

Colquitt, GA (Fig. 4.15) location had the greatest differences between the two epochs. The largest difference in minimum temperatures at Colquitt occurred in July, where post irrigation average minimum temperatures increased by 0.946°C. This led to a 0.744°C increase of summer average minimum temperatures. June average dew point temperatures showed the greatest increase, not July, as the average dew point temperatures increased by 0.768°C. The summer average dew point temperatures at Colquitt increased by 0.594°C. This station displayed the expected results of areas where irrigation intensity increased over time.

There were also stations that showed precipitation, minimum, and dew point temperatures in the analysis November minimum temperatures increased by 0.92°C in a subset of eight stations that displayed summer increases in minimum temperatures. A subset of six stations showed an average increase of 1.08°C in November post irrigation temperatures. Average November precipitation increased 24.6 mm during the post irrigation epoch as well. It is believed that these findings are not related to irrigation, but it is speculated that irrigation late into the

growing season has created a positive soil moisture anomaly in November, a time of year when evaporative demand is low.

4.5 Conclusion

It was hypothesized that irrigation would increase minimum and dew point temperatures, and reduce maximum temperatures during the post irrigation epoch. Impacts on precipitation varied from region to region with evidence that irrigation enhances downwind precipitation. It was expected that precipitation would decrease in heavily irrigated areas during the summer months within the region. Minimum and dew point temperatures responded as expected for some stations in the region. Maximum temperatures in the pre-irrigation epoch were generally warmer, but the differences between the two epochs were not significant at many of the stations analyzed, which was not the hypothesized results to increasing irrigation. In the analysis region, precipitation showed a decrease during the growing season and summer months. Further investigation is needed before attributing the decrease in growing season and summer precipitation to increased irrigation during the post irrigation epoch.

Total average precipitation, maximum temperature, minimum temperature, and dew point temperature differences between two 38-year epochs were analyzed. The epochs consisted of a pre-irrigation epoch (1938-1975) and a post irrigation epoch (1976-2013). A total of 19 stations were analyzed and of those eight showed statistically significant increased minimum temperatures and there were six stations that had increased dew point temperatures during the post irrigation epoch. Five of these stations were in areas where irrigation density was high. The station located in Alma does not reside in an area where irrigation is as high. The station in Alma

has been presented as possible case for advection of moisture as there was no increase in maximum temperatures associated with the decrease in minimum and dew point temperatures. Precipitation between the two epochs was impacted the most in April, July, and November. Post irrigation precipitation decrease in April and July. The magnitude of the decrease was above 20 mm. Although the April decrease is not directly attributed to irrigation, it could increase the demand to irrigate if the onset of the growing season is drier now than in previous times. Less rain in July will also increase the need to irrigate as the evaporative demand is highest during this time of year. An increase in November precipitation was found, and further investigation is needed to determine the cause of this increase. One possible explanation is an increase in soil moisture due to late growing season (April – September) irrigation. The effects of irrigation in the region appear to impact local scales. There are also possible confounding factors, i.e. urbanization, increasing aerosols and other influences that could minimize the expected signal seen in irrigated regions. This study was not designed to address the unique microclimate that may be possible at stations analyzed. There is clear evidence that irrigation has impacted the hydroclimate in some areas, and the poor quality of observations may limit the coherency of the effect of irrigation.. There appears to be a net loss of water in the region, as decreases in growing season precipitation accompany the known excess water introduced to the surface via irrigation. Future work includes conducting a modeling study where the possible confounding factors introduced in this study are minimized.

4.6 References

Adegoke, J. O., Pielke, R. A., Eastman, J., Mahmood, R., & Hubbard, K. G. (2003). Impact of

Irrigation on Midsummer Surface Fluxes and Temperature under Dry Synoptic Conditions: A Regional Atmospheric Model Study of the U.S. High Plains. *Mon. Wea. Rev. Monthly Weather Review, 131*(3), 556-564. doi:10.1175/1520-0493(2003)1312.0.co;2

Adegoke, J. O., Pielke, R., & Carleton, A. M. (2007). Observational and modeling studies of the impacts of agriculture-related land use change on planetary boundary layer processes in the central U.S. *Agricultural and Forest Meteorology, 142*(2-4), 203-215. doi:10.1016/j.agrformet.2006.07.013

Barnston, A. G., & Schickedanz, P. T. (1984). The Effect of Irrigation on Warm Season Precipitation in the Southern Great Plains. *J. Climate Appl. Meteor. Journal of Climate and Applied Meteorology, 23*(6), 865-888. doi:10.1175/1520-0450(1984)0232.0.co;2

Bonfils, C., & Lobell, D. (2007). Empirical evidence for a recent slowdown in irrigation-induced cooling. *Proceedings of the National Academy of Sciences, 104*(34), 13582-13587. doi:10.1073/pnas.0700144104

Changnon, D., Sandstrom, M., & Schaffer, C. (2003). Relating changes in agricultural practices to increasing dew points in extreme Chicago heat waves. *Climate Research Clim. Res., 24*, 243-254. doi:10.3354/cr024243

Deangelis, A., Dominguez, F., Fan, Y., Robock, A., Kustu, M. D., & Robinson, D. (2010). Evidence of enhanced precipitation due to irrigation over the Great Plains of the United States. *J. Geophys. Res. Journal of Geophysical Research, 115*(D15). doi:10.1029/2010jd013892

Diem, J. E., & Mote, T. L. (2005). Interepochal Changes in Summer Precipitation in the Southeastern United States: Evidence of Possible Urban Effects near Atlanta, Georgia. *Journal of Applied Meteorology J. Appl. Meteor., 44*(5), 717-730.

Douglas, E., Beltrán-Przekurat, A., Niyogi, D., Pielke, R., & Vörösmarty, C. (2009). The impact of agricultural intensification and irrigation on land–atmosphere interactions and Indian monsoon precipitation — A mesoscale modeling perspective. *Global and Planetary Change, 67*(1-2), 117-128. doi:10.1016/j.gloplacha.2008.12.007

Douglas, E. M., Niyogi, D., Frolking, S., Yeluripati, J. B., Pielke, R. A., Niyogi, N., . . . Mohanty, U. C. (2006). Changes in moisture and energy fluxes due to agricultural land use and irrigation in the Indian Monsoon Belt. *Geophys. Res. Lett. Geophysical Research Letters, 33*(14). doi:10.1029/2006gl026550

FAO. (2014). Did you know...? Retrieved May 24, 2016, from http://www.fao.org/nr/water/aquastat/didyouknow/index3.stm

Kueppers, L. M., & Snyder, M. A. (2011). Influence of irrigated agriculture on diurnal surface energy and water fluxes, surface climate, and atmospheric circulation in California. *Clim Dyn Climate Dynamics, 38*(5-6), 1017-1029. doi:10.1007/s00382-011-1123-0

Misra, V., Michael, J., Boyles, R., Chassignet, E. P., Griffin, M., & O'Brien, J. J. (2012). Reconciling the Spatial Distribution of the Surface Temperature Trends in the Southeastern United States. *Journal of Climate J. Climate, 25*(10), 3610-3618. doi:10.1175/jcli-d-11-00170.1

Moore, N., & Rojstaczer, S. (2002). Irrigation's influence on precipitation: Texas High Plains,

U.S.A. *Geophys. Res. Lett. Geophysical Research Letters, 29*(16). doi:10.1029/2002gl014940

Pei, L., Moore, N., Zhong, S., Kendall, A. D., Gao, Z., & Hyndman, D. W. (2016). Effects of Irrigation on Summer Precipitation over the United States. *Journal of Climate J. Climate, 29*(10), 3541-3558. doi:10.1175/jcli-d-15-0337.1

Pervez, M. S., & Brown, J. F. (2010). Mapping Irrigated Lands at 250-m Scale by Merging MODIS Data and National Agricultural Statistics. *Remote Sensing, 2*(10), 2388-2412. doi:10.3390/rs2102388

Salazar, M., Hook, J., Garcia, A. G., Paz, J., Chaves, B., & Hoogenboom, G. (2012). Estimating irrigation water use for maize in the Southeastern USA: A modeling approach. *Agricultural Water Management, 107*, 104-111. doi:10.1016/j.agwat.2012.01.015

Segal, M., Garratt, J. R., Pielke, R. A., Schreiber, W. E., Rodi, A., Kallos, G., & Weaver, J. (1989). The Impact of Crop Areas in Northeast Colorado on Midsummer Mesoscale Thermal Circulations. *Mon. Wea. Rev. Monthly Weather Review, 117*(4), 809-825. doi:10.1175/1520-0493(1989)1172.0.co;2

Shukla, S. P., Puma, M. J., & Cook, B. I. (2013). The response of the South Asian Summer Monsoon circulation to intensified irrigation in global climate model simulations. *Clim Dyn Climate Dynamics, 42*(1-2), 21-36. doi:10.1007/s00382-013-1786-9

Sridhar, V. (2013). Tracking the Influence of Irrigation on Land Surface Fluxes and Boundary Layer Climatology. *Journal of Contemporary Water Research & Education, 152*(1), 79-93. doi:10.1111/j.1936-704x.2013.03170.x

USDA. (2014, November). Irrigation: Results from the 2013 Farm and Ranch Irrigation Survey. Retrieved May 24, 2016, from https://www.agcensus.usda.gov/Publications/2012/Online_Resources/Highlights/Irrigation/Irrigation_Highlights.pdf

Zhao, F., & Shepherd, M. (2012). Precipitation Changes near Three Gorges Dam, China. Part I: A Spatiotemporal Validation Analysis. *J. Hydrometeor Journal of Hydrometeorology*, *13*(2), 735-745. doi:10.1175/jhm-d-11-061.1

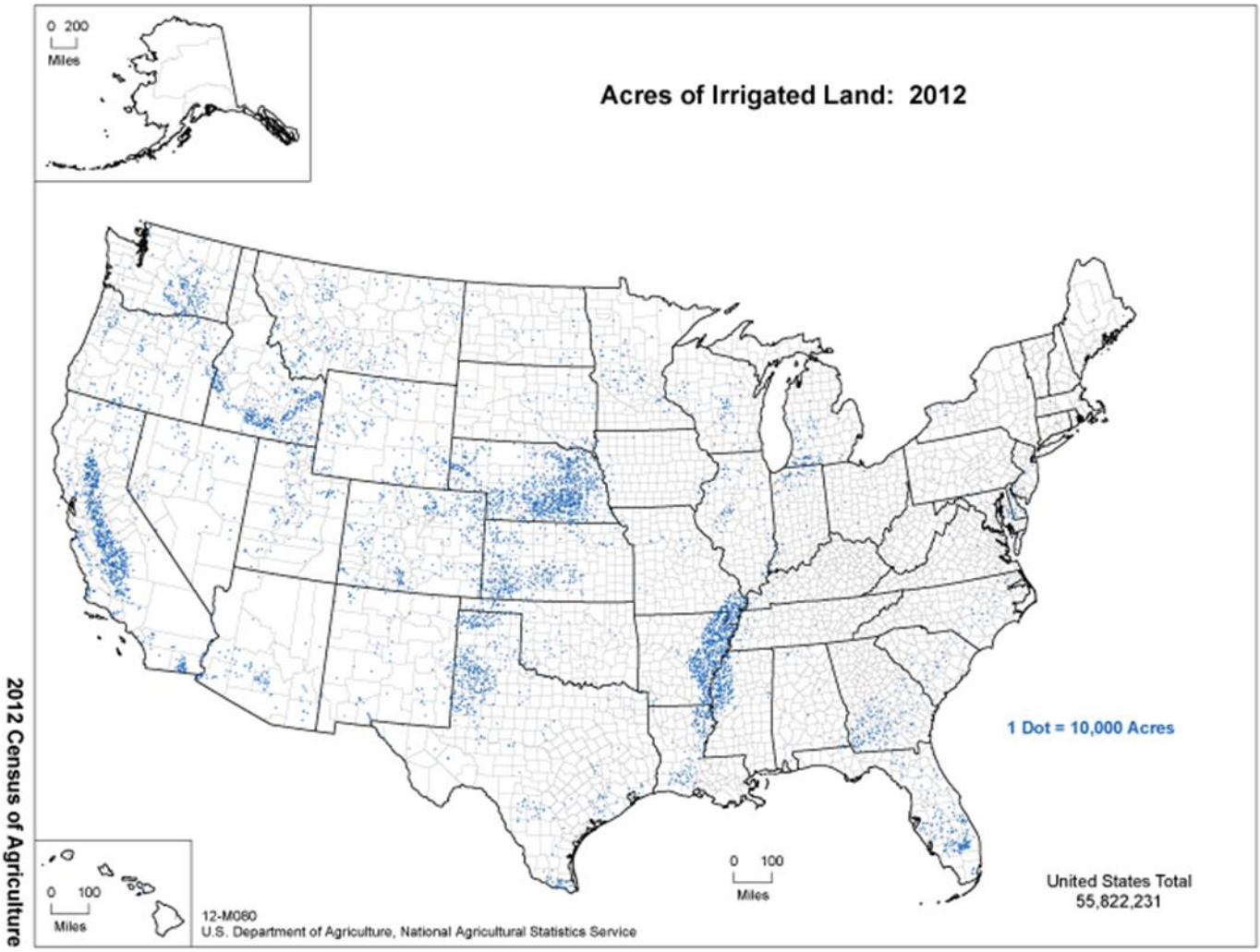

Figure 4.1: 2012 Irrigated acres in the United States. Photo credit to USDA Census of Agriculture

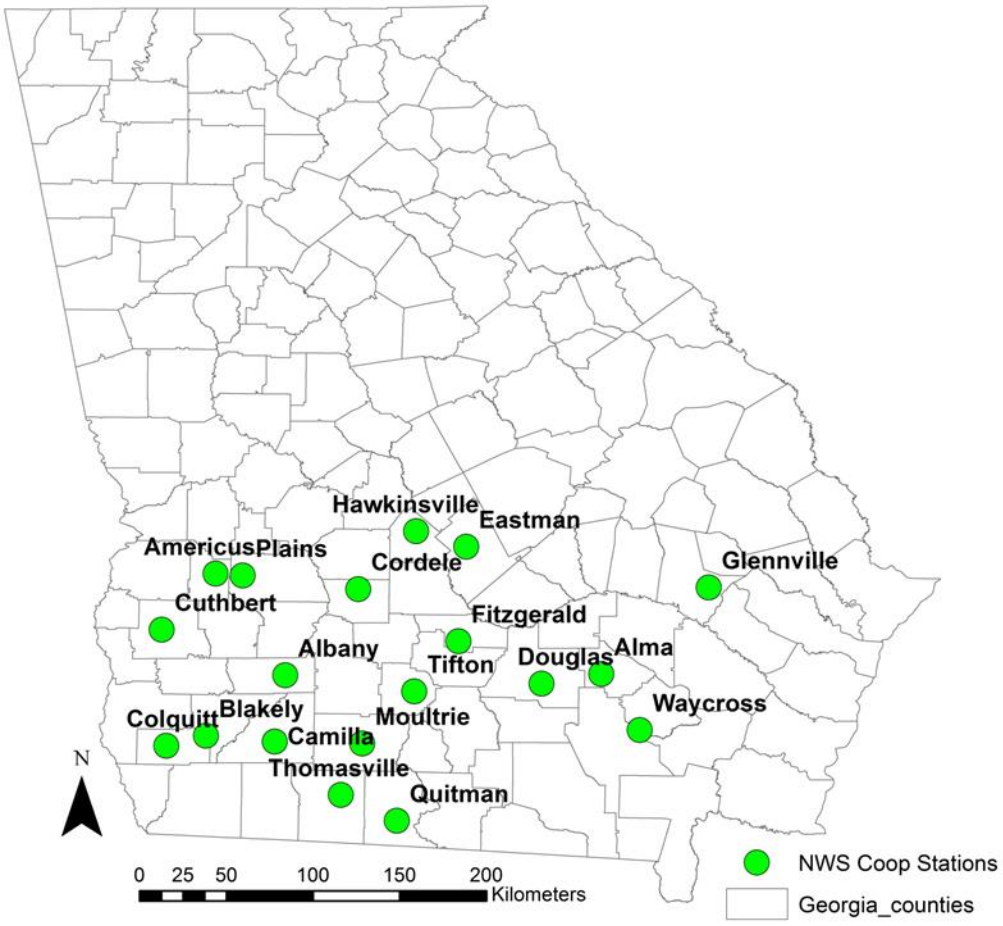

Figure 4.2: Map of 19 NWS Coop stations used in analysis

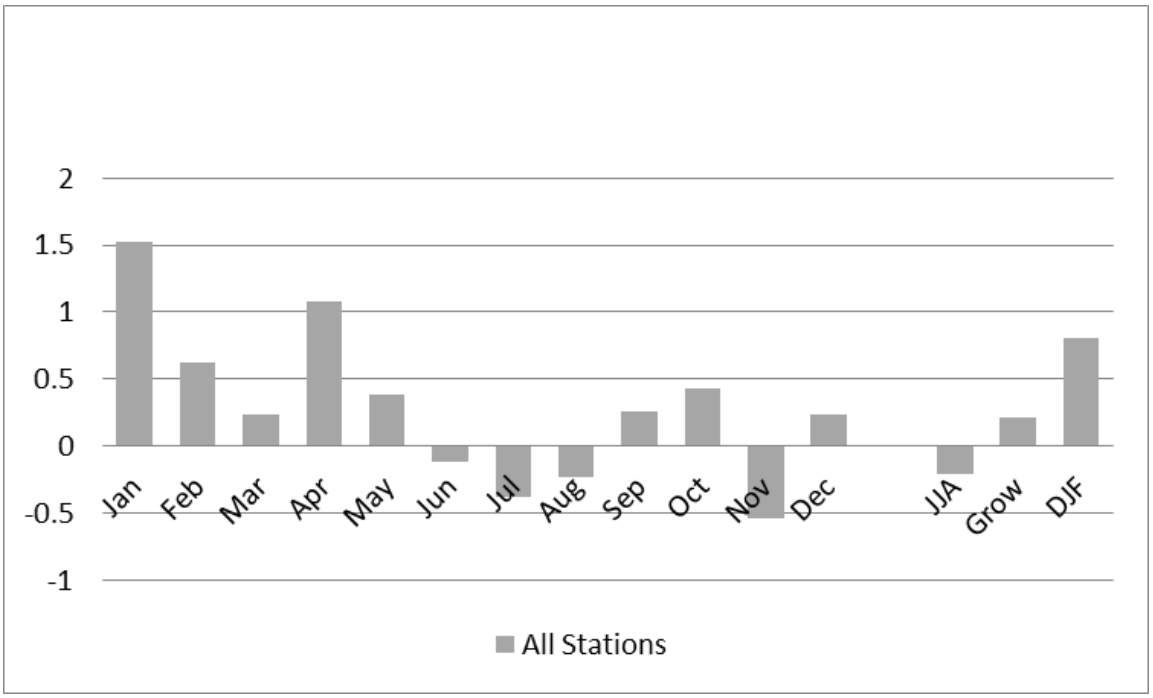

Figure 4.3: Pre and Post Irrigation minimum temperature difference graph. Calculated by subtracting post irrigation average from pre irrigation average. Averages for all 19 stations shown.

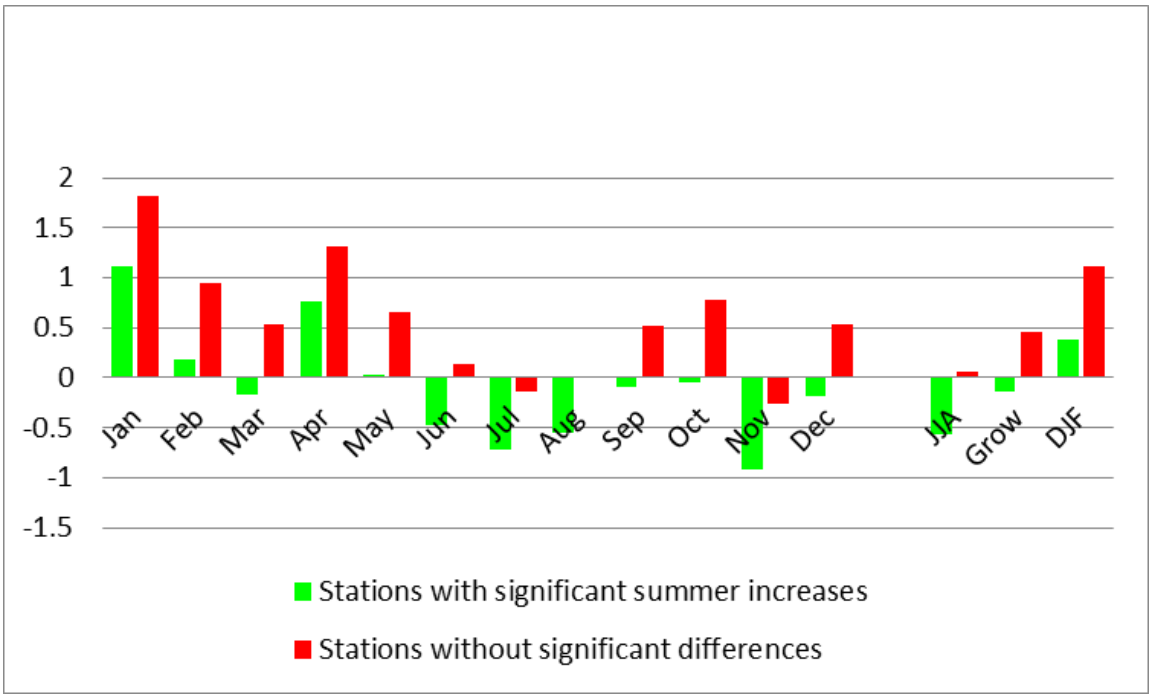

Figure 4.4: Pre and Post Irrigation minimum temperature difference maps. Green denotes stations that had significant increases in June, July, and August minimum temperatures during the post irrigation epoch. Red denotes averages for the 13 remaining stations

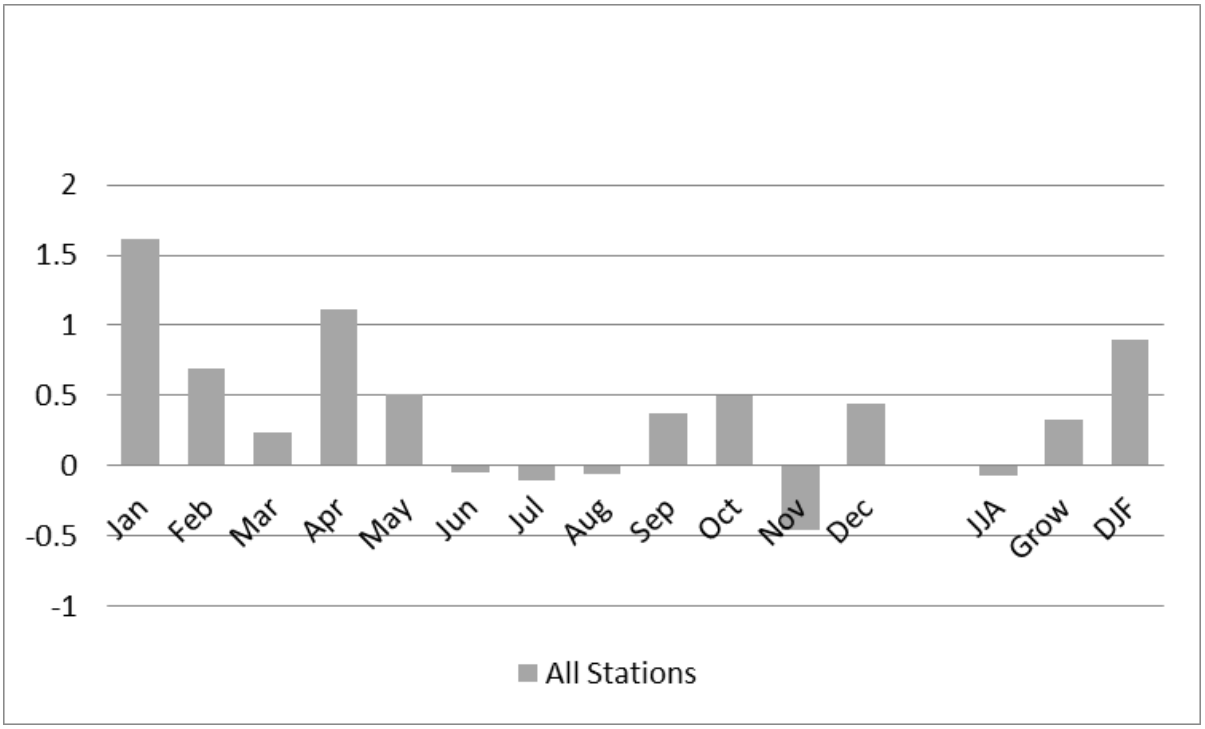

Figure 4.5: Pre and post irrigation dew point temperatures for all 19 stations

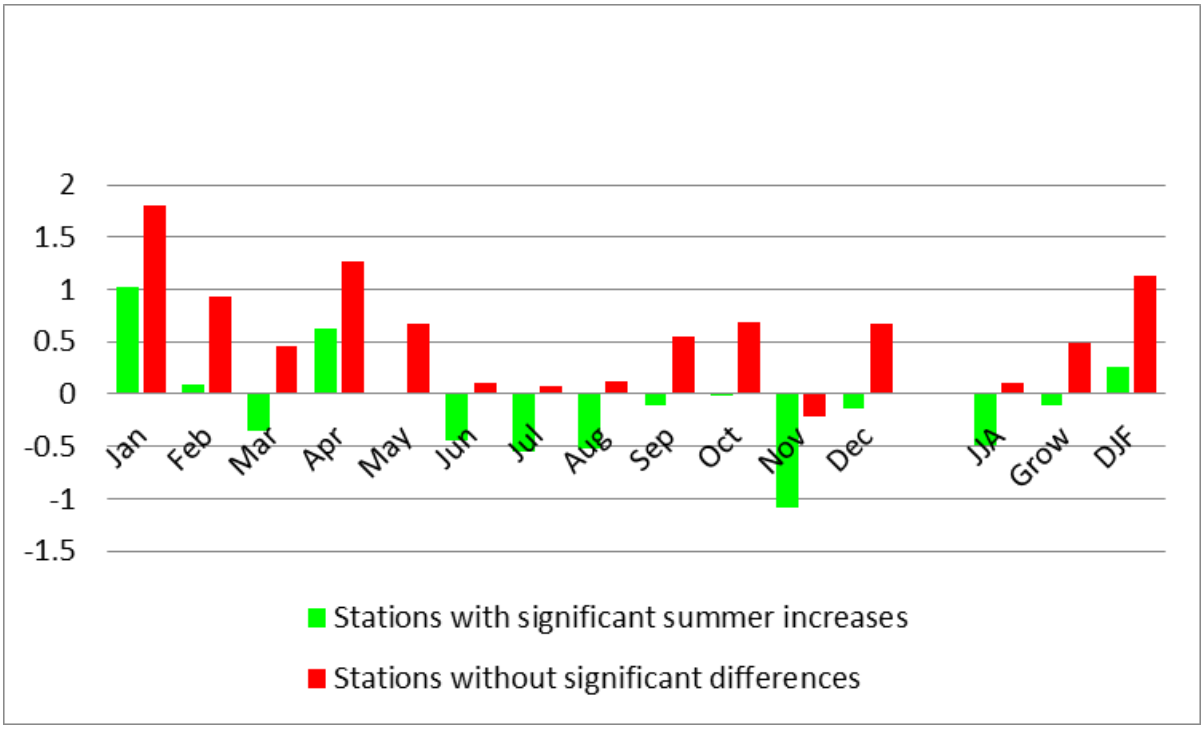

Figure 4.6: Pre and Post Irrigation dew point temperature difference maps. Green denotes stations that had significant increases in June, July, and August dew point temperatures during the post irrigation epoch. Red denotes averages for the 13 remaining stations

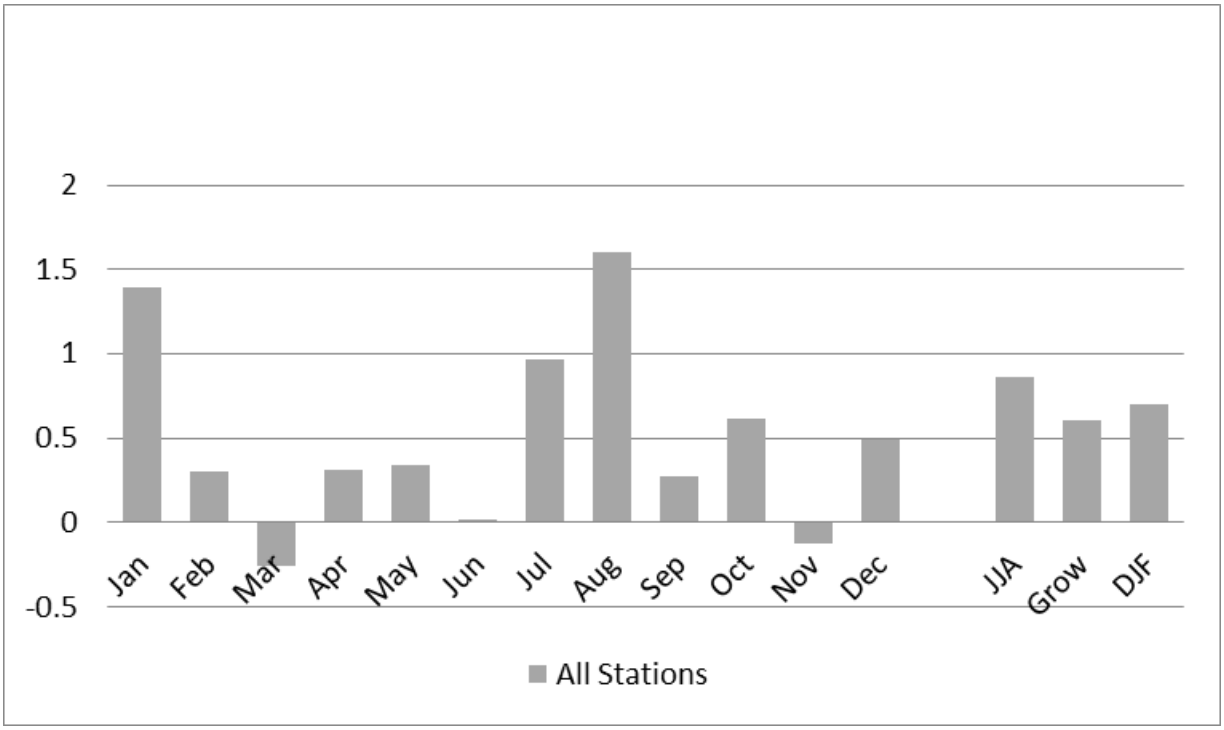

Figure 4.7: Pre and post irrigation maximum temperature difference for all 19 stations.

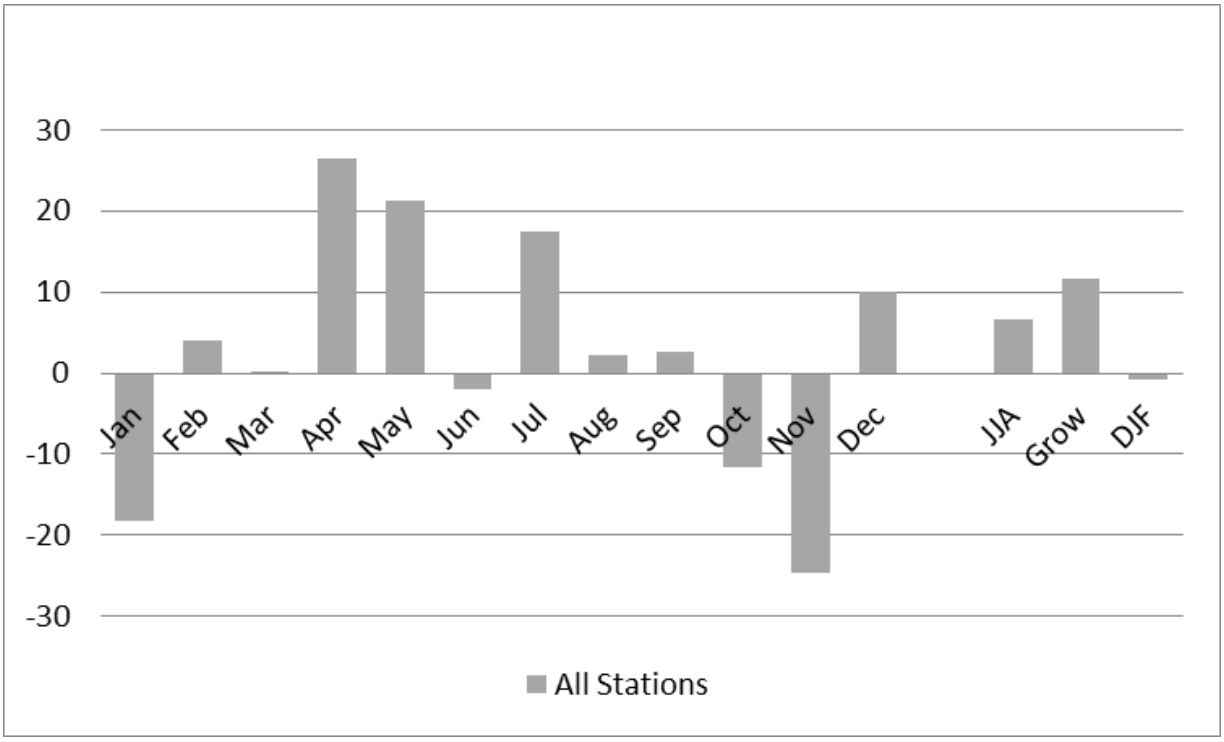

Figure 4.8: Pre and post irrigation precipitation difference for all 19 stations.

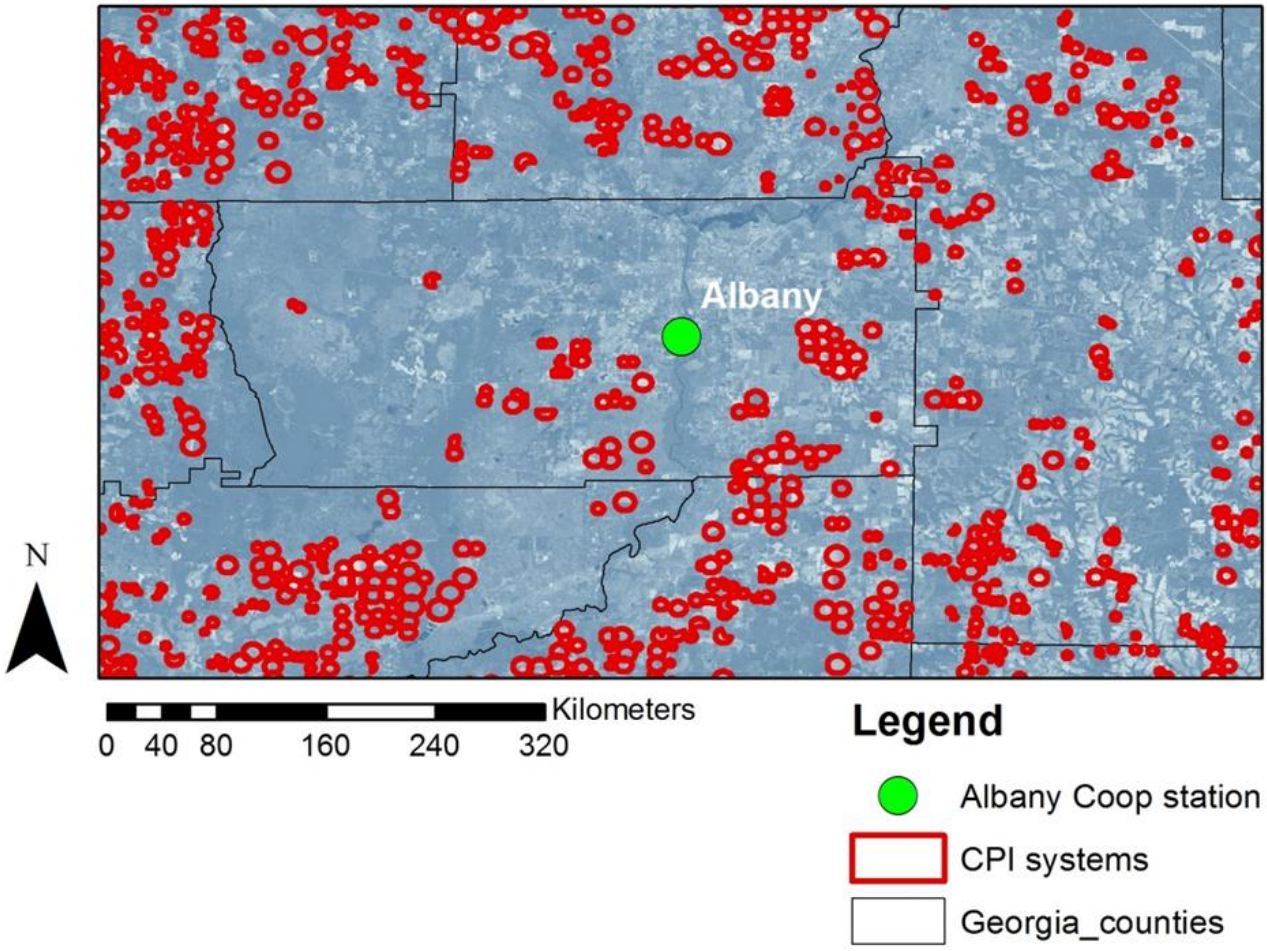

Figure 4.9: Map showing location of Albany NWS Coop station (green circle). The red circles represent mapped center pivot irrigation (CPI) systems for 2008.

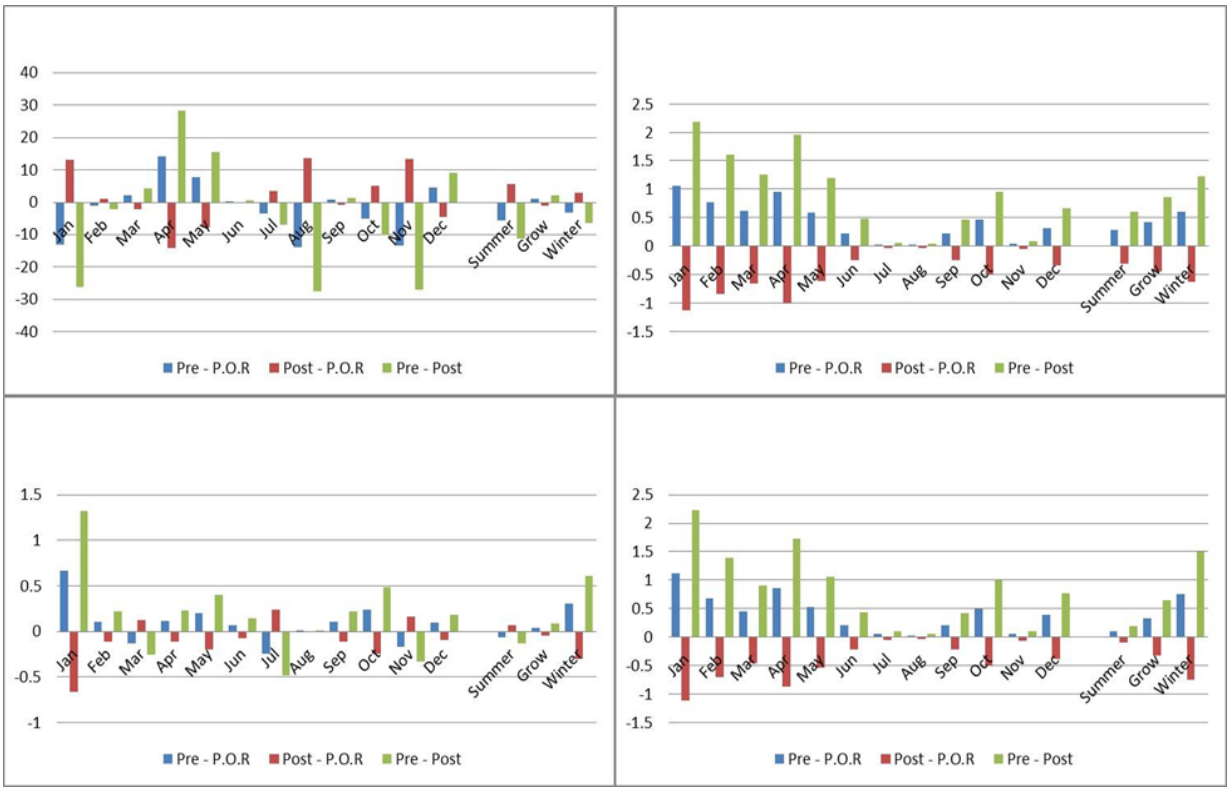

Figure 4.10: Albany, GA pre and post irrigation difference graphs for precipitation (upper left), minimum temperature (upper right), maximum temperature (lower left), and dew point temperatures (lower right). Blue represents the pre-irrigation averages minus the 1938-2013 period of record (P.O.R.). Red represents post irrigation minus P.O.R. and green represents post irrigation minus pre irrigation values.

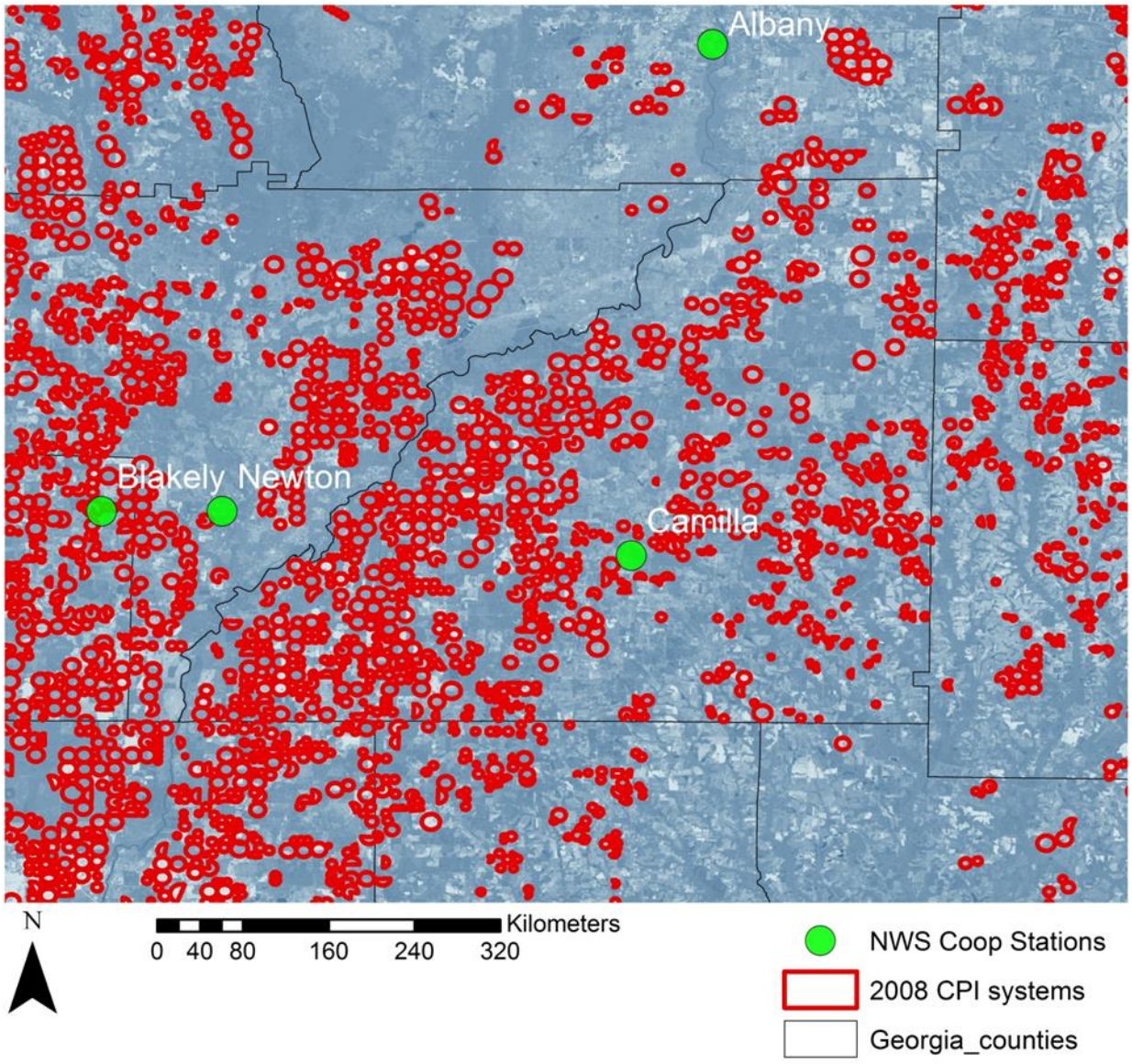

Figure 4.11: Map showing location of Camilla NWS Coop station (green circle). The red circles represent mapped center pivot irrigation (CPI) systems for 2008.

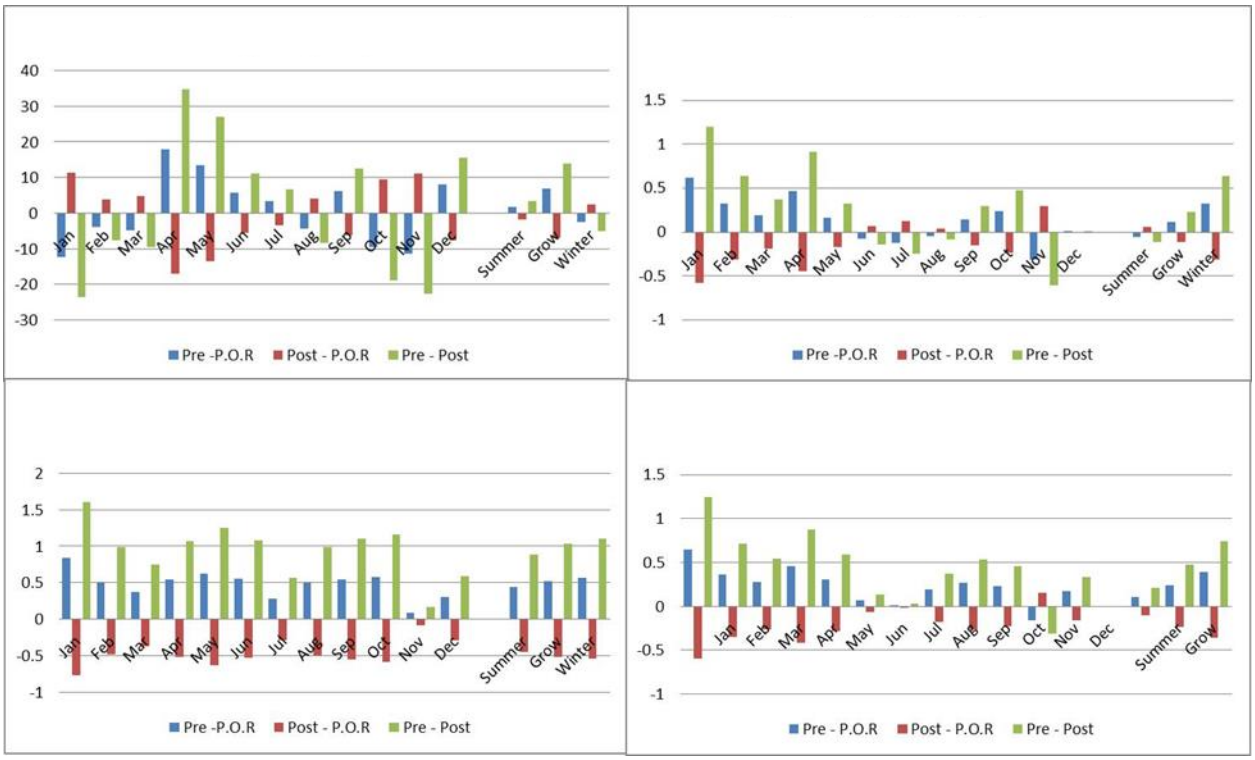

Figure 4.12: Camilla, GA pre and post irrigation difference graphs for precipitation (upper left), minimum temperature (upper right), maximum temperature (lower left), and dew point temperatures (lower right). Blue represents the pre-irrigation averages minus the 1938-2013 period of record (P.O.R.). Red represents post irrigation minus P.O.R. and green represents post irrigation minus pre irrigation values

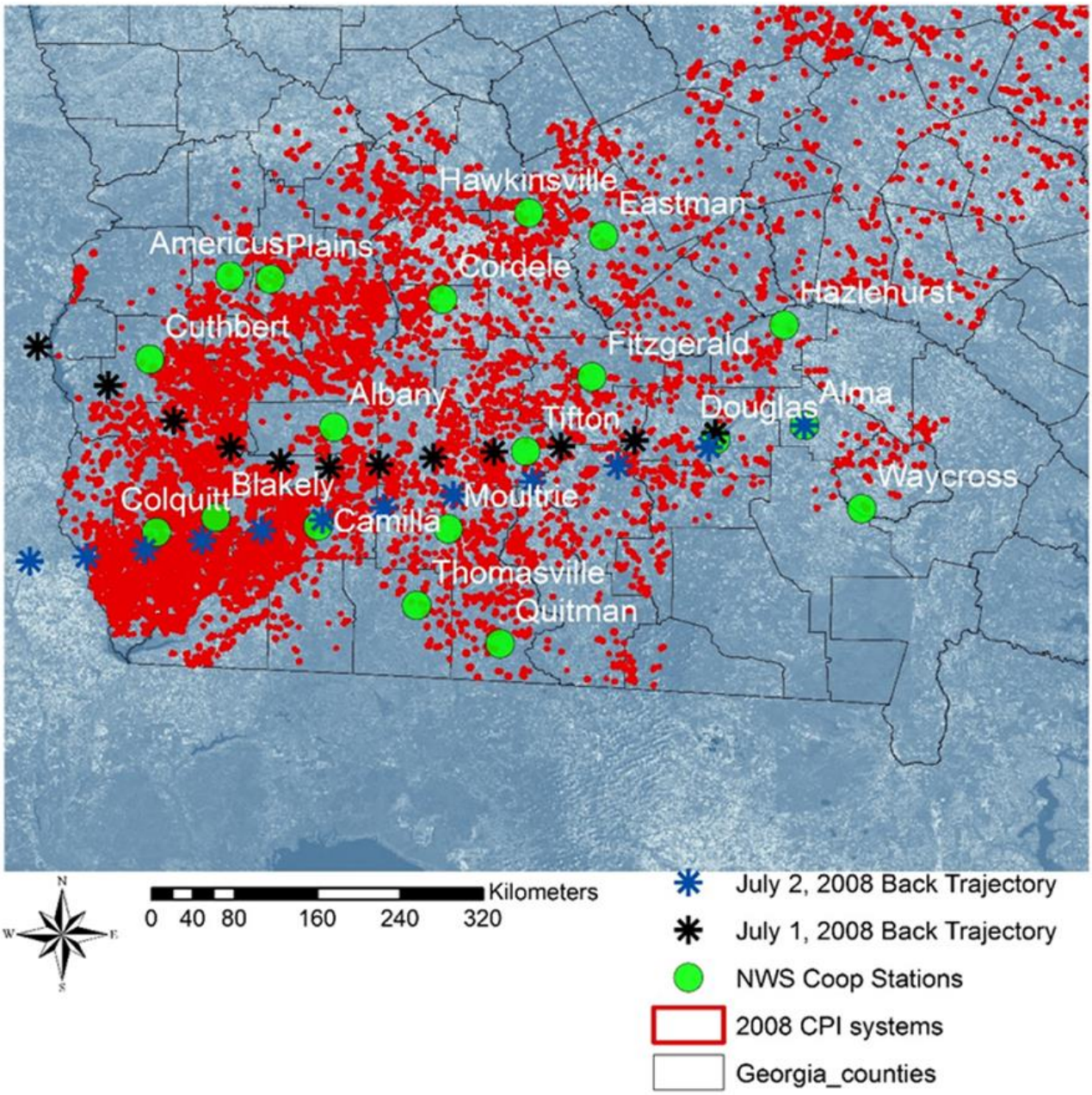

Figure 4.13: Map of HYSPLIT back trajectory calculations for Alma, GA. Black and blue asterisks represent trajectory calculations for July 1st and 2nd respectively. Red represents the mapped CPI systems in 2008.

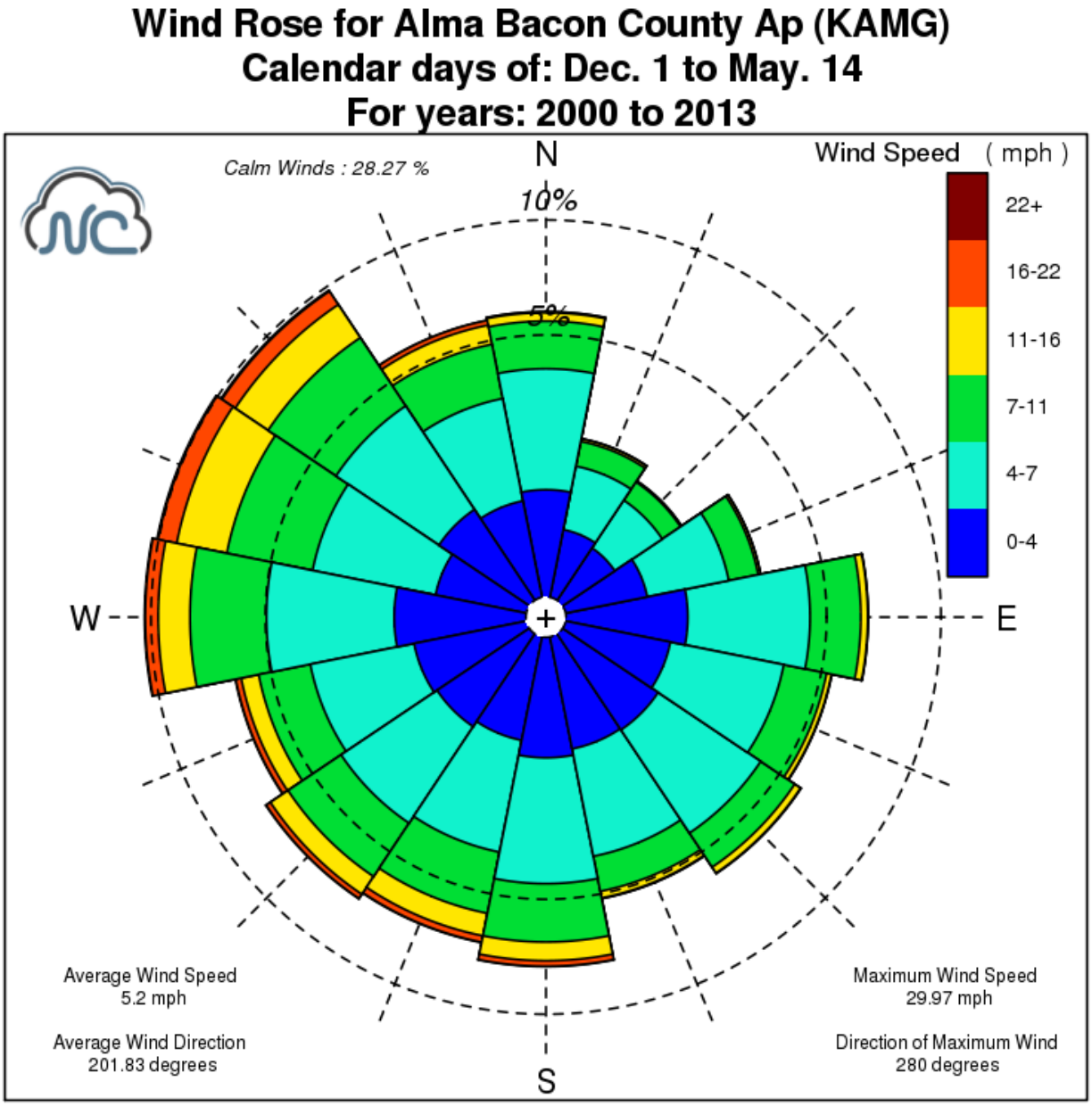

Figure 4.14: Wind Rose diagram for Alma, GA

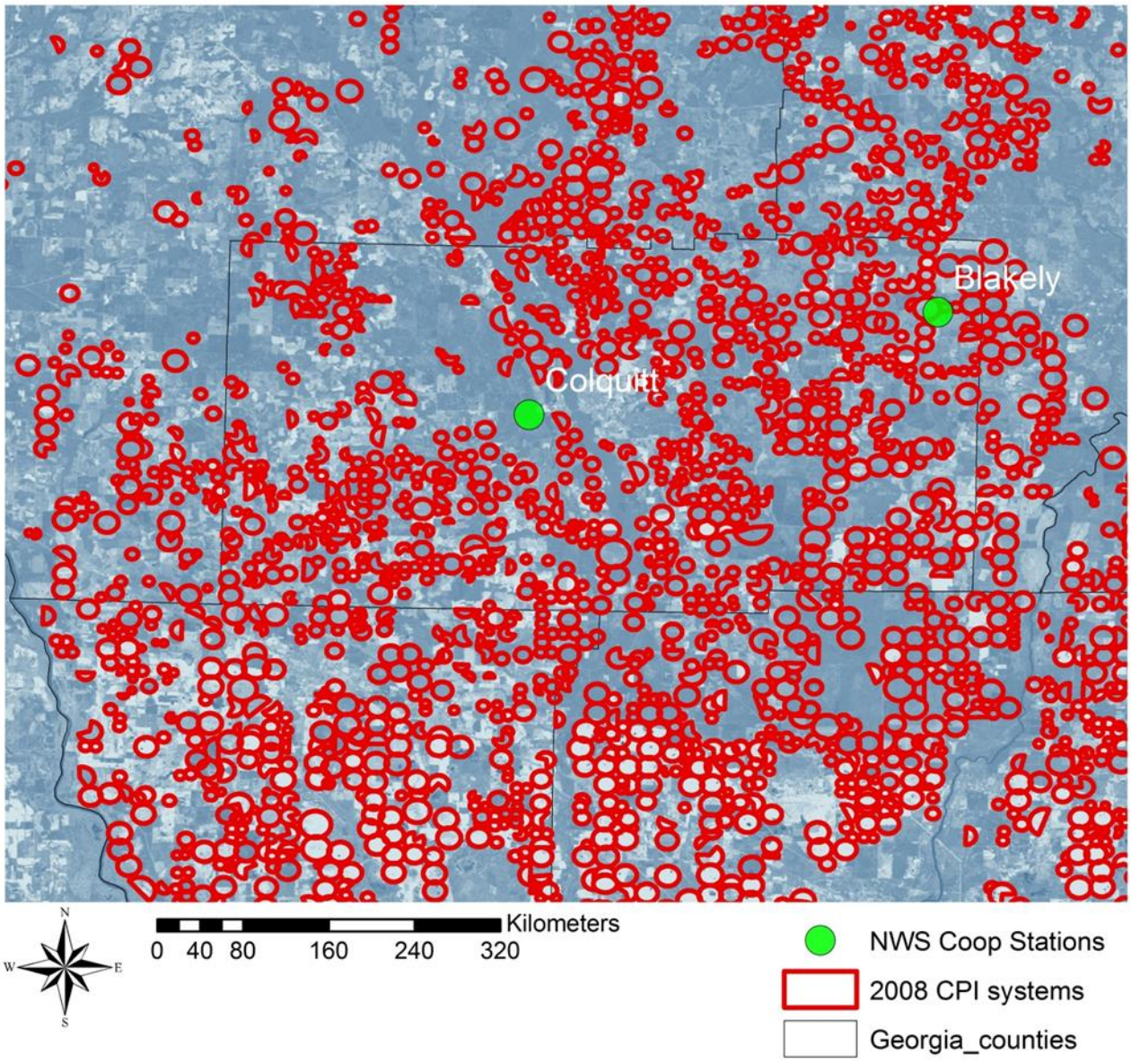

Figure 4.15: Map showing location of Colquitt NWS Coop station (green circle). The red circles represent mapped center pivot irrigation (CPI) systems for 2008.

5) ON THE IMPACT OF IRRIGATION ON SUMMERTIME SURFACE FLUXES AND PRECIPITATION IN SOUTHWEST GEORGIA: A MODEL SENSITIVITY APPROACH

Abstract

There is substantial evidence that irrigation alters the hydrologic cycle and the surface energy budgets. Since the early 1970s, southwest Georgia has experience rapid growth in acres artificially irrigated. There is limited understanding on the impacts on this land cover change on the hydroclimate in the region. Long-term observations are sparse in southwest Georgia, so a modeling approach is useful to investigate these potential changes. The Weather Research and Forecasting (WRF) model is employed to simulate relative differences between unirrigated and irrigated land cover scenarios. Sensitivity experiments of this nature are prevalent in the literature, as a modeling approach removes potential confounding factors and allows for the exploration of physical differences that occur when the land cover transitions from unirrigated to irrigated agriculture. The differences in land cover amongst the simulations created local differences as opposed to regional, broad scale differences. Sensible and latent heat fluxes appeared as high/low couplets in the simulations, and changes in land cover shifted the spatial occurrence of these high low couplets. Some shifts produced differences in surface fluxes on the order of 400-500 W/m^2. Grid cell maximum accumulated precipitation, or the totaled amount of precipitation that fell at each grid point, was higher for the irrigated land cover in the two runs where precipitation occurred.

5.1 Introduction and Literature Review

Beginning in the 1970s, Georgia experienced rapid growth in agricultural intensity, as there was a substantial increase in irrigated acreage from 1970 to 1992 (Tyson and Harrison, 1993). Much of this growth was fueled by the expansion of center pivot irrigation technology and general growth of agriculture in the late seventies (Tyson and Harrison, 1993). The increase in irrigated acreage continued, although the rate of increase slowed as regulations on agricultural water withdrawals were put into place by the Georgia Environmental Protection Division (EPD) in the late 1980s. Agriculture is the largest industry in Georgia and contributed more than $72 billion to the state's economy in 2015 (Georgia Farm Bureau) with one out of every seven residents of the state working in agriculture of forest related fields (UGA Cooperative Extension, 2011).

Irrigation is the single largest anthropogenic water use with much of the source of water for irrigation being derived from groundwater that accounts for over 60% of agricultural water demands (Braneon and Georgakakos, 2011). Irrigation is highest in the southwest portion of the state, with minimal amounts of irrigation occurring above the fall line (Tyson and Harrison, 1993) as the Flint, Central, and Coastal regions of Georgia comprise about 95% of crop production and irrigated acreage (Guerra et al., 2005). During the April – September growing season irrigation water use is estimated to account for 90% in southwest Georgia (Braneon, 2014) and saw a 1,320% increase in agricultural water withdrawals from 1970 -1990 (Marella et al, 1990). Competing water demands amongst municipal, industrial, agricultural, and ecological sectors make water resources and planning challenging for policy makers and stakeholders. A

changing climate can also place an additional strain on water resources. It is important to identify any potential changes to the climate system irrigation poses in the region.

Research has shown that irrigation affects the hydrologic cycle and the surface energy budget. The impacts on the hydrologic cycle include altering precipitation patterns, modifying water storage in the atmosphere via increased evapotranspiration, and modifying groundwater storage through water withdrawals for irrigation (Fig 5.1). Precipitation is often increased downwind of heavily irrigated areas (Barnston and Schickedanz, 1984; DeAngis et al., 2010; Harding and Synder, 2012; Pei et al., 2016). Boucher et al. (2004) conducted a set of model simulations that showed irrigation increases water vapor concentrations in the lower levels of the atmosphere, and resulted in a significant cooling of 0.8K over irrigated continental regions. The primary impact of irrigation on the surface energy budget is the modification of the Bowen ratio, which is the partitioning of incoming solar radiation between latent and sensible heating (Fig 5.2). Through the introduction of moisture at the surface, irrigation increases surface evapotranspiration and near surface humidity; which can lead to changes in the planetary boundary layer (Qian and Huang et al., 2012). Modeling and empirical studies in various regions have demonstrated that soil moisture from irrigation leads to decreases in simulated average and maximum temperatures (Adegoke et al., 2003).

The relationship between irrigation and climate in Georgia has not been as widely studied as other regions. The literature is more robust on the hydrologic impacts of irrigation in Georgia as it has been shown that irrigation impacts groundwater resources and streamflows (Braneon 2014, Hicks and Golladay 2009; Mitra et al., 2016; Rugel et al., 2011). In one of the few studies

to investigate the climatic response to irrigation in Georgia Misra et al. (2012) found that irrigation had a meaningful impact on summer minimum and maximum temperature trends. Their analysis showed than maximum temperatures cooled by 0.5°F per century and that minimum temperatures increased by 3.5°F per century. There is evidence that irrigation influences climate in Georgia, but the lack of quality long term meteorological observations make it difficult to quantify the relationship. Therefore, a modeling approach would serve as a theoretical foundation to broaden the knowledge of the relationship between irrigation and climate in Georgia.

This analysis investigates the relative differences between non irrigated and irrigated land cover. The questions of interest are: (1) can irrigation modify surface latent and sensible heat fluxes; and (2) are there any spatial differences in precipitation patterns between irrigated and unirrigated land surfaces. Model simulations are a widely recognized approach to answer the hypothesized questions. Models allow for a controlled environment that remove confounding factors that often exist in empirical analysis. The only changes in this experiment are to the land cover type, as both simulations share the meteorological input used to initiate the model run. The analysis investigates the relative differences amongst the land surfaces and is not an attempt to simulate realistic forecasts. This theoretical approach is a first step in gaining an understanding of the effects of irrigation on the regional hydroclimate.

5.2 Methodology

Two distinct land cover scenarios were used as the foundation for the sensitivity experiments. The first scenario, NO IRRIGATION (NO-IRR), represents land cover based on

the United States Geological Survey (USGS) 24-class land use classification implemented in WRF (Table 5.1). This scenario represents the dominant land cover in the region before rapid irrigation occurred prior to the mid-1970s (Fig 5.3).The second scenario, IRRIGATION (IRR), represents the likely land cover after the rapid expansion of irrigation in Georgia. Williams et al. (2016) provided an assessment of irrigation changes in the region and found substantial increases in acres irrigated. The increased irrigated acreage was converted from existing non-irrigated agriculture. For the IRR (Fig 5.4), the dryland, cropland and pasture is replaced with 'irrigated cropland and pasture' to represent the transition to artificial irrigation in the region, as identified by Williams et al. (2016), and a closer depiction of the current land cover. The soil moisture availability parameter was changed from .5 to .8, to represent a value closer to saturation. A simulation for each land cover is conducted for duration of 36 hours. The three periods for the simulation which are June 29th-30th, July 10th-11th, and July 17th-18th during the 2014 summer. These days were selected because they represent days of moderate and light precipitation in the domain. In the created difference maps, the IRR field is subtracted from the NO-IRR field. If a positive difference is referenced, it implies that NO-IRR modeled output is greater that IRR modeled output for the time or times being referenced. Table 5.1 provides information on the differences in model surface parameters

WRF and Model Configuration

The Weather and Research and Forecasting (WRF) model (Shamrock et al., 2008) is a numerical weather prediction (NWP) and atmospheric simulation system designed for both research and operational applications. It is a compressible, non-hydrostatic, Euler equation,

mesoscale meteorological model. WRF features multiple dynamical cores (ARW, NMM), a 3-dimensional variational (3DVAR) data assimilation and portable code that is efficient in computing environments ranging from parallel supercomputers to laptops. This study uses the Advanced Research WRF (ARW) core version of WRF.

The simulations used three nested domains (Fig 5.5), D1, D2, and D3 with horizontal grid resolutions of 15 km, 5 km, and 1 km, respectively. The largest domain, D1, covers most of the Southeastern United States and includes parts of the Atlantic and Gulf of Mexico water bodies. The second domain contains the entire states of Alabama, Georgia, and South Carolina as well as portions of Mississippi, Tennessee, North Carolina, and Florida. This domain also covers portions of the Atlantic and Gulf of Mexico. The innermost domain, D3, covers the southwest portion of the Georgia Coastal Plain. The model uses 30 vertical levels, with the top set at 100 hPa, and 4 soil levels.

The basic atmospheric packages used in all cases were Kain-Fritsch for cumulus cloud parameterization and WRF single-moment class 3 microphysics. The innermost domain explicitly resolves precipitation; therefore no cumulus cloud parameterization was needed. Table 1 provides additional information on the configuration of the WRF model. All scenarios are initialized with the North American Regional Reanalysis (NARR) dataset (Mesinger et al., 2006), which has a horizontal resolution of 32 km.

5.3 Results and Analyses

Sensible and Latent Heat Flux

The simulation for June 30th, 2014 is initialized at 12z on June 29th. The results herein are discussed in the context of D3, the domain where the land cover changes were made. The first 12 hours of the model run are used for spin up and disregarded in the analysis. The spatial distribution of sensible heat flux for the NO-IRR (Fig 5.6.), and IRR (Fig 5.6) simulations 12 h into the simulation are shown in Figure 5.6. The fluxes in both simulations have initial differences roughly around 70 W/m^2 (Fig 5.6). As radiative energy from the sun decreases, the differences in sensible heat flux between the surfaces begin to dissipate, and differences reach a minimum around 10z on June 30th. At 14z, a few hours after sunrise, differences between the two surfaces develop in the eastern portion of D3. Sensible and latent heat fluxes were plotted for the two runs at a grid cell near 31.5N and -83.0W (Figure 5.7). Latent heat fluxes during the day were higher than sensible heat fluxes in IRR and NO-IRR simulations. Precipitation could be influencing the fluxes. Peak latent heat flux value occurred at 18z for both simulations, with a higher peak of approximately 30 W/m^2. At the 18z simulation time, many localized differences in latent heat flux began to develop between the NO-IRR and IRR simulations. The differences in available soil moisture, albedo, and surface roughness between the two land cover scenarios do not appear great enough to produce large scale differences in sensible heat flux at the scale of this study. An emerging pattern of a shift in local minimum and maximum fluxes between the two scenarios begins to materialize on this day. It appears that there are not any large changes in the value amongst latent heat fluxes, but spatial differences on where these minimum and

maximum values occur begin to create large local differences between the two simulations. These differences can represent areas of rising air, called thermals. Thermals indicate the development of shallow cumulus clouds. Spatial changes in areas of maximum sensible heat flux could lead to spatial changes where cumulus clouds develop. An example of this is seen in the 20z sensible heat plots (Fig 5.8). In the lower right corner of the domain, NO-IRR run has a local maximum latent heat flux of 470 W/m^2. This local maximum is located in Coffee, county Georgia (approx. 31°30'N & 83°W) and is surrounded by areas of very low sensible heat flux. The local maximum in latent heat flux is shifted south in the IRR simulation and is slightly higher, 497 Wm^2. If subtracted directly, this would only result in a small difference in sensible heat flux. The spatial shift in local maximum between the two scenarios creates a positive difference of 462 W/m^2 and a decrease of 501 W/m^2. It is possible that the differences in latent heat flux can modify precipitation or local cloud cover. At the 21z simulation time latent and sensible heat fluxes sharply decline in the NO-IRR run (Fig 5.7). Values remain higher in the IRR run at 21z as the latent heat flux is 281 W/m2 higher and the latent heat flux is greater by 131 W/m2. This could indicate the presence of clouds in the NO-IRR run that are not present in the IRR run.

The simulation on June 10^{th} 2014 followed a similar pattern as the prior simulation. Localized differences between the two scenarios began to develop around 12z for this day and again, the greatest differences were in the eastern portion of the domain. The largest differences in sensible heat flux occurred at 18z in Coffee County, and the surrounding counties of Bacon and Jeff Davis. The northwest quadrant of the domain also began to develop flux difference

couplets at 18z (Fig 5.9). The July 17th – 18th simulation was a relatively dry day. This day yields interesting results as the differences in fluxes for this simulation closely follow the spatial pattern of where the land cover was converted from unirrigated agriculture to irrigated agriculture, as shown in figure. The 18z time frame illustrates the point well (Fig 5.10). Differences in latent heating resembled the general spatial pattern displayed by sensible heating, with the sign of the difference between changing direction as expected. The high/low flux couplets in latent heating were not as large spatially as they were in sensible heating.

Precipitation

There was a marginal amount of precipitation in the July 17-18th simulation so the results of those simulations are not discussed here. For the remaining simulations the differences in daily totals are presented. Figure 5.11 shows that the model produces precipitation that was observed on June 29th. On both days, there appears to a shift in daily maximum values of precipitation. Like the pattern shown in sensible and latent heating, there are some increase/decrease couplets which signal a shift in where the maximum amount of precipitation is located. Coffee County, an area of large latent heat differences, displayed a decline in total precipitation in the IRR simulation (Fig 5.12). The June 29-30th domain total cumulative precipitation amounts were 72,139.5 mm for the NO-IRR simulation compared to 70,347.9 mm for the IRR simulation. Despite producing higher total precipitation values, the IRR simulation produced the highest daily precipitation amount at 41.46 mm compared to 35.82 mm for the NO-IRR run. There is an area in the upper right quadrant of the domain were total precipitation increased by more than a 25 mm during the IRR simulation. Most changes are confined to the

upper right quadrant on the June 29th-30th simulation. Precipitation is more widespread during the July 10th-11th simulation (Fig 5.13). The domain total cumulative precipitation in this simulation was higher for the IRR run. A total of 178,285 mm of precipitation fell in the IRR run compared to 155,662 mm in the NO-IRR run. The IRR run produced the highest grid cell maximum cumulative precipitation, an amount of 68.77 compared to 63.64 for the NO-IRR run. The additional soil moisture associated with the IRR simulations appears to increase storm total precipitation amounts.

5.4 Summary

It was clearly shown that there were relative differences in sensible and latent heat flux and precipitation between the NO-IRR and IRR simulations, which is in agreement with the results of similar studies. The duration and scale of the simulations did not allow for a full quantification enhancing precipitation downwind, but the local shifts in precipitation that were found could lead to enhanced downwind precipitation over time. The meteorological conditions were the same for both simulations, with the only differences occurring in the land cover. The differences in albedo, surface roughness, and available soil moisture between the two land cover scenarios did not appear to create any large scale differences during the three 36 h simulations. The differences between the scenarios were localized. Although the changes appear to be local; it is reasonable to assume these changes found between the two land cover types increase over longer simulations. The differences in latent and sensible heat flux appear to occur in areas where unirrigated and irrigated land cover bordered other land cover types, such as forested land cover. Coffee County

is an example of this mixed land cover scenario. The differences between the two simulations appeared to occur in high/low couplets, which implies that the differences in the land cover types created a shift in local minimum and maximum values of fluxes and precipitation rather than changed the magnitude of the fluxes and precipitation totals. This shift can be the difference of a surplus of rain at a farm or a summer of little or no rain. In the two simulations where moderate rainfall was produced, the grid cell maximum accumulated precipitation was higher for IRR runs. A natural logical next step in future research is to see if these differences manifest themselves over larger spatial scales during longer simulations.

5.5 References

State and Private Forestry Fact Sheet: Georgia 2016. (2016, February 2). Retrieved May 20, 2016, from http://www.stateforesters.org/sites/default/files/publication-documents/GAFY2016Standard.pdf

Adegoke, J. O., Pielke, R. A., Eastman, J., Mahmood, R., & Hubbard, K. G. (2003). Impact of Irrigation on Midsummer Surface Fluxes and Temperature under Dry Synoptic Conditions: A Regional Atmospheric Model Study of the U.S. High Plains. *Mon. Wea. Rev. Monthly Weather Review*, *131*(3), 556-564. doi:10.1175/1520-0493(2003)1312.0.co;2

Barnston, A. G., & Schickedanz, P. T. (1984). The Effect of Irrigation on Warm Season Precipitation in the Southern Great Plains. *J. Climate Appl. Meteor. Journal of Climate and Applied Meteorology*, *23*(6), 865-888. doi:10.1175/1520-0450(1984)0232.0.co;2

Boucher, O., Myhre, G., & Myhre, A. (2004). Direct human influence of irrigation on

atmospheric water vapour and climate. *Climate Dynamics, 22*(6-7). doi:10.1007/s00382-004-0402-4

Braneon, C., & Georgakakos, A. (2011). Climate change impacts on Georgia agriculture and irrigation demand. *2011 Georgia Water Resources Conference* (pp. 1-2).

Braneon, C. V. (2014). *Agricultural Water Demand Assessment in the Southeast U.S. Under Climate Change* (Doctoral dissertation, Georgia Tech, 2014) (pp. 1-240). Atlanta, GS: Georgia Institute of Technology.

Deangelis, A., Dominguez, F., Fan, Y., Robock, A., Kustu, M. D., & Robinson, D. (2010). Evidence of enhanced precipitation due to irrigation over the Great Plains of the United States. *J. Geophys. Res. Journal of Geophysical Research, 115*(D15). doi:10.1029/2010jd013892

Georgia Trend. (2007). The Longleaf Pine: Georgia's First Tree. Retrieved May 21, 2016, from http://www.georgiatrend.com/April-2007/The-Longleaf-Pine-Georgias-First-Tree/

Guerra, L. C., Garcia y Garcia, A., Hoogenboom, G., Hook, J. E., Harrison, K. A., & Boken, V. K. (2005). Impact of local weather variability on irrigation water use in Georgia. In *2005 Georgia Water Resources Conference* (pp. 1-4). Athens: Institute of Ecology.

Hicks, D. W., & Golladay, S. W. (2009). Impacts of Agricultural pumping on selected streams in southwest Georgia. *J.W. Jones Ecological Research Center*, 1-29.

Lobell, D. B., & Bonfils, C. (2008). The Effect of Irrigation on Regional Temperatures: A Spatial and Temporal Analysis of Trends in California, 1934–2002. *Journal of Climate J. Climate, 21*(10), 2063-2071. doi:10.1175/2007jcli1755.1

Marella, R. L., Fanning, J. L., & Mooty, W. S. (1990). Estimated Use of Water in the Apalachicola Chattahoochee-Flint River basin during 1990 with State summaries from 1970 to 1990. *Water-Resources Investigations Report 93-4085,* 1-45.

Mesinger, F., Dimego, G., Kalney, E., Mitchell, K., Shafran, P. C., Ebisuzaki, W., . . . Shi, W. (2006). North American Regional Reanalysis. *Bulletin of the American Meteorological Society,* 343-360.

Misra, V., Michael, J. P., Chassignet, E. P., Griffin, M., & O'Brein, J. J. (2012). Reconciling the Spatial Distribution of the Surface Temperature Trends in the Southeastern United States. *Journal of Cliamte, 25,* 3610-3618. http://dx.doi.org/10.1175/JCLI-D-11-00170.1

Mitra, S., Srivastava, P., & Singh, S. (2015). Effects of Irrigation Pumpage during Droughts on Groundwater Levels and Groundwater Budget Components in the Lower Apalachicola-Chattahoochee-Flint River Basin [Abstract]. *ASABE 1st Climate Change Symposium: Adaptation and Mitigation,* 1-4. doi:10.13031/cc.20152143182

Pei, L., Moore, N., Zhong, S., Kendall, A. D., Gao, Z., & Hyndman, D. W. (2016). Effects of Irrigation on Summer Precipitation over the United States. *Journal of Climate J. Climate, 29*(10), 3541-3558. doi:10.1175/jcli-d-15-0337.1

Qian, Y., Huang, M., Yang, B., & Berg, L. K. (2013). A Modeling Study of Irrigation Effects on Surface Fluxes and Land–Air–Cloud Interactions in the Southern Great Plains. *J. Hydrometeor Journal of Hydrometeorology, 14*(3), 700-721. doi:10.1175/jhm-d-12-0134.1

Rugel, K., Jackson, C. R., Romeis, J. J., Golladay, S. W., Hicks, D. W., & Dowd, J. F. (2011).

Effects of irrigation withdrawals on streamflows in a karst environment: Lower Flint River Basin, Georgia, USA. *Hydrol. Process. Hydrological Processes, 26*(4), 523-534. doi:10.1002/hyp.8149

Skamarock, W. C., & Klemp, J. B. (2008). A time-split nonhydrostatic atmospheric model for weather research and forecasting applications. *Journal of Computational Physics, 227*(7), 3465-3485. doi:10.1016/j.jcp.2007.01.037

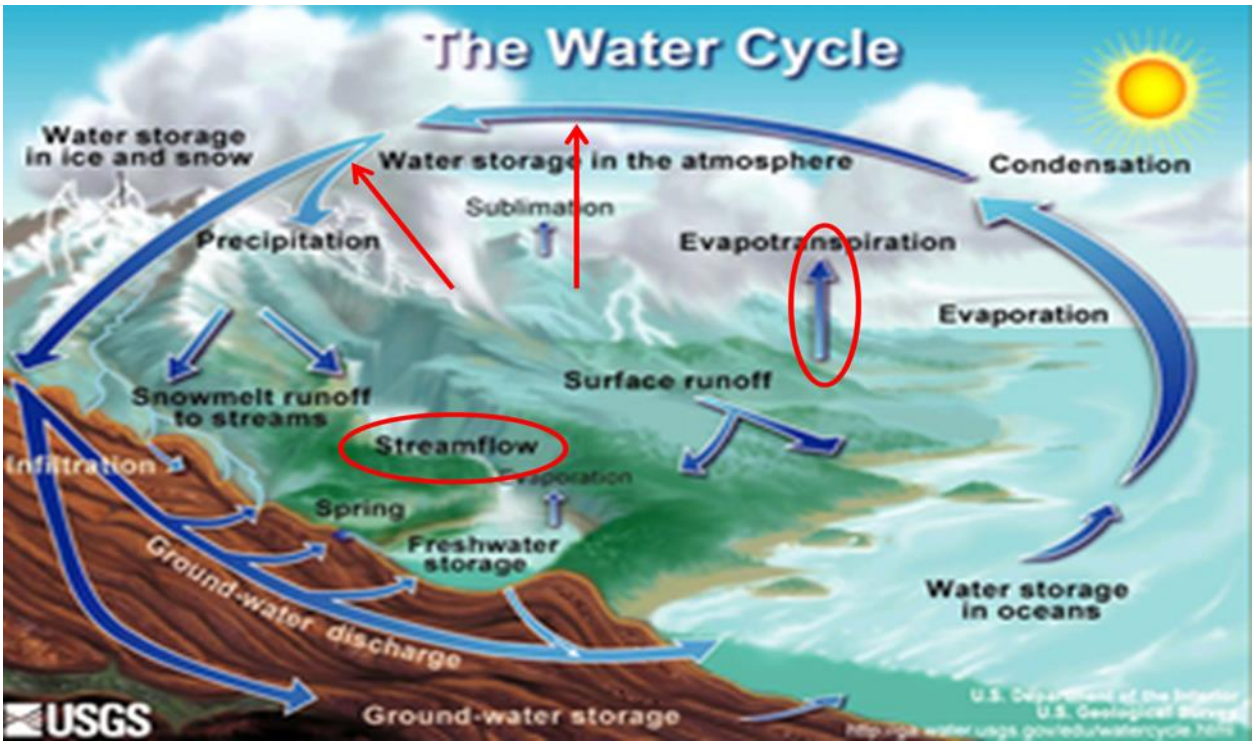

Figure 5.1: Depiction of the water cycle and alterations caused by irrigation. Image obtained from the United States Geological Survey.

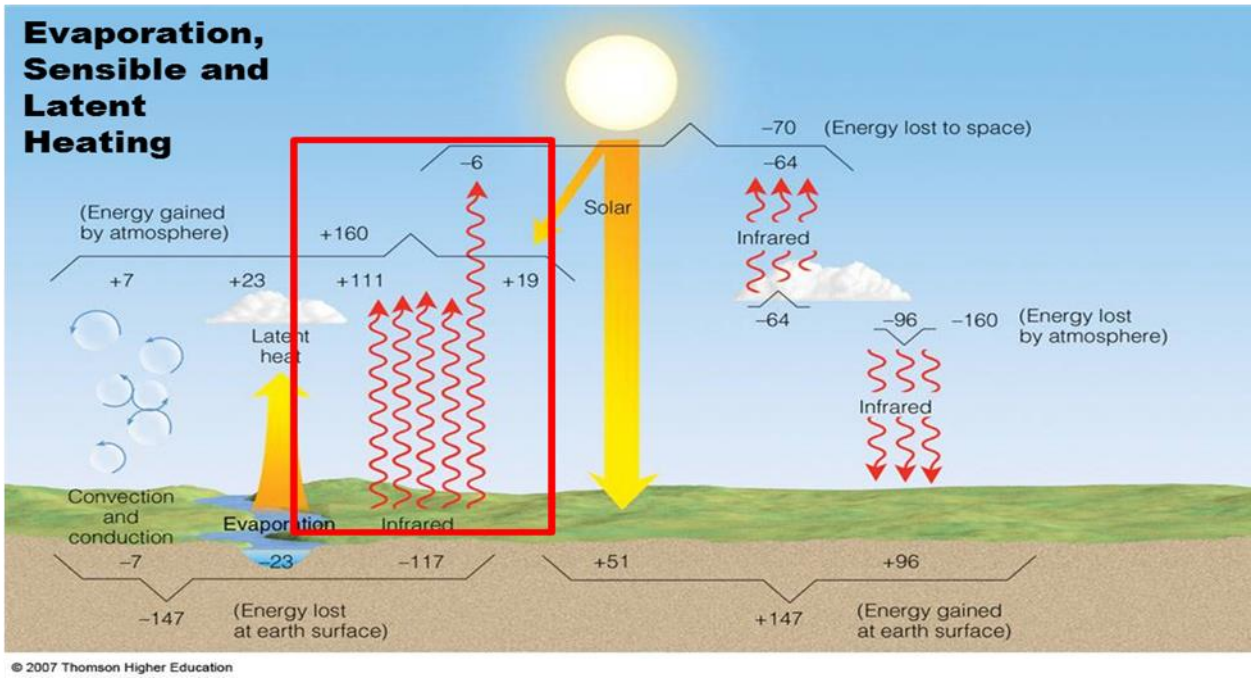

Figure 5.2: Depiction of the surface energy budget and the modifications caused by irrigation. Image courtesy of Lyndon State University department of Meteorology.

Land Use Category	Land Use Description
1	Urban and Built-up Land
2	Dryland Cropland and Pasture
3	Irrigated Cropland and Pasture
4	Mixed Dryland/Irrigated Cropland and Pasture
5	Cropland/Grassland Mosaic
6	Cropland/Woodland Mosaic
7	Grassland
8	Shrubland
9	Mixed Shrubland/Grassland
10	Savanna
11	Deciduous Broadleaf Forest
12	Deciduous Needleleaf Forest
13	Evergreen Broadleaf
14	Evergreen Needleleaf
15	Mixed Forest
16	Water Bodies
17	Herbaceous Wetland
18	Wooden Wetland
19	Barren or Sparsely Vegetated
20	Herbaceous Tundra
21	Wooded Tundra
22	Mixed Tundra
23	Bare Ground Tundra
24	Snow or Ice

Table 5-1: 24-class land use classification used in the WRF simulations derived from USGS.

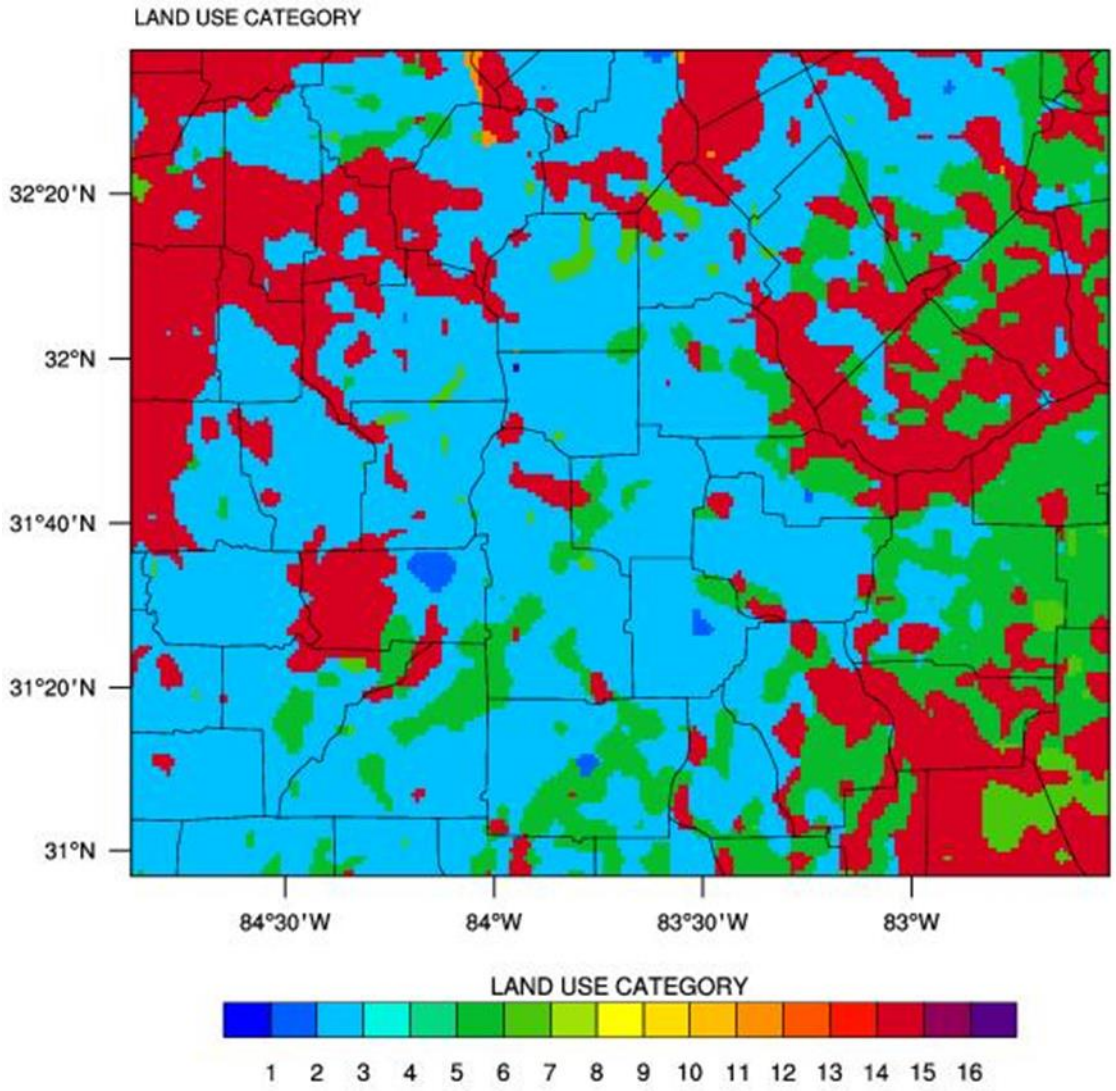

Figure 5.3: Land use category for NO-IRR model simulations.

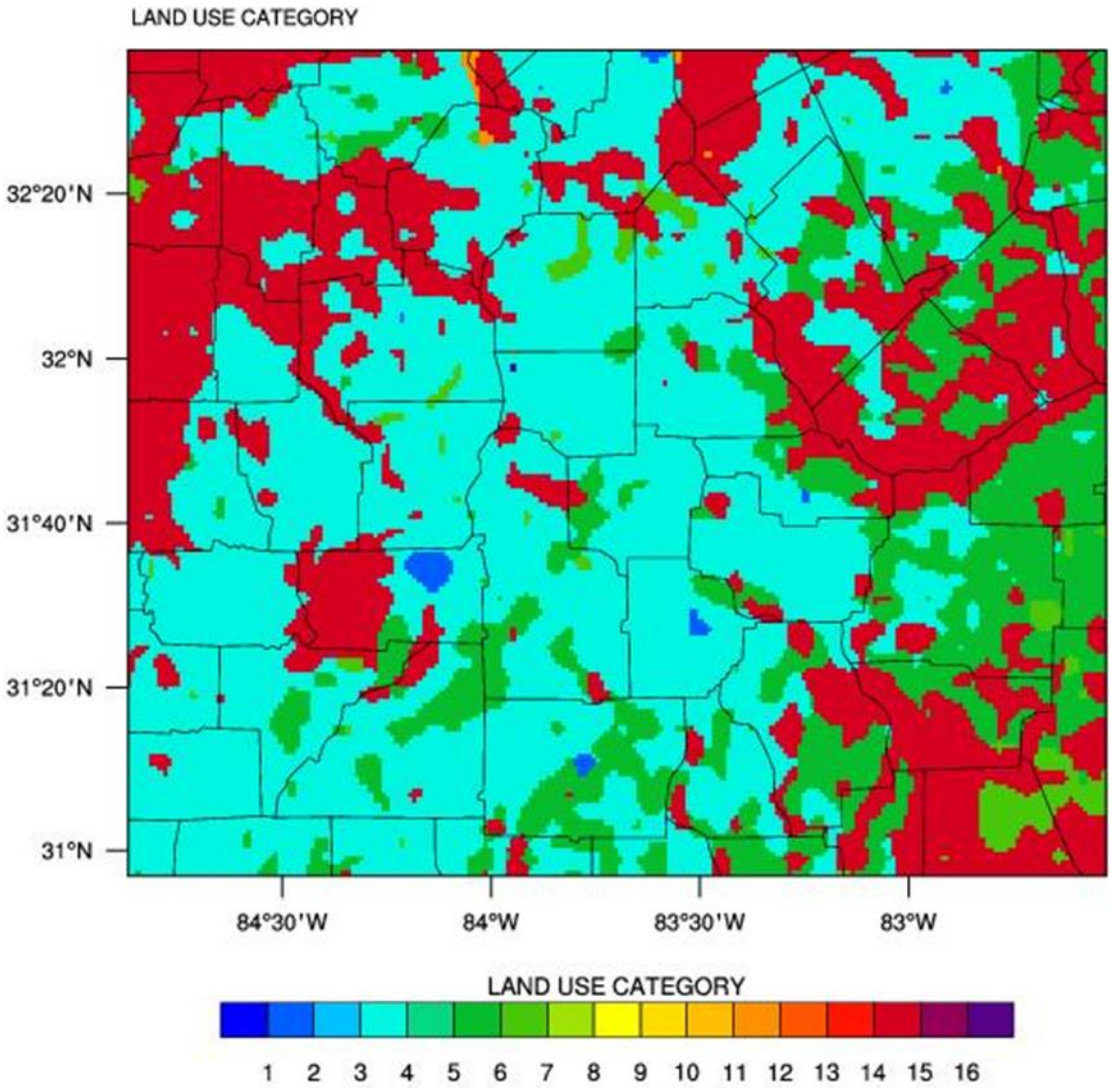

Figure 5.4: Land use category for IRR model simulations.

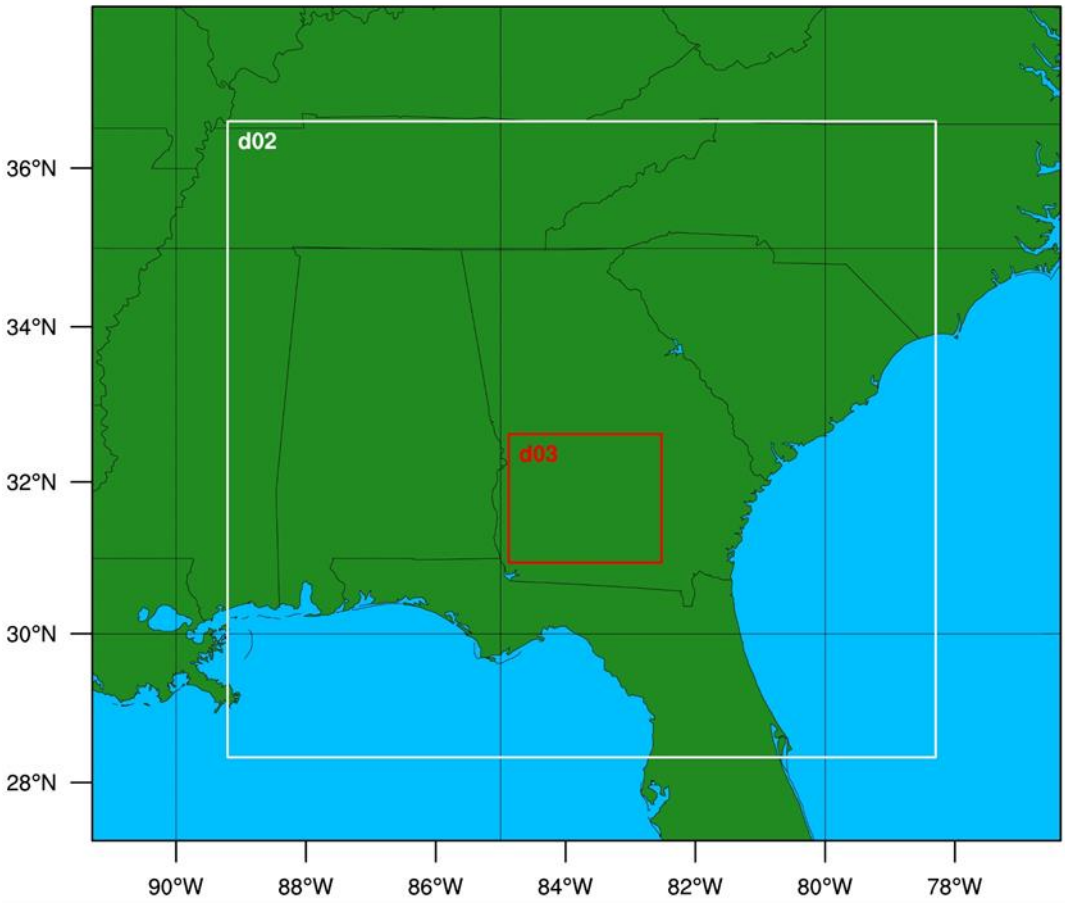

Figure 5.5: Image of model domain set up. Largest domain D1 has a horizontal resolution of 15km, medium domain D2 has a horizontal resolution of 5km, and innermost domain D3 has a horizontal resolution of 1km.

Model Land Cover Parameters	ALBD	SLMO	SFZ0	SCFZ	Classification
NO-IRR	.17	.3	15	2.71	Dryland Crop and Pasture
IRR	.10	.5	10	2.20	Irrigated Cropland and Pasture

Table 5-2: Table showing land surface parameters for the NO-IRR and IRR model simulations.

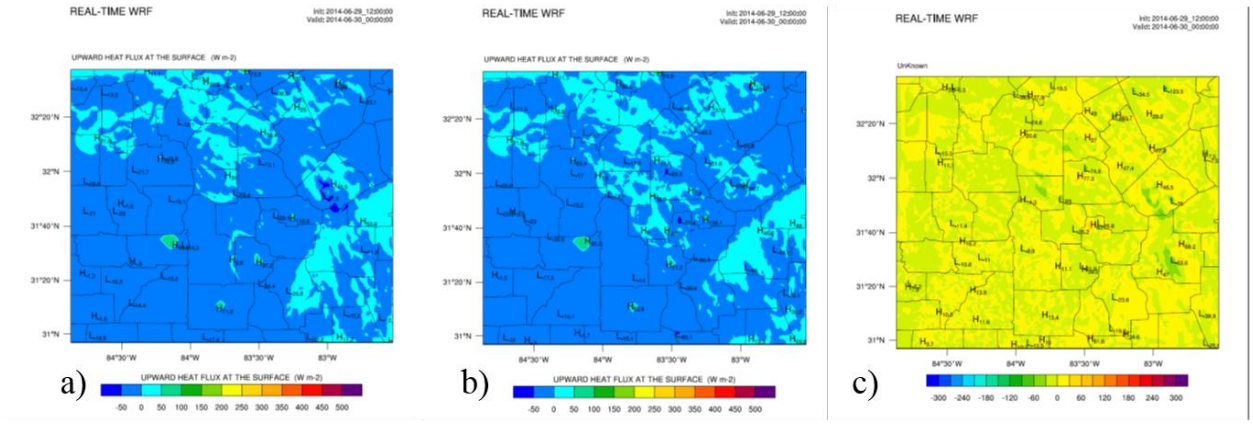

Figure 5.6: June 30th sensible heat flux for a) NO-IRR, b) IRR, and c) the differences in sensible heat flux between the two simulations.

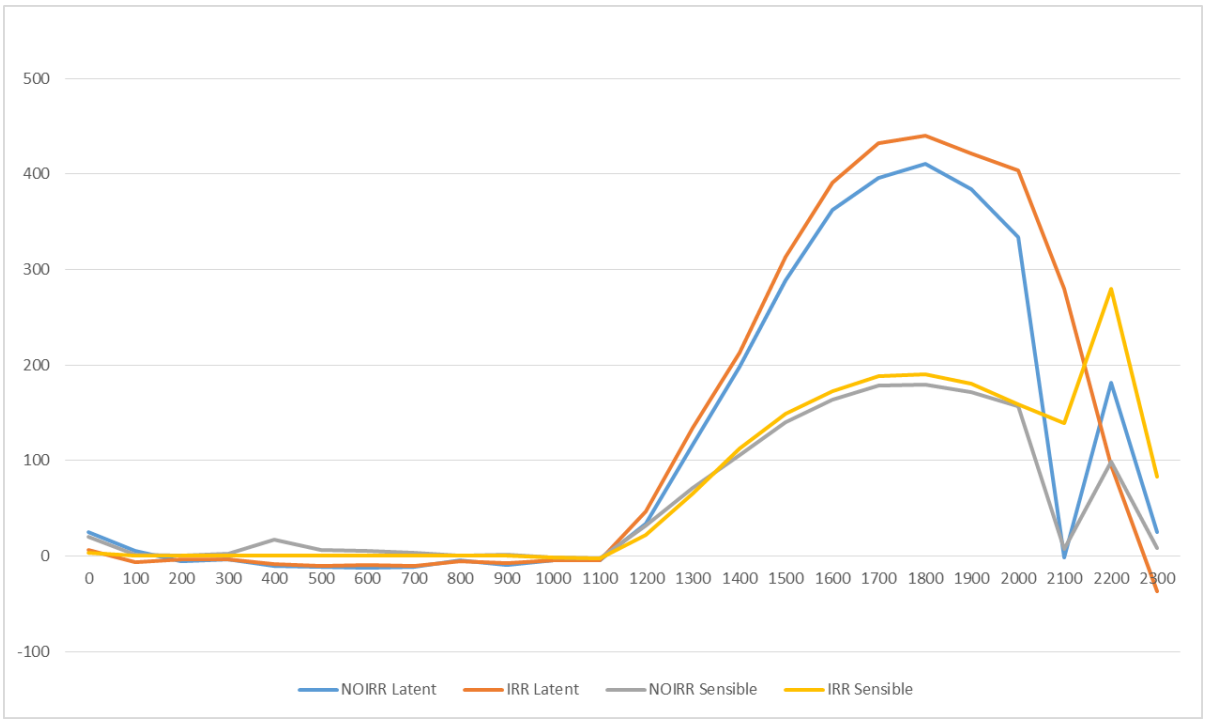

Figure 5.7: Sensible and Latent heat flux for NO-IRR and IRR simulations. Plots are for grid point near 31.5N and -83.5W (Coffee County). Blue and yellow lines represent NO-IRR latent and sensible heat fluxes respectively. Red and grey lines represent IRR latent and sensible heat fluxes, respectively.

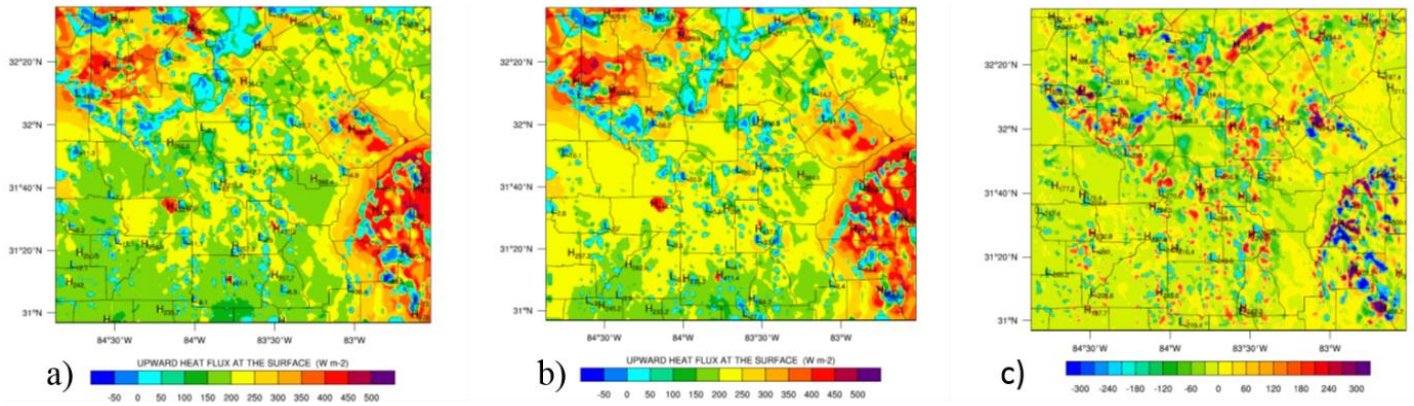

Figure 5.8: 20z June 30 sensible heat flux for a) NO-IRR, b) IRR, and c) the difference in flux between the two surfaces.

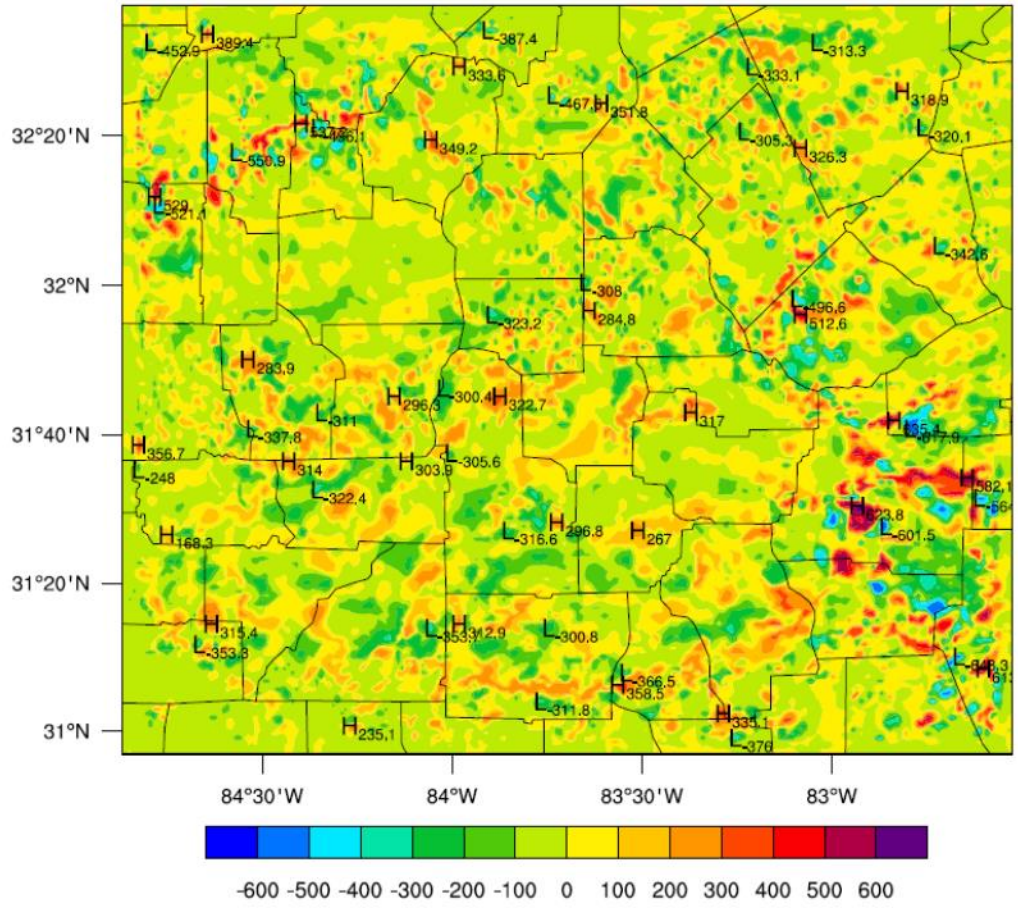

Figure 5.9: 18z July 11th differences in latent heat flux between NO-IRR and IRR simulations (W/m^2).

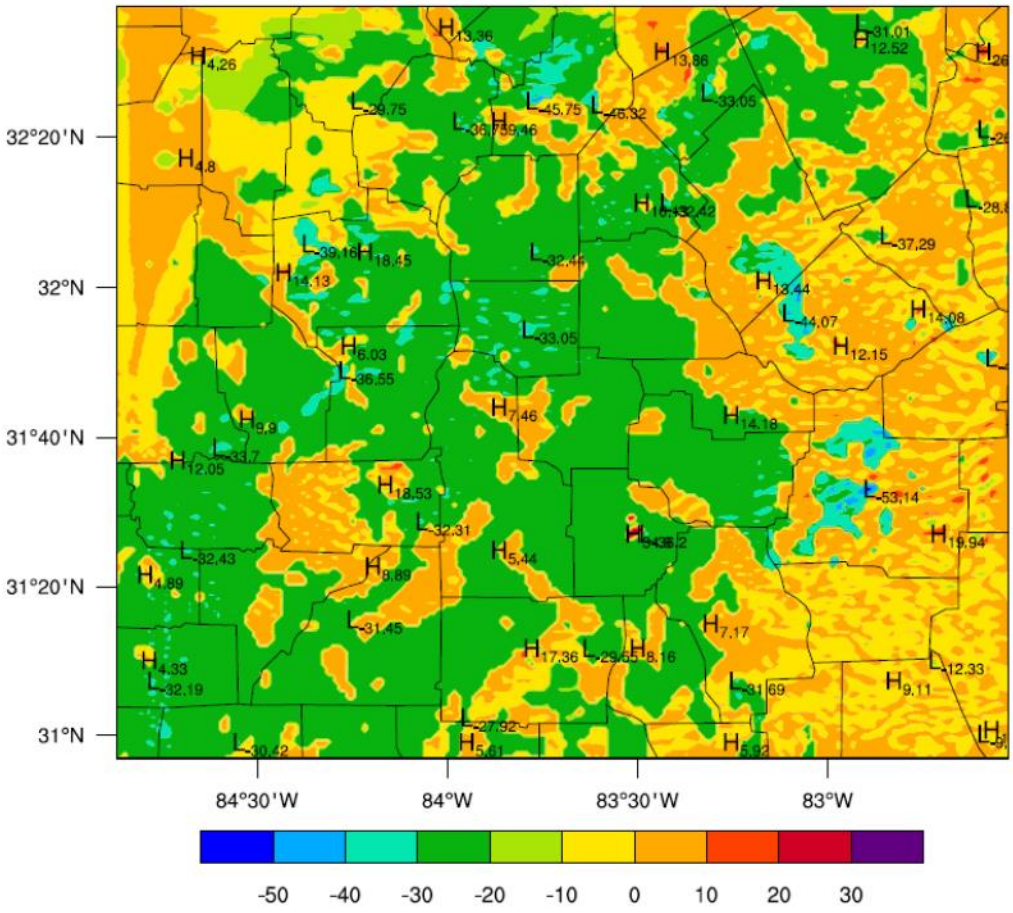

Figure 5.10: Sensible heat flux for 18z July 18th 2014 (W/m^2).

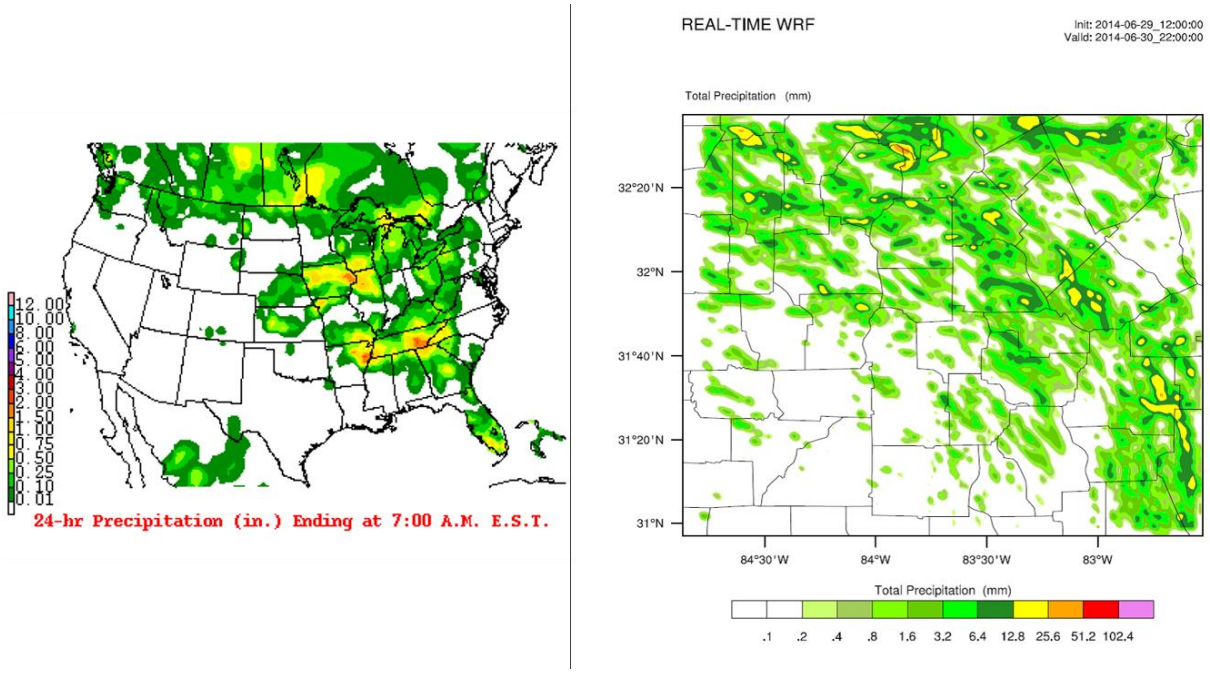

Figure 5.11: Image showing observed 24-hr precipitation on left hand side and model accumulated precipitation on June 30th, 2014. Obeserved precipitation photo credit to NCEP (http://www.wpc.ncep.noaa.gov/dailywxmap/index_20140630.html)

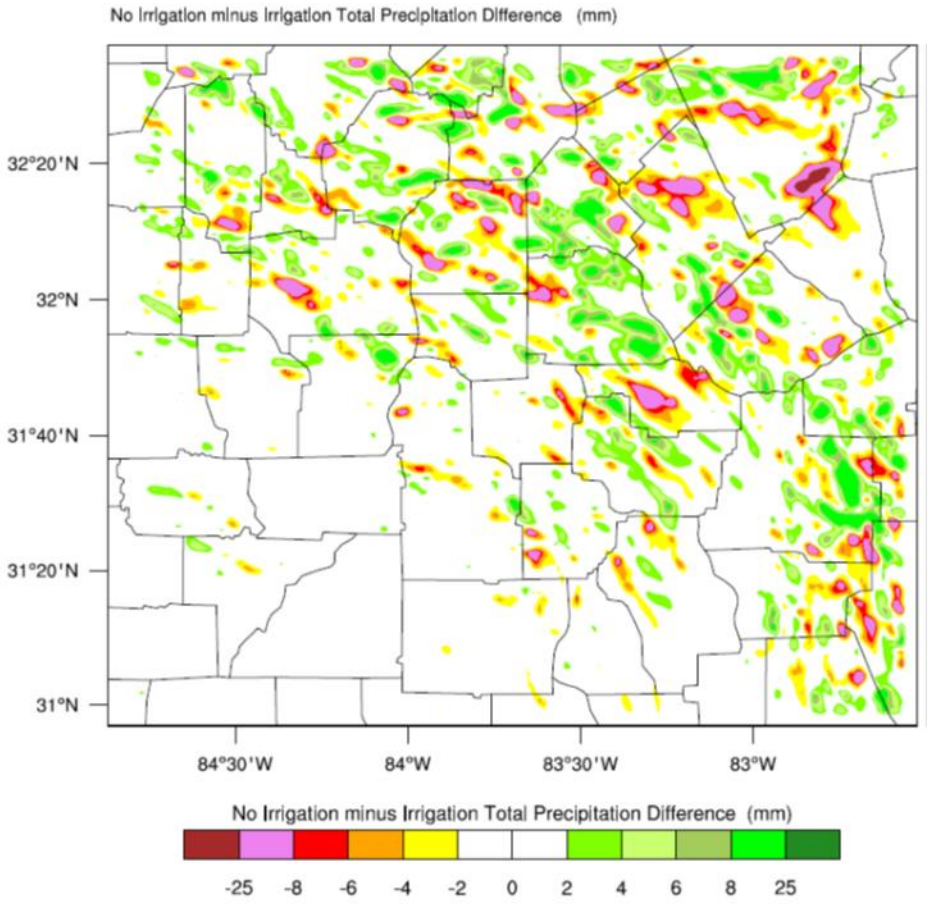

Figure 5.12: Total simulation precipitation difference map for NO-IRR and IRR June 29ht-30th simulation.

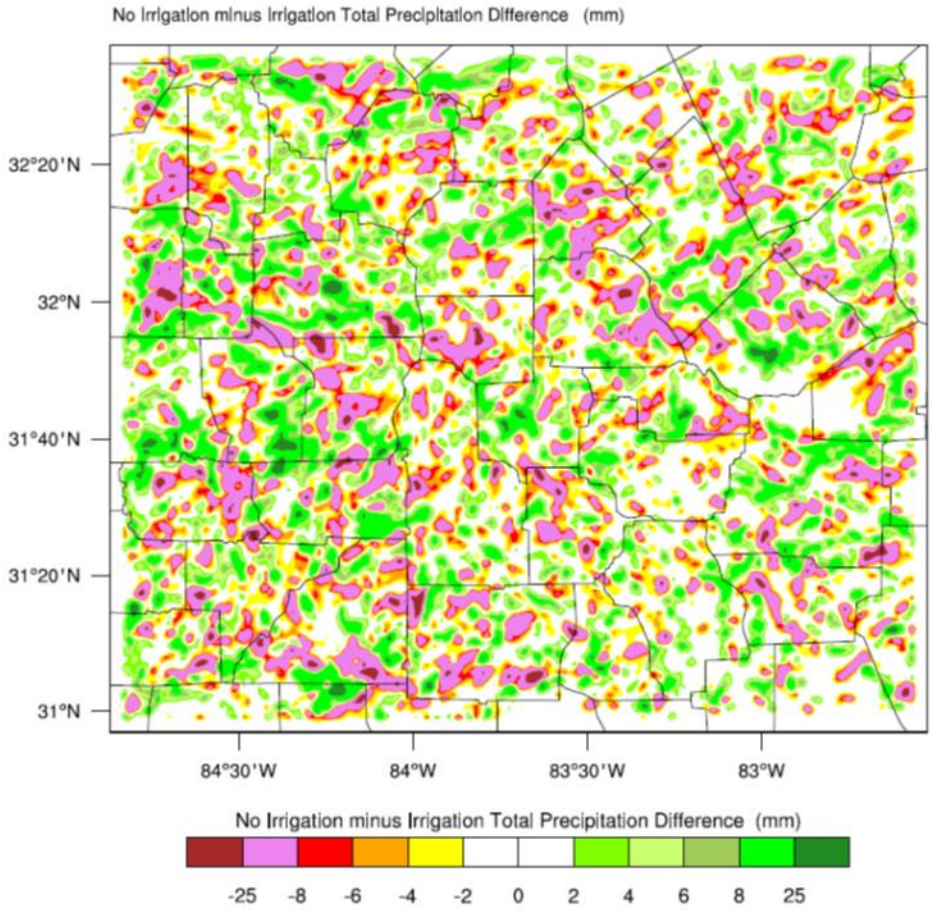

Figure 5.13: Total simulation precipitation difference map for NO-IRR and IRR July 10th-11th simulation.

6) SUMMARY AND CONCLUSIONS

6.1 Overview

Georgia has a humid subtropical climate, and climates of this type are generally perceived to have minimal irrigation needs. However, the increasingly sporadic nature of summertime and growing season precipitation in the region has made irrigation an attractive and more reliable alternative to relying on precipitation for agricultural crop production. Georgia has experienced rapid growth in irrigated acreage since the 1970s and the irrigated acreage continues to grow in the region. Evidence suggests that the increased irrigation often results in a net loss of water in irrigated areas, thus creating a positive feedback that strengthens the need to irrigate. Competing water use needs among private, municipal, and agricultural industries exacerbates the need to understand the impact of irrigation on the climate in Georgia.

This study addresses the need for a better understanding of the role of irrigation in Georgia's past and current climate. The objectives of this dissertation are to map the spatial and temporal development of irrigation in Georgia (Chapter 2). Chapter 3 addresses the limited availability to analyze long term changes in humidity by creating an adequate dew point temperature estimation method, tailored specifically for Georgia. Chapter 4 applies this method to assess the pre- and post-irrigation differences in climate. Chapter 5 uses the WRF model to address the climatic impact of transitioning from unirrigated agriculture to irrigated agriculture.

6.2 Conclusions

The findings from this dissertation extend existing knowledge on the impact of irrigation on climate and provide new perspectives that have been sparsely represented for the Southeastern U.S., particularly within the Coastal Plains region of Georgia. The results indicate that Georgia has experienced rapid growth in irrigated acreage since the mid-1970s. An analysis of remotely sensed data spanning 38 years (1976-2013) revealed a 4,500% increase in Center Pivot Irrigation (CPI) systems that corresponded to an approximate 2,000% increase in total area of CPI-irrigated land. The bulk of the total acreage irrigated is located in southwest Georgia, as seven counties in the region contained 38% of the total acreage irrigated in 2013. One of the first mapped time series of irrigated acreage in Georgia was created as a result of this analysis.

To assess long-term changes in moisture in the region, it was critical to analyze long-term dew point temperatures. The lack of long-term daily average dew temperatures created the need for the development of an adequate estimation method. Dew point temperatures were estimated and evaluated at 14 NWS Coop stations in southwest Georgia using linear regression models and artificial neural network (ANN) analysis. Estimation methods were drawn from simple and readily available meteorological observations, therefore only temperature and precipitation were considered as input variables. Both methods produced adequate estimates of daily averaged dew point temperatures with the ANN displaying the best overall skill. On average, the ANN reduced root mean square error (RMSE) by 6.86% and mean absolute error (MAE) by 8.30% when compared to the best performing linear regression model. The ability to assess long-term changes

in dew point temperature in areas outside of first order stations was also a by-product of the work performed in this dissertation.

In an era defined as post-irrigation since the installation of artificial irrigation structures such as center pivot irrigation (CPI) in the mind 1970s in the Georgia Coastal Plain, empirical analysis suggests that increased irrigation has modified summer humidity and temperatures. A total of 19 stations in the Georgia Coastal Plain were analyzed to determine differences in the hydroclimate in pre-irrigation and post-irrigation epochs. Analysis found that summer minimum and dew point temperatures were most impacted. Precipitation was most impacted in April and November. Further research is needed to determine if or how the changes in precipitation are influenced by irrigation. The poor data quality in the region made it difficult to isolate the impact of irrigation as many stations had multiple years of missing data. There were also confounding factors that make it difficult to isolate the impact of irrigation empirically. To limit the influence of poor data quality and confounding factors created by the microclimate of each observation station, this analysis was extended via a modeling approach.

To investigate the relative differences between non-irrigated and irrigated land cover scenarios, three 36h model simulations were conducted using version 3.5 of the WRF Model. The case study analysis showed that the differences in land cover created spatial shifts in latent and sensible heat fluxes. The irrigated land cover had higher sensible and latent heat fluxes for all three case studies and produced higher grid cell maximum accumulated precipitation. The increase in near surface moisture impacts where local minimum and maximum fluxes occur and this local shift impacts local development of convection.

Agriculture is the largest industry in Georgia and its continued growth and maintenance is vital to the state's economy. Combined with climate changes and recent transitions in the types of crops produced in Southwest Georgia, continued increases in artificial irrigation are expected. With the expected continuing reliance on irrigation, it is of utmost important to continue to monitor and map irrigation in the region beyond this study. The research presented here suggests that irrigation has impacted the hydroclimate in Georgia, and this relationship is expected to strengthen as irrigated acreage increases in the future. The greatest impacts of irrigation in the state are local, but the cumulative impacts have already begun to cause larger problems. Results shown here suggest that minimum and dew point temperatures were impacted the most, which is in agreement with other studies of this nature. Other studies have also noted that irrigation causes a reduction in summer maximum temperatures, but that result was not as conclusive in the Georgia Coastal Plain. Early growing season and summer precipitation decreased during the more intensely irrigated time period, but further research must be conducted before directly attributing this decrease to irrigation. One issue that arose was the lack of complete and consistent long term climate observations in the region. Improvements in data quality can provide a better context on the long term impacts of irrigation discussed in this study

The ongoing dispute between Alabama, Florida, and Georgia known as the "Tri-State Water Wars" provides an example of the wide reaching impacts of irrigation within Georgia. The dispute began over allocation of water resources in the Alabama-Coosa-Tallapoosa (ACT) and Apalachicola-Chattahoochee-Flint (ACF) river basins. Irrigation density and water withdrawals are highest in the Lower Flint basin in Georgia. This removal of water upstream has reduced the

water reaching Florida, and has negatively impacted Florida's multi-million dollar shellfish industry. Results found here provide evidence that increased near surface moisture caused by irrigation has resulted in a net loss of water in the region. The net water loss strengthens the need to irrigate in the future. This reliance on irrigation can potentially create a positive feedback and introduce wide reaching negative ecological and economic impacts as seen in the Tri-State Water Wars.